SKY-FI - Internet Everywhere

DSE Group 13

S. Angelovski	4055403	J.H. Freiherr von der Goltz	4206037
Y. A. Antonio	1544039	G.R.W. ten Hove	4150023
G. de Jong	4210034	T. Bussink	4153693
A. Carrera	4060865	K. Rado	4212169
Y. Chen	4142136	J.K. El Sioufy	4192729

Final Report

Design Synthesis Excercise

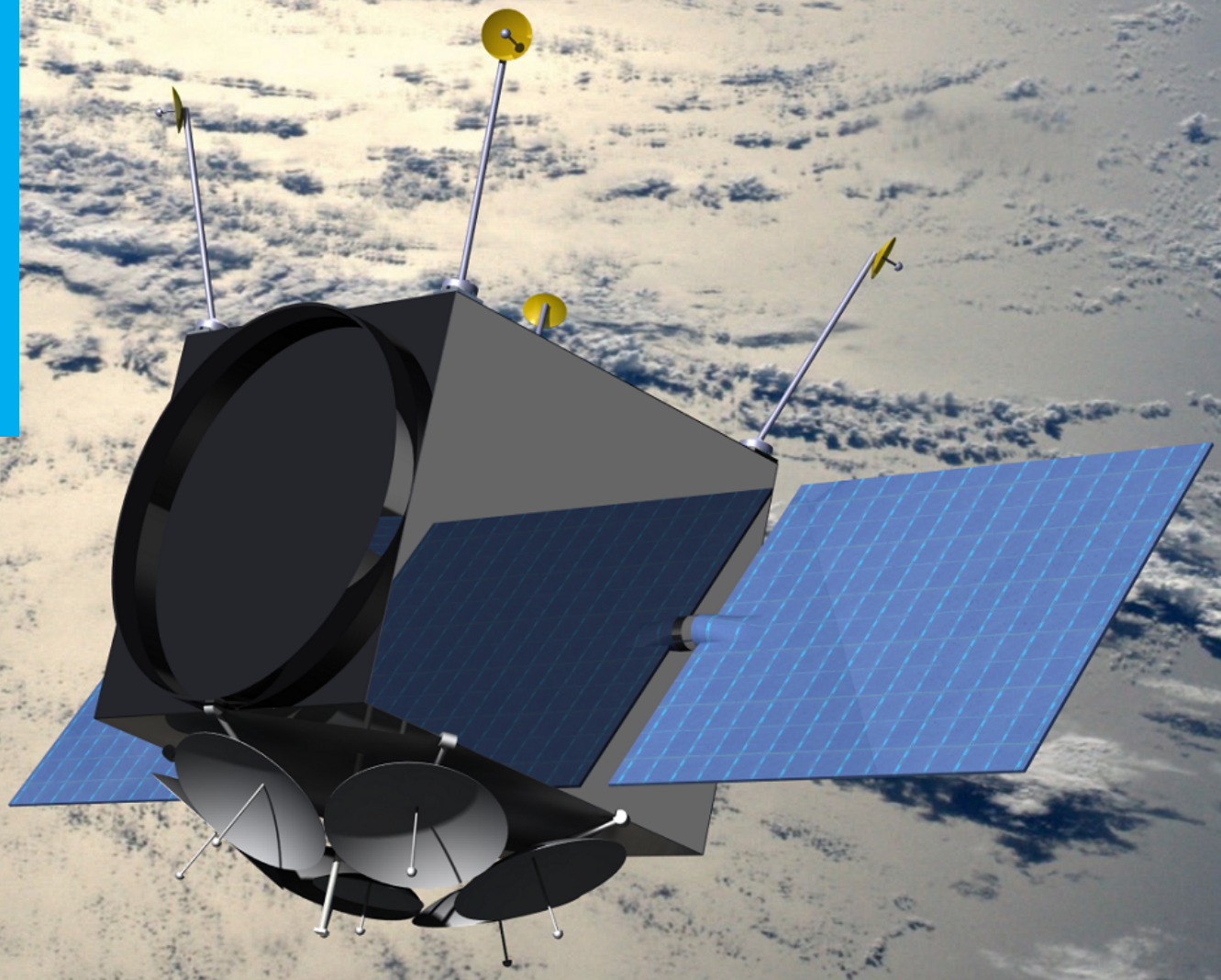

TU Delft Delft University of Technology

Aerospace Engineering

Version 1.0

June 30, 2015

Preface

This Final Report is made within the scope of the Design Synthesis Exercise (DSE) of group 13. The DSE is a 10 week project where groups of 10 students design an aerospace related system. The project concludes the Bachelor of Aerospace Engineering at TU Delft. The task is to design a global communication system which can provide services like SMS, phone calls, Internet connection and a Search And Rescue (SAR) function. The group is working on a satellite system named Sky-fi. This project intends to give insight into the entire development process of a system starting with nothing but a demand and a budget and the group will combine what they have learned in the past 3 years in order to find the best solution.

We would like to thank our tutor Ernst Schrama for his continuing support and constant feedback which always helps us to stay on track and think into the right direction, also we would like to thank our coaches Zi-Xuan Zheng and Martin Schmelzer as well as our external experts Arancha Dominguez and Wouter Jan Ubbels for offering their assistance. Additionally we would like to thank to thank the experts that helped us with several subsystems. For the sustainability we would like to thank Eelco Doornbos, for the antenna design we would like to thank Dink Tran, Prem Sundaramoorthy and Alexander Yarovoy and for the link budget we would like to thank Angelo Cervone. For the power subsystem we would like to thank Nuno Baltazar dos Santos.

Summary

This report presents the outcome of the DSE of Group 13 in spring 2015. The goal of the exercise is to complete the conceptual and preliminary design of a satellite communication system called SKY-FI.
Key requirements of the SKY-FI mission are global coverage, voice communication, text messaging, Internet connectivity and Search and Rescue (SAR) tracking capability. The data rates provided must be sufficient to perform basic internet tasks like emailing, or other low-bandwidth services. Furthermore there must be connection success probability of 90%.

It was estimated that approximately one million users will subscribe to the service out of which 5% are active at the same time. An average data rate of 2kpbs and a peak data rate of 10kbps will be provided. Under special circumstances, single users can be assigned higher data rates up to 50kbps if no other users are connected to a satellite or by reducing the data rates of other users.
The satellite constellation is made of 209 satellites in 19 orbital planes with 82 degrees inclination at an altitude of 550km. There are 19 spare satellites, one per plane. They will be deployed by a Rockot launcher from the Plesetsk Cosmodrome in Russia.
Each satellite has a mass of 104kg and has a size of 60cm $\times$ 60cm $\times$ 65cm. The satellites have a design lifetime of ten years, after that they will de-orbit due to atmospheric drag within approximately 6 years. A mono-propellant propulsion system is used for orbit and constellation maintenance and debris avoidance.
Inter-satellite communication, an additional ground station and gateway antenna and smart digital onboard signal routing allow for fast connections, low latency and reduced need for expensive ground operations. The communication payload consists of four transponders which are made of flight-proven and reliable components, accommodating 245 users per satellite. By extracting the Doppler frequency shifts of the communication channels, SAR tracking can be provided and even scientific data can be gathered in an unprecedented extent.
The communication system drives the power requirement of the spacecraft, the power subsystem is designed accordingly. The total spacecraft power is 104W, which is provided by two solar arrays with each having a surface area of 0.432m^2 and a battery for the eclipse with 60Wh capacity.
The satellites will have an Attitude Determination and Control System (ADCS) that provides three-axis control to point the antennas to their destination and the solar panels to the sun. This is accomplished with a redundant magnetic torquers assembly.
A thermal control system makes sure that the electronics and the propulsion system can operate within their designed temperature ranges. To achieve that, heaters are implemented to protect the electronics from the temperature occurring in eclipse.

All hardware is designed to be simple and low-cost. Economics of scale and proven technology make it possible to build the system within the budget of €500 million, while fulfilling all data rate, coverage, performance and other mission requirements.

Contents

List of Figures

List of Tables

Acronyms

ADCS Attitude Determination & Control System.

AOCS Attitude Orbit and Control System.

BMS Battery Management System.

CS Communication Satellite.

DOT Design Option Tree.

DSE Design Synthesis Exercise.

ECEF Earth Centred Earth Fixed.

ECI Earth Centred Inertial.

EIRP Effective Isotropic Radiation Pattern.

EPC Electronic Power Conditioner.

EPS Electric Power Subsystem.

FDMA Frequency-Division Multiple Access.

HET Hall Effect Thruster.

ICD Interface Control Document.

IF Intermediate Frequency.

ISL Inter Satellite Link.

ITAR International Traffic in Arms Regulations.

ITU International Telecommunication Union.

LAF Location Adjustment Factor.

LEO Lower Earth Orbit.

LNA Low Noise Amplifier.

MEMS Microelectromechanical System.

MLI Multi Layered Insulation.

MSS Mobile Satellite Services.

PMU Power Management Unit.

QPSK Quadrature Phase Shift Keying.

RAMS Reliability, Availability, Maintainability and Safety.

SAR Search And Rescue.

SEC United States Securities and Exchange Commission.

SLOC Source Lines of Code.

SNR Signal to Noise Ratio.

SSCM Small Satellite Cost Model.

TDD Time-Division Duplexing.

TDMA Time-Division Multiple Access.

TFU Theoretical First Unit.

TLE Two-Line-Element.

TWT Traveling Wave Tube.

UD User Device.

VLEO Very Low Earth Orbit.

Nomenclature

Latin

Δf Doppler frequency shift [Hz]

ΔR_{drag} Change in orbit radius due to atmospheric drag $[m]$

$\Delta V_{hohmann}$ Delta V needed for a Hohmann transfer $[\frac{m}{s}]$

ΔV_{total} Total velocity increment required for orbital maneuvers $[kg]$

$\frac{A}{m}$ Area-to-mass ratio $[\frac{m^2}{kg}]$

$\frac{dR_o}{dt}$ Decay rate $[\frac{m}{s}]$

$\frac{dr}{dt}$ Range rate $[\frac{m}{s}]$

$\frac{S}{N}$ Signal-to-Noise Ratio [-]

$\vec{x}_u$ User position vector

A Cross-sectional area of launch adapter [m^2]

a Semi-major axis $[km]$

A_s Satellite area illuminated by the sun $[m^2]$

A_u Satellite surface area in flight direction $[m^2]$

A_{adcs} ADCS Area $[m^2]$

A_{bat} Area of Battery $[m^2]$

a_{drag} Acceleration $[\frac{m}{s^2}]$

A_{ins} Insulated Area $[m^2]$

A_i Radiated area of surface i $[m^2]$

A_j Radiated area of surface j $[m^2]$

A_{maxorb} Surface Area of MAXORB layer $[m^2]$

A_{mylar} Surface Area of Aluminized Mylar layer $[m^2]$

A_{prop} Area of Propelant Tank $[m^2]$

A_{sc} Total Spacecraft Area $[m^2]$

A_{solar} Area of solar panel$[m^2]$

B Ballistic coefficient $[\frac{m^2}{kg}]$

B Channel Bandwidth [Hz]

C Channel Capacity [bit/s]

c Speed of light, 3×10^8 $[\frac{m}{s}]$

C_D Drag coefficient [-]

c_{pa} Center of aerodynamic pressure $[m]$

C_{PMSE} Cost of program management and systems engineering [$]

c_{ps} Center of solar pressure $[m]$

C_{satSW} Cost of flight system software maintainence [$]

D Drag $[N]$

d orbital debris diameter $[cm]$

D_y Degradation per year [-]

d_{sp} Distance from center of solar panel to the motor $[m]$

E Eccentric anomaly [°]

E Young's modulus of elasticity [Pa]

e Eccentricity [-]

$EIRP$ Transmitter power $[dBW]$

F	Co-rotation and wind correction factor [-]
F	Flux $[\frac{Impacts}{m^2 year}]$
f_n	Fundamental frequency [Hz]
f_t	Transmitting frequency [Hz]
F_{i-j}	Radiative view factor [-]
g_0	Gravitational acceleration at sea level $[\frac{m}{s^2}]$
G_r	Gain of receiving antenna $[dBW]$
G_t	Gain Transmitter Antenna $[dBW]$
h	Orbit altitude $[km]$
h	altitude$[km]$
I	Mass moment of inertia $[kgm^2]$
I	Moment of inertia [kgm^2]
i	Inclination of the orbit [°]
I_d	Inherent degradation [-]
i_{min}	Minimum inclination [°]
I_{sp}	Moment of inertia of half the solar panel$[kgm]$
I_{sp}	Specific impulse $[s]$
k	Boltzmann's constant $[dB\frac{W}{K}]$
K_{buck}	Buckling coefficient, depends on edge boundary conditions and aspect ratio
L	Length from beam root to center of mass [m]
L_a	Atmospheric Loss $[dBW]$
L_d	Life degradation [-]
L_l	Line Loss $[dBW]$
L_s	Free Space Loss $[dBW]$
L_s	Satellite lifetime $[years]$
L_θ	Pointing loss $[dBW]$
l_{sp}	length of half the solar panel $[m]$
M	Mass of beam [kg]
M	Mean anomaly [°]
M	Moment applied on launch adapter [Nm]
m	mass $[kg]$
M_{dry}	Satellite dry mass $[kg]$
M_{earth}	Magnetic moment of the earth $[Tm^3]$
M_{prop}	Propellant mass $[kg]$
m_{sp}	mass of half the solar panel $[kg]$
N	Number of parts [-]
n	Mean motion [°/s]
N_sat	Number of manufacturd Satellites [-]
P	Applied load on spacecraft launch adapter [N]
P	Orbital period $[s]$
P_t	Tank pressure $[Pa]$
P_{tot}	Total Power required$[W]$
q	Reflectance factor of the satellite surface [-]
Q_{ins}	Insulated Internal Heat [W]
$Q_{internal}$	Internal Power dissipation $[W]$
q_{IR}	Eart Infra Red Flux $[\frac{W}{m^2}]$
q_s	Solar Flux $[\frac{W}{m^2}]$
R	Bit Rate $[bits]$
R	Reliability [-]
r_1	departure circular radius $[km]$
r_2	arrival circular radius $[km]$
R_E	Average Earth radius $[km]$
R_o	Radius of the orbit $[m]$
r_t	Tank radius $[mm]$
$R_{S/C}$	Distance between spacecraft and centre of the Earth $[km]$
r_{sat}	radius of the footprint $[km]$
S	13-month smoothed solar radio flux$[10^4 Jy]$

s	Distance between spacecraft and Earth $[m]$
S_{in}	Solar flux$[\frac{W}{m^2}]$
T	External torque acting on the satellite $[Nm]$
t	Tank wall thickness $[mm]$
t	date$[year]$
t	time $[s]$
T_s	Noise Temperature $[dBK]$
$T_{ins-adcs}$	ADCS Insulated Temperature [K]
$T_{ins-bat}$	Battery Insulated Temperature [K]
$T_{ins-prop}$	Propelant Tank Insulated Temperature [K]
T_{ins}	Insulated Internal Temperature [K]
t_{mis}	time from the start of the mission [year]
T_{mt}	Magnetorquer torque $[Nm]$
T_{nins}	Non-insulated Spacecraft Heat [K]
T_{sc}	Net heat of spacecraft $[K]$
t_{sp}	Time for solar panel to orbit $[s]$
T_s	Sink Heat $[K]$
Tq_{sp}	Torque of the solar panel$[Nm]$
u	Temperature $[K]$
U	Radiation Intensity [W/m^2]
$u(x, y, t)$	Temperature, exact solution to the PDE [K]
U_0	Radiation Intensity of an isotropic antenna [W/m^2]
$U^n_{i,j}$	Discreet temperature $[K]$
V	Orbital velocity $[\frac{m}{s}]$
w_{sp}	width of inertia of half the solar $[m]$
x	Horizontal coordinate [m]
y	Distance of moment line [m]
y	Vertical coordinate [m]
C$_{grSW}$	Cost of ground system software maintainence [$]
C$_{op}$	Operating cost [$]
C$_{SW}$	Software cost [$]
C$_{TFU}$	Cost of the first theoretical model [$]
C$_{TL}$	Cost of the total number of satellites [$]
dB	$10log_{10}$ relative to 1 Watt
dBi	$10log_{10}$ relative to an isotropic antenna
dBm	$10log_{10}$ relative to 1 miliWatt
dBmW	$10log_{10}$ relative to 1 miliWatt
dBW	$10log_{10}$ relative to 1 Watt
EIRP	Effective Isotropically Radiated Power [dBW]
FTE$_{eng}$	Cost of full time equivalent of engineers [$]
N$_{eng}$	Number of engineers [-]
T	Yearly turnover from subscriptions [$]

Greek

α	Solar absorptivity [-]
α_{sat}	Angular acceleration of the satellite $[\frac{^\circ}{s^2}]$
α_{sp}	Angular acceleration of the solar panel$[\frac{^\circ}{s^2}]$
β	Orbital drift at specific time [°]
ϵ	Minimum elevation angle [°]
ϵ_θ	Pointing loss [°]
η_{BOL}	Solar efficiency at the beginning of life [-]

η_{sol}	Solar panel efficiency [-]
γ	Safety factor [-]
κ	Thermal diffusivity $[\frac{m^2}{s}]$
λ	Failure rate of a part [1/year]
λ	Longitude [deg]
λ_{ert}	Angle deviation from normal of Earth's surface [°]
λ_{sp}	Angle deviation from normal of spacecraft surface [°]
μ	Standard gravitation parameter $[\frac{km^3}{s^2}]$
ν	Poisson's ratio
ν	True anomaly [°]
Ω	Right ascension of ascending node [°]
ω	Argument of perigee [°]
ω_0	Initial angular velocity$[\frac{^\circ}{s}]$
ω_{sp}	angular velocity $[\frac{^\circ}{s}]$
ϕ	Latitude [deg]
ϕ	geocentric semi-angle [°]
ρ	Density$[\frac{kg}{m^3}]$
ρ_r	Slant range $[km]$
ρ_{alb}	Albedo factor [-]
σ	Internal stress of the structure [Pa]
σ	Stefan–Boltzmann constant $[\frac{W}{m^2K^4}]$
σ_y	Yield stress $[Pa]$
θ	Incidence angle [°]
θ	Mean Anomaly [°]
θ_{nadir}	Satellite pointing offset from the nadir vector [°]
θ_{sp}	required angle[°]
ε_{ins}	Effective Emissivity [-]
ε_{IR}	Infrared emissivity [-]
ε_{maxorb}	Emissivity of MAXORB layer [-]
ε_{mylar}	Emissivity of Aluminized Mylar layer [-]
q_{av}	Average Heat Flux [W/m^2]
q_j	Heat Flux from Body j [W/m^2]

Introduction

The world relies on information technologies, however there are vast areas around the globe which lack communication coverage. Airplanes enter areas of radio silence when crossing the world's oceans. Ground users cannot reach the outside world when they are not in the coverage area of a terrestrial tower. This report will describe the concept and preliminary design phase and its result for a constellation of satellites providing communication with worldwide coverage. It becomes clear how this sector has become a field of interest in the last few years, now that companies like OneWeb Ltd. [1] are partnering with aerospace contractors like Airbus Defence and Space to build large communication satellite constellations in Lower Earth Orbit (LEO).

Following on the Project Plan, the Baseline Report and the Midterm Report, this report is the last in a series of four reports in the Design Synthesis Exercise (DSE). The DSE is a ten week project that concludes the Bachelor of Science programme of Aerospace Engineering at the TU Delft. The purpose of this Final Report is to present the result of the DSE, namely a Very Low Earth Orbit (VLEO) communication satellite constellation that was chosen in the Midterm Report. The constellation and service that is offered is called SKY-FI. The report elaborates on the detailed technical design of satellite bus and payload, constellation design, manufacturing and operation of SKY-Fi.

The report will be structured in the following way. It will be divided in two parts. The first part will be Technical Design. This part of the report will comprise of the Technical Development and Requirements in Chapter 1. In this chapter the requirements of the system will be discussed. This will be followed by the System Interfaces and Functional Breakdown in Chapter 2. After that the constellation design and orbit propagation will be reviewed in Chapter 3. The satellite constellation is designed based the theory presented in this chapter. Chapter 4 will discuss the communication payload, including antenna design and Chapter 5 will describe the user tracking subsystem. The TT&C subsystem is described in Chapter 6. The power subsystem is presented in Chapter 7. Chapter 8 discusses the attitude laws for solar array pointing which is followed by Chapter 9 about the Attitude Determination and Control Subsystem. The Thermal Control Subsystem and the satellite bus structure are described in Chapter 10 and Chapter 11. Chapter 12 will discuss the sustainability approach concerning our system. Subjects such as orbital decay and debris avoidance manoeuvres will be discussed. Based on the sustainability approach the propulsion subsystem is designed in Chapter 13. At the end of the Technical Design part a requirement a requirement compliance check is done in Chapter 15.

The second part of the report will concern itself with Operations management. This part will start with the launch vehicle and site choice in Chapter 16. In Chapter 17 a market analysis will be made for the final concept. A risk assessment will be performed in Chapter 18. After that a sensitivity analysis will be presented. Furthermore, operations and logistics will reviewed in Chapter 20, a production plan will be given in Chapter 21 and a Reliability, Availability, Maintainability and Safety Characteristics analysis will be performed in Chapter 23.

Part I

Technical Design

Chapter 1

Technical Development and Requirements

1.1 Mission Need and Project Objective

The need for low-orbit, space-based, communication systems is ever increasing, as the developed world increases its mobile communication and Internet usage. However, the Internet and regular cellphone coverage are geography specific and due to the lack of infrastructure in large parts of the world, they are non-existing. Providing this to the whole world is the major challenge upon which the project is based. Therefore, the Project Objective Statement lists the objectives, resources and the constrains of the design as follows:

> *Designing the infrastructure of a global, two-way, mobile communication system with emergency tracking capability with 10 students and a virtual 500M € budget within ten weeks.*

The mission need statement, on the other hand, states the needed performance, resources and time constraints of the overall product. It is formulated as follows:

> *Provide satellite-based voice, text, image transfer, basic Internet and tracking functionality to affordable, low-power, portable devices anywhere on the planet for a ten year period.*

Following from the definition of these statements, requirements have been derived, for which the system is designed.

1.2 Requirements List

The requirements that describe what the system needs to provide for the given mission are summarized in the Requirements Matrix, shown in Table 1.1. The requirements are split into their respective level (Top, System or Subsystem) and are rated based on three categories which are: Killer, Key and Driving. The killer requirements are the ones that drive the group's design to unacceptable extent. The Key requirements are important from the customer's perspective, while driving are the ones that drive the design more than average. Top requirement 2, 4 and 13 (defined in the group's Baseline Report [2]) are combined since the requirement for the coverage was in total assumed to be 90%, for either text messaging and phone calls and picture sending.

Table 1.1: Requirements matrix.

Req. ID.	Description	Level (Rating)
Req-Top-1	The system shall be able to connect users to Internet.	Top-Level (Key)

Req-Top-2	The system shall provide full coverage of the earth at any time with success rate of 90%.	Top-Level
Req-Top-3	The system shall be able to transcieve text messages at a data rate of 1 kilobit per minute.	Top-Level (Key)
Req-Top-5	The system shall be able to connect a phone call or send a picture at a data rate of 10 kilobit per second.	Top-Level (Key)
Req-Top-6	The whole system's operation time shall be 10 years.	Top-Level (Key)
Req-Top-7	A portable device with an omnidirectional antenna shall be able to establish communication to the space segment when there is a non-obstructed field of view.	Top-Level
Req-Top-8	The system shall be realized within an initial (virtual) budget of 500 M€.	Top-Level (Killer)
Req-Top-9	At the end of its life, the spacecraft shall have a minimal impact on the space debris density.	Top-Level (Driving)
Req-Top-10	The spacecraft shall comply with the International Traffic in Arms Regulations (ITAR) regulations.	Top-Level
Req-Top-11	The spacecraft shall comply with the International Telecommunication Union (ITU) regulations.	Top-level (Killer)
Req-Top-12	The system shall be able to locate the user within a 2 km radius within 1 hour.	Top-Level (Driving)
Req-Top-14	The user shall be able to successfully connect to the system within a period of 15 minutes.	Top-Level
Req-Sys-1	The satellite shall de-orbit 25 years after End-of-Life.	System Level (Driving)
Req-Sub-Payl-1	The payload shall provide a maximum data rate of 0.49 Mbits/s.	Subsystem-Level (Key)
Req-Sub-ADCS-1	The Attitude Determination & Control System (ADCS) shall have a pointing accuracy of 5° with 3 sigma in 3 axes for the communication system.	Subsystem-Level

Req-Top 11 is identified as killer, as the spacecraft will not be able to communicate to the ground if ITU regulations are not met. Furthermore, the ITU is responsible for assigning frequency ranges that are part of a lengthy and expensive process. Taking this into account, would drive the total mission cost to an undesirable level and most likely over the 500 M€ mark.

Requirements such as Req-Top-9 and Req-Sys-1 are driving the design, as one of the major considerations the group has made is in terms of sustainability. It is required for the satellite to leave as little (or none whatsoever) of space-debris as possible during its entire mission life.

Table 1.1 will be used in the Requirement Compliance Matrix in Chapter 15, in order to verify whether the provided design in this report fulfills all the requirements.

Chapter 2

System Interfaces and Functional Breakdown

2.1 Defining System Interfaces

The following Chapter would represent all the system elements considered in this report. This is visually represented by the N2 chart that is shown in Table 2.1. This chart analyzes functional and physical interfaces between the system elements. The functional interfaces are represented in the Functional Flow Diagram shown in Figure 2.1. Most of the subsystem level requirements come out from analyzing these functional interfaces.

The check mark shown in the N2 diagram indicates that there is an interface between the two system elements. If the box is blank, it means that there are no interfaces between the respective entities. The input/output relationships flow clockwise, meaning, for example, attitude control has input (yaw rate for intersatellite links) with communication payload. On the other hand, the feedback is the output (pointing accuracy) from communications.

2.2 Functional Flow Diagram

The Functional Flow Diagram defines the functional interaction between system elements during the entire mission. There are three main parts of the mission that interact simultaneously and they are identified as Space, User and Ground Segments.

The differences between the Functional Flow Diagram from Baseline report [2], are that the diagram has been expanded to a subsystem level. The functions of the different subsystems that support the payload has been added and the logical flow of tasks they perform, has been indicated in the figure. Furthermore, the Ground segment has been added which describes the how the Telemetry and Tracking part

2.3 Functional Breakdown Structure

The Functional Breakdown Structure is depicted in Figure 2.2. It labels all the tasks under the three mission segments.

Table 2.1: N2 Chart.

Attitude Control	✓	✓	✓	✓	✓		✓	✓	✓	✓	✓		
✓	Attitude Determination	✓	✓	✓	✓		✓	✓	✓	✓	✓	✓	
✓	✓	Power Production	✓	✓	✓					✓	✓	✓	
✓	✓	✓	Comm. Payload	✓			✓	✓	✓	✓	✓	✓	
✓	✓	✓	✓	Thermal Control	✓	✓						✓	
✓	✓			✓	Propulsion		✓	✓					✓
✓			✓	✓	✓	Structure							✓
✓	✓	✓	✓	✓	✓		Orbit Selection	✓	✓	✓	✓		✓
✓	✓	✓	✓		✓		✓	Constellation	✓	✓	✓	✓	✓
✓	✓	✓	✓				✓	✓	User Tracking	✓	✓	✓	
✓	✓		✓				✓	✓	✓	Ground Comm.	✓	✓	✓
✓	✓						✓	✓	✓	✓	Inter-satellite comm.	✓	
									✓	✓		Data Storage	
✓	✓					✓	✓	✓					Launcher

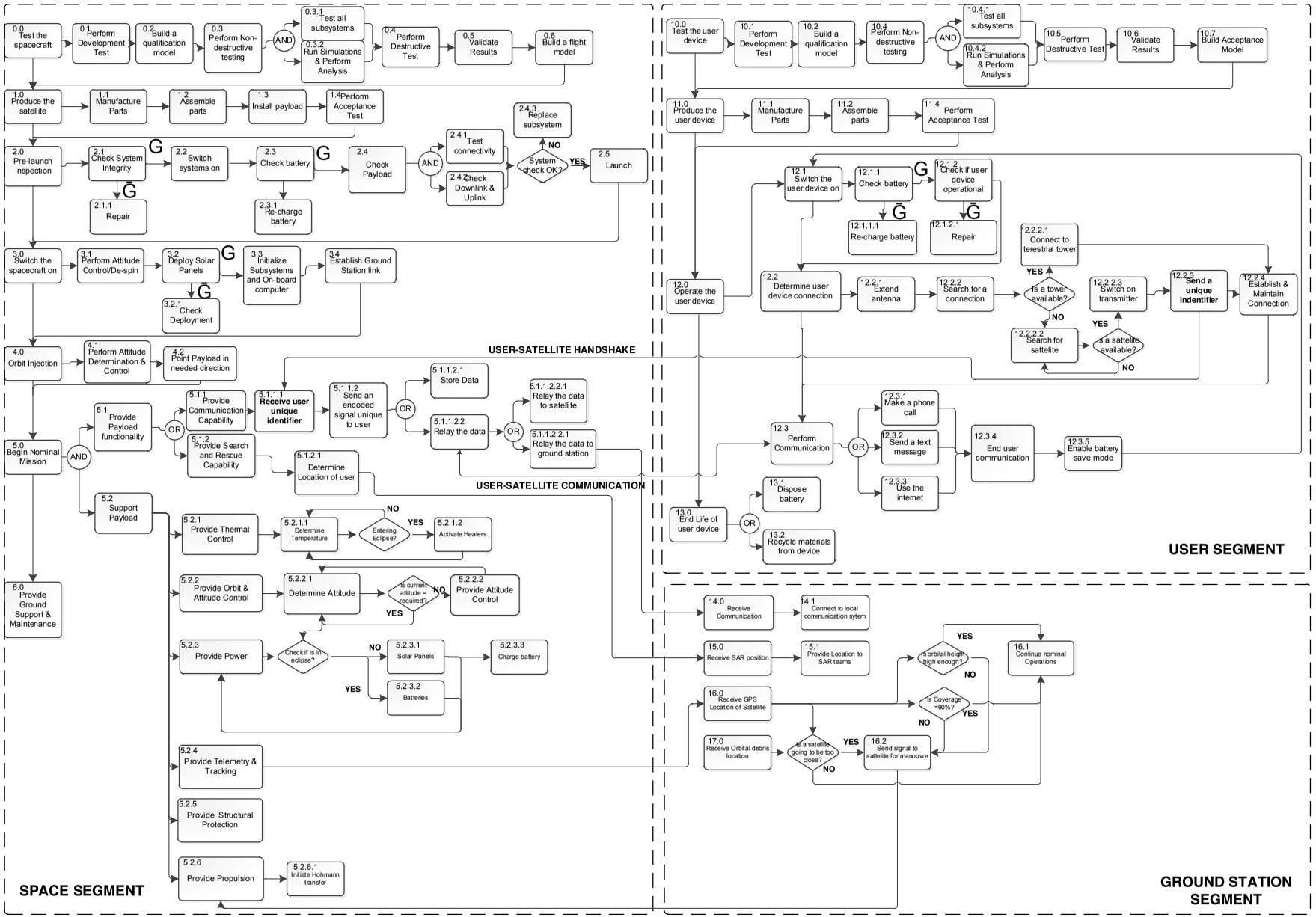

Figure 2.1: Functional flow diagram between the three mission segments: User, Ground and Satellite.

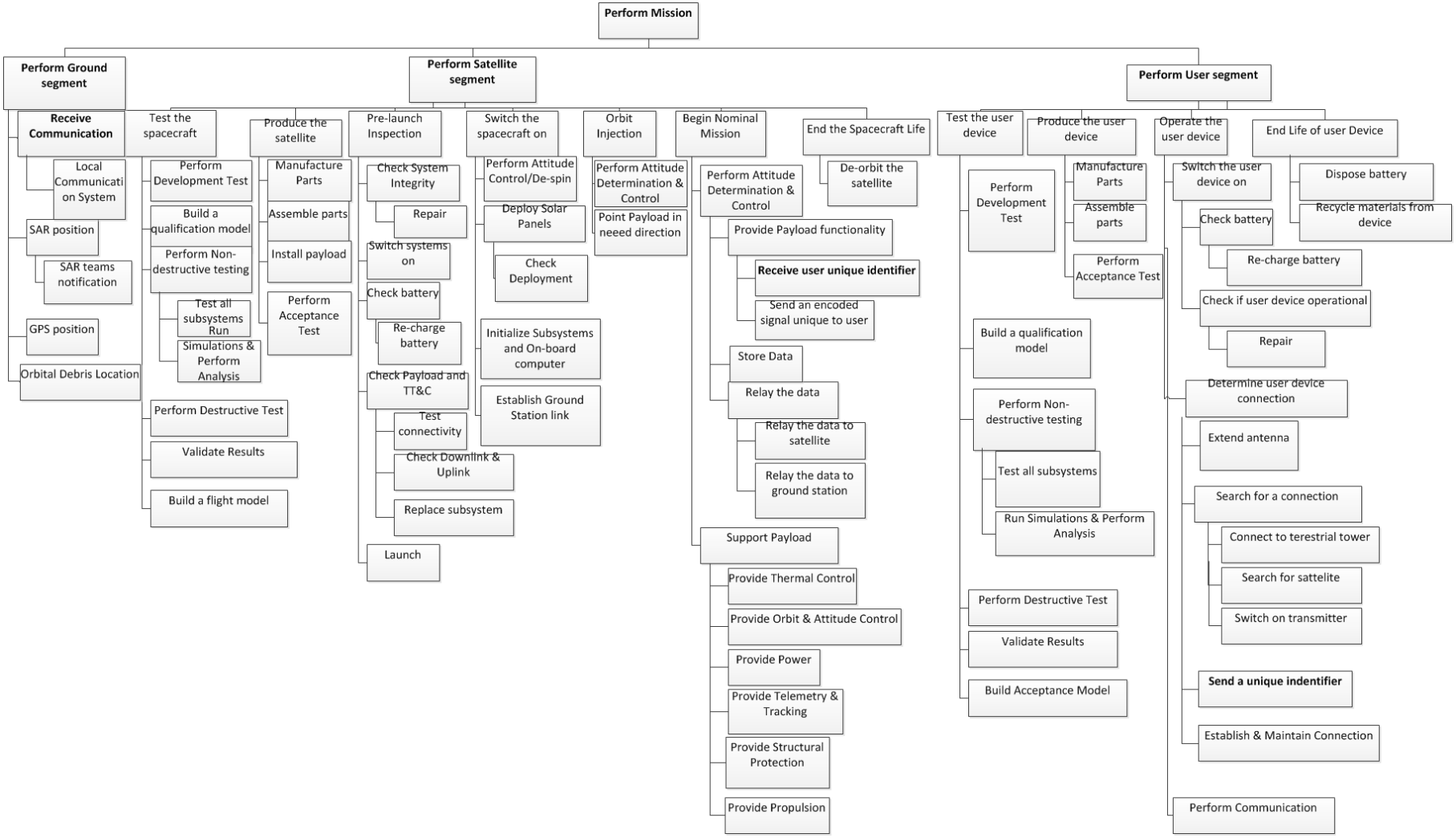

Figure 2.2: Functional Breakdown Structure.

Chapter 3

Orbit and constellation simulation

In this chapter the calculations for the orbit characteristics of satellites are discussed, as well as the theory behind the constellation design. After the theory is explained, the simulation that was made using the theory is explained, verified and validated and lastly used to design the constellation needed for this mission.

3.1 Orbit Characteristics

The first step in the process of making a simulation of a constellation is to create an orbit and its characteristics for a single satellite. This section will discuss the Kepler equations for the orbiting bodies. Equation 3.1 [3] gives a satellite position, which can be simplified. These simplifications are dictated by the constellation choice.

3.1.1 Governing equations

The first of the governing equations is given in Equation 3.1. This equation is a fundamental equation to describe a position in the orbit in a clear and simple manner.

$$R_{S/C} = \frac{a\ (1-e^2)}{1+e\ \cos(\nu)} \tag{3.1}$$

$R_{S/C}$ is the distance between the spacecraft and the centre of the Earth. The semi-major axis is denoted by a. Eccentricity is denoted by e. ν is used to describe to true anomaly. A full orbit can be simulated if calculation is repeated for a range of angles ν from 0 to 360°. However, a proper orbit analysis requires a position to be related to time. The use of the mean anomaly M and eccentric anomaly E [3] will help to accomplish this.

$$n = \frac{360}{T} = \sqrt{\frac{\mu}{a^3}} \tag{3.2}$$

$$M(t) = n\ t = \sqrt{\frac{\mu}{a^3}}t \tag{3.3}$$

$$M(t) = E(t) - e\ \sin(E(t)) \tag{3.4}$$

$$\nu = 2\ \arctan(\sqrt{\frac{1+e}{1-e}}\tan(\frac{E}{2})) \tag{3.5}$$

It is important to note that Equation 3.4 does not have a closed-form solution. Hence, an algorithm should be used to converge to the solution. A simple and powerful solution to this problem is the Newton-Raphson method [4]. Equation 3.4 needs to be rewritten to Equation 3.6, which will result in the scheme given in Equation 3.7. The solution will be achieved when the value $\|E_{k+1} - E_k\|$ get below a defined threshold, and the last updated value for E can be considered the solution.

$$f(E) = M - E + e\ \sin(E) = 0 \tag{3.6}$$

$$E_{k+1} = E_k - \frac{f(E)}{f'(E)} = E_k - \frac{M - E_k + e\ \sin(E_k)}{e\ \cos(E_k) - 1} \tag{3.7}$$

The Keplerian elements now make it possible to determine an orbit. Two important effects need to be taken into account, which are the Earth rotation and the J2 effect. The J2 effect is the drift the spacecraft experiences during one orbit. This drift is caused by a mass bulge at the Earth equator. The J2 effect will not cause a change in inclination, as it solely causes a westward shift in this model, which is constant. Equation 3.9 [5] shows the shift per orbit due to the J2 effect.

$$\delta_{J2} = \frac{3\ \pi\ J2\ Re^2\ \cos(i)}{(Re + h)^2\ (1 - e^2)^2} \tag{3.8}$$

$$\tag{3.9}$$

The rotation of earth can be approximated using Equation 3.10 and 3.11. Orbits with an inclination up to 90° are called direct orbits, whereas orbits with an inclination higher than 90° are called retrograde orbits.

$$dL1 = 360 - (\frac{P}{60 \times 3.988})\text{: direct orbit} \tag{3.10}$$

$$dL1 = 360 + (\frac{P}{60 \times 3.988})\text{: retrograde orbit} \tag{3.11}$$

3.1.2 Orbit Simplifications

In the Mid-term Report [6] the decision to design a satellite constellation in VLEO is documented. It is determined that the constellation should provide a constant coverage with circular orbits. Also, elliptical orbits is not possible due to inefficiency with global coverage, and were discarded because of it. A number of assumptions are then made:

- Orbit are circular
- Satellites are equally spaced in an orbit
- Earth is assumed to be a sphere
- J2 effect will be incorporated in the total satellite drift
- The reference frame is Earth Centred Earth Fixed (ECEF)

3.1.3 Reference Frame

The reference frame in which the orbit is plotted is an Cartesian coordinate system. This coordinate system is ECEF, which is right-handed and able to determines the y-axis. The origin for it is at the centre of Earth with an x-axis going through the intersection of the 0° latitude (equator) and 0° longitude (Greenwich). The z-axis, on the other hand, goes through the North Pole at 90° latitude.

3.2 Foot Print

The footprint of a single satellite can be calculated using Figure 3.1, where the geocentric semi angle ϕ are calculated. The equation for the geocentric semi angle can be seen in Equation 3.12

$$\phi = -\epsilon + \arccos(\frac{R_E}{R_E + h}\ \cos(\epsilon)) \tag{3.12}$$

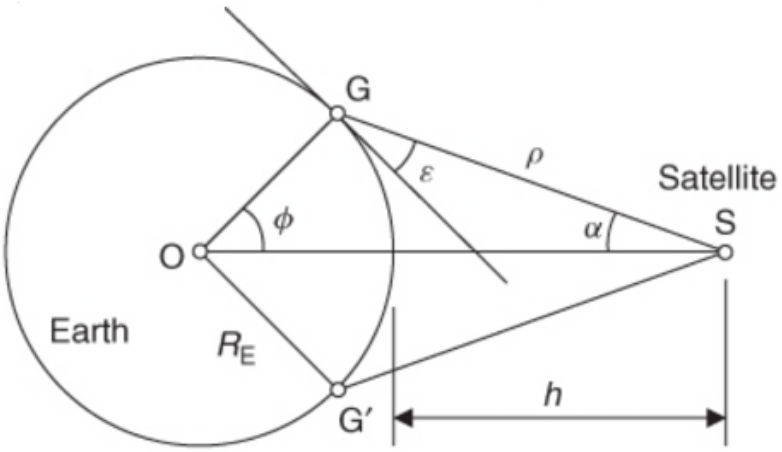

Figure 3.1: Typical ground coverage geometry [7].

Where R_E is the average earth radius, h is the altitude of the satellite, ϕ is the geocentric earth angle and ϵ is the minimum elevation angle. The elevation angle was assumed to be 20°, due to the fact that the slant range cannot be too large in order to limit the power requirement for the communication subsystem. The slant range will be further explained in Section 3.3. From this elevation angle and altitude, the geocentric earth angle ϕ can be calculated, which means the radius of the footprint can be calculated using Equation 3.13.

$$r_{sat} = \phi \; R_E \tag{3.13}$$

3.3 Constellation Design

By knowing the designed footprint and orbit characteristics, the constellation can now be designed. The Midterm report shows that a walker star constellation with an inclination smaller than 90° is chosen [3, 6]. The minimum inclination that is needed to have polar coverage is calculated using the equation 3.14.

$$i_{min} = 90 - \frac{r_{sat} \; \cos(30)}{R_E} \tag{3.14}$$

Now that the type of constellation is known, the spacing between satellites and planes can be determined, as well as the phase difference between different planes.

The spacing between the satellites in a plane is equally spaced, and thus in the simulation it will be the amount of the data points of a single orbit divided by the amount of satellites.

The phase difference of the first satellite in the next westwards plane is defined by where this satellite will be, which is in between the first and second satellite of the designated plane. For the simulation, this means that the phase difference is half the number of data points than that of the spacing between the satellites of the designated plane.

The plane spacing for a walker star constellation with a polar orbit can be seen in Figure 3.2. Here it can be seen that due to the non-synchronized orbits between the first and last orbit, a different plane spacing is needed there. This is due to the fact that the first plane and the last plan,e the descending node of the first plane and the ac ending node of the last plane, and vice versa), will go in a different direction. The spacing between these non-synchronized orbits has to be the r_{sat} due to the fact that they have to be able to fill the dips of the other orbit. As such, the plane spacing for this case is equal to $180 + \phi$ divided by number of planes for a polar orbit.

The drift will also have an influence on the plane spacing, as it will cause the constellation to leave a gap westwards of the first plane. Figure 3.3 shows what happens if this drift is not taken into account

with the plane spacing. In this example, 4 planes can be seen from the north pole. It shows that there is a drift away from westward position of the first plane, which cause a large gap to appear here.

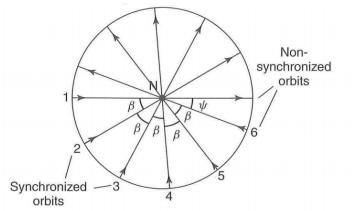

Figure 3.2: Walker star constellation with six polar orbits [7].

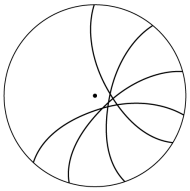

Figure 3.3: Orbits with small drift as seen from the north pole.

Since the drift angle for half an orbit is already known and explained in Section 3.1.1, this means that the plane spacing has to increase to $180 + \phi + (dL1 + \delta_{J2})/2$ divided by the total number of planes.

Now that all the plane and satellite spacings and phase differences are known, the total constellation can now be found. The coverage can then be calculated by plotting the amount of users randomly over the earth and then to check for every user whether a satellite is in view. A user will have a 1 if a satellite is in view and a 0 if not, which is further explained in Section 3.4 This is calculated using the slant range, which calculation can be seen in Equation 3.15.

$$\rho_r = R_E \frac{\sin(\phi)}{\sin(\frac{\pi}{2} - \epsilon - \phi)} \tag{3.15}$$

The slant range ρ_r is the maximum range a user can be to still have contact to the satellite, as can be seen in Figure 3.1. Therefore, if the absolute distance between the user and satellite is smaller than the maximum allowed slant range, the user will be in range of the satellite. This is done for all the users with all the satellites at any time. By using this, the amount of users that are in contact with a satellite at a given time can be found.

A plot is also made to show the amount of users that have contact with a satellite, and thus the coverage, over time. This is also used to determine the percentage of users that are connected, which can be linked to the requirements of 90% coverage from the requirement Table 1.1. Another use is that the maximum time that a user is not in contact with a satellite can be determined which can be linked to the requirement of a maximum time of no coverage of 15 minutes. An example of this plot can be seen in Figure 3.7. In this figure, the average connectivity can be found over time. For instance, a value of 0.93 coverage means that 93% of the users have a connection with a satellite.

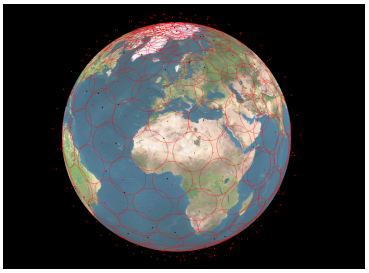

Figure 3.4: Constellation still image where the red dot and circle are the satellite and its coverage circle.

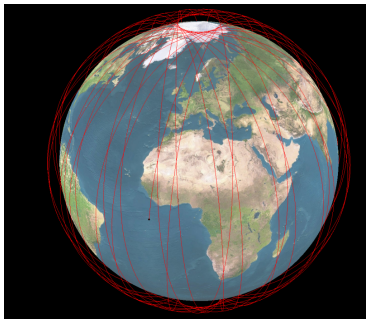

Figure 3.5: Drift after 25 orbits of a sattelite at an altitude of 550 km with an inclination of 82°.

3.4 Orbit Propagation and Coverage Software

The theory discussed in the Sections 3.1, 3.2 and 3.3 leads to a software package in Matlab. The ICD can be found in Appendix A.1. How the theory is exactly used to create the software can be found below.

First, the system calculates the orbit propagation of the planes by using the theory explained in Section 3.1. The orbit will be propagated for the amount of orbits selected, as seen in Figure 3.5. The satellites will then be evenly spaced on the first orbit, where the satellite and plane spacing is explained in Section 3.3. For these given satellites, the footprint can be plotted as explained in Section 3.2. This whole constellation can be plotted over time along the orbit lines.

Now that the satellites are plotted with there designated footprint, The users can be randomly distributed over the Earth. For each user, over time it will be checked whether or not the satellites are in view. From this it can be found for a certain user at each time slot, whether a connection is possible if a satellite is in view. This is then use to make the average over time, an example of which can be seen in Figure 3.7.

3.5 Verification and Validation

The orbital characteristics and the footprint, as well as the verification and validation for this part, were already calculated in the Mid-term Report [6]. This means that most of the simulation has already be verified and only the only thing checked is the users were included in the model and the ability to connect to a satellite Therefore, the verification and validation are done for the coverage value.

This is done by plotting 4 satellites in 3 planes and counting the amount of satellites a single user can see. Also, it checks whether these values correspond to the values obtained from the example graph seen in Figure 3.7. This is done by counting all the black dots(users) that are in the coverage circles of the satellites. The graphical (plotted coverage and users on sphere) and numerical (output value average coverage) results of the initial state of the simulation were compared and determined to be the same. This means this part of the simulation is also verified and thus the total simulation is verified.

To validated this simulation, the Iridium constellation can be used, due to the similar use and constellation type. In figure 3.6, the iridium constellation is simulated.

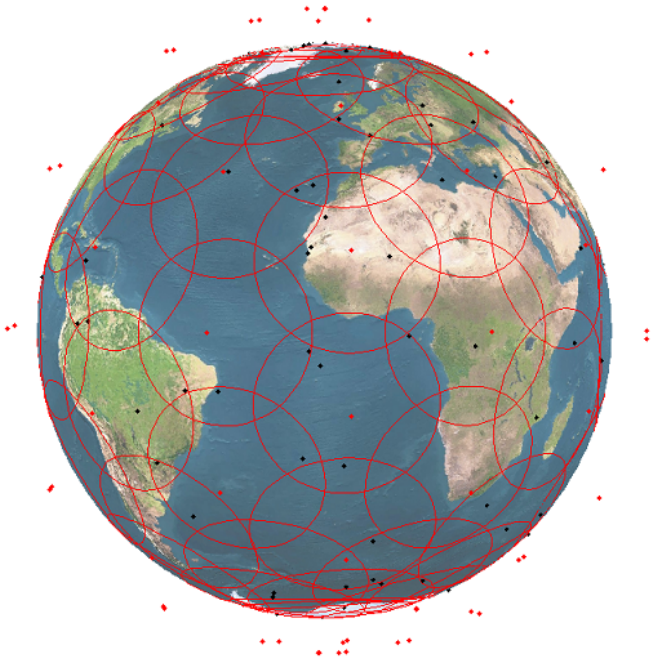

Figure 3.6: Iridium constellation still image with the coverage of each satellite (red dot) shown as red circles.

Using the simulation, it is found that the average coverages is 99%. Iridium on the other hand, has a coverage of 100%. The 1% difference is due to the fact that the precise plane spacing, satellite spacing

and phase difference between the different planes are unknown and have to be guessed. Another reason for this is because the assumptions made of the orbit characteristics can create difference in drift which in term then create a difference in coverage over time.

Due to this small difference, the simulation can be considered validated. In practice, the rate of success of Iridium will be lower due problems such as atmospheric conditions. However, these problems are not included in the coverage model. As such, the connection is assumed to be successful if the spacecraft is in view to the ground user according to conditions discussed in Section 3.2, and thus a 100% coverage for Iridium is used for validation.

3.6 Orbit and Constellation design

The altitude of 550 km was chosen from the Mid-term Report [6]. From the simulation previously explained, the orbital and coverage characteristics can be determined, in order to reach the coverage requirements, as found in Chapter 1. This can be seen in table 3.1, while the coverage is shown in Figure 3.7. A still image at time = 0 of the final constellation can also be seen in Figure 3.4.

Table 3.1: Orbital and Constellation characteristics.

Height [km]	550
No of Planes [-]	19
No of satellites (per plane) [-]	11
Inclination [°]	82
Orbital Period [min]	95.5
Elevation angle [°]	20
Circular Velocity [km/s]	7.58
Drift per orbit [°]	23.9
Plane spacing [°]	11.8
Satellite spacing [°]	33
Coverage radius [km]	1124.8
Coverage [%]	94
Maximum non connection time [min]	13

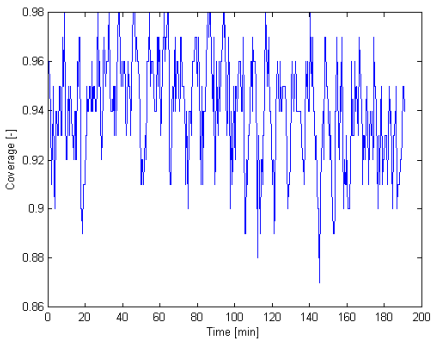

Figure 3.7: Coverage plot of final design.

In Table 3.1 it can be seen that this constellation meets the requirements for both the 90% coverage and maximum time there is no connection time of 15 minutes. The Coverage is 94% due to the fact that

the pointing accuracy was not taken into account in this simulation which has a negative effect on the coverage.

Chapter 4

Communication

The main function of the satellite is providing communication. This chapter will go into detail on the design of the communication systems. These include the link budget, antenna design, communication hardware block diagrams, weight and power estimations, and the detailed deployment mechanism and antenna design.

4.1 Communications Architecture

Creating a satellite communication system is a complicated task. This section will give an overview of the architecture of the systems and how the users will send and receive data.

There are two types of satellite communication architectures: The *bent pipe* architecture and the *regenerative* architecture. In the *bent pipe* architecture, the signal from the user terminal is returned to another terminal that is in line of sight of the satellite. There is no processing of the signal, but it could involve changing the carrier frequency. This makes the system simple but less flexible and requires a ground station always in sight of the satellite. As the constellation of satellites is at a very low altitude the *bent pipe architecture* would require at least 219 ground stations to ensure global coverage, making it unfeasible. The *regenerative* architecture on the other hand makes use of on-board data processing such that the signal can be more efficiently routed to its destination. This means there is no need to have a ground station in sight at all times. Combined with the use of an Inter Satellite Link (ISL), it allows satellites to relay data to other satellites in the constellation. The main advantage is that it requires less ground stations than the *bent pipe* method. However, the addition of the cross link antennas and on-board routing adds extra complexity to the payload hardware and software, and the ADCS. Due to current developments in electronics performance and size, it was decided that the *regenerative* architecture is feasible and that it is better than the *bent pipe* architecture. A brief overview of the communication diagram can be seen below in Figure 4.1.

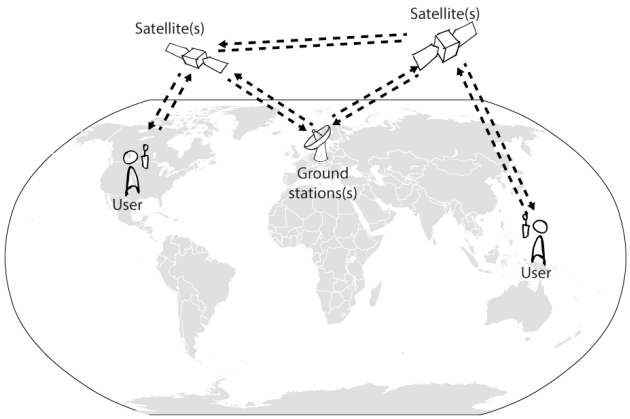

Figure 4.1: Overview of Communications Architecture.

4.2 Frequency Use

The correct frequency selection is of paramount importance for the communications system. In general, higher frequencies need more power for communication, as the free space loss is proportional to the inverse of the wavelength. On the other hand, higher frequencies also allow for higher data rates. As such the trade-off between frequency and power needs to be made carefully. There are three links where the frequency needs to be chosen, as can be seen in Figure 4.1. The frequency choice cannot be made solely based on the satellite requirements, since it also has to comply with the ITU regulation. The ITU is an agency of the United Nations (UN), which concerns itself with information and communication systems [8]. As such to avoid interference caused by many sources using the same frequencies, it has the power to license out specific frequencies to certain users. This way, if the frequencies are licenced by a certain company they cannot be used for anything else. An application to get access to a frequency is a very expensive and labour intensive, and getting the license for a frequency can take several years. As this project concerns itself with communication satellites, a frequency will need to be applied for at the ITU, however it is beyond the scope of this project to apply for a frequency allocation. For more information regarding the financial and budget can be found in section 14. To give an idea of the complexity, an overview of the frequency allocation for region 1 can be seen in Figure 4.2 (note that the ITU covers 3 such regions).

The regulation has been consulted to confirm that the frequencies used for communications are indeed allocated for satellite communications.

A low frequency is possible to utilize to serve the ground user, because a large area will be radiated and the data rate requirement Top Level Requirement 5 is not too restricting. The decision to with a frequency of 2.2GHz which falls in the S-Band, was based on the fact that it can provide sufficient data rate for the communications. It is a frequency that is widely used for satellite to ground communications. Furthermore there are 0.2GHz set aside for mobile communications [8].

The ground station link will have a similar coverage area as the ground user antenna. However, it is possible for the ground antenna to be larger and effectively does not have a power or dimension constraint. Furthermore, one ground station will have to upload more data than one satellite will have to communicate to the ground. Data which needs to be communicated to other satellites though ground links will be included. As such the only solution is to use a higher frequency of 12GHz in the Ku-band. Communicating in this frequency bands uses more power but the difference in power will be made up with higher gains of the ground station antennas.

For the ISL a high data rate needs to be used. a frequency, which is not suitable for communication to the earth due to atmospheric excessive attenuation will be chosen. This has the advantage of shielding the ISL from interference with the ground sources. Furthermore, as the location of the satellites is known exactly, high gain antennas can be used to keep the communication power down. The decision was made to go with a frequency of 30GHz which is in the Ka-band for the inter satellite links.

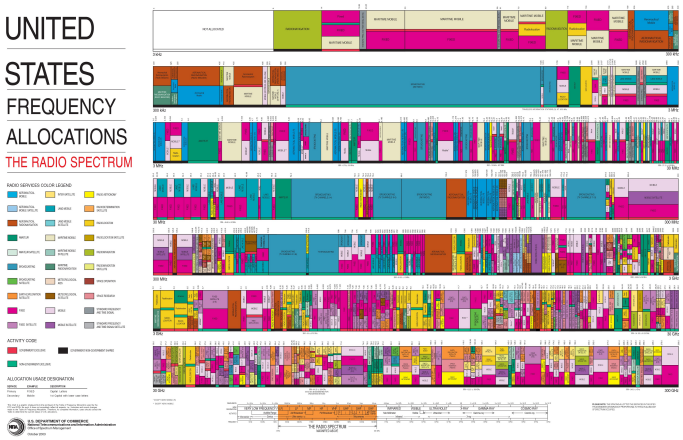

Figure 4.2: ITU frequency allocation table for Region 1 in 2003.[8]

4.3 Multiple Access Schemes

To make sure that more than one user can access the satellite at once it is necessary to have a multiple access scheme. The following possibilities are considered:

- **Space-Division Multiple Access (SDMA):** The simplest method, where every user is divided by a dedicated position in space which is for example covered by one dedicated antenna. This however requires the satellite to have multiple antennas or one pointable antenna.
- **Frequency-Division Multiple Access (FDMA):** Every user has an own dedicated carrier frequency on which he communicates with the satellite. However frequency bandwidth is a scarce resource as such it is best to use as little as possible (it also needs to be approved by the ITU).
- **Time-Division Multiple Access (TDMA):** Every user has an own dedicated time slot, while all users use the same frequency and same space, however for the user to achieve a certain data rate it is necessary to increase the data rate of the satellite as the user only has a limited time to to load the data.

It is also possible to combine different multiple access schemes to exploit their advantages more efficiently. This was done in this design. The schemes used are SDMA, FDMA and TDMA. SDMA is used by dividing the coverage area in seven cells, each covered by an own antenna. Every antenna transmits and receives at seven subcarrier frequencies which adds FDMA. Every frequency has five time slots, with one slot assigned to one user for the TDMA. However, the cells are not covered at the same time: The system cycles periodically through the antennas so that only one cell is radiated at once. This adds another layer of TDMA. So the total number of users that a satellite can serve is: $7\,\text{cells} \times 7\,\text{frequencies per cell} \times 5\,\text{time slots per frequency} = 245\,\text{user slots}$. The ground station link and ISL only use TDMA but with a higher data rate. Figure 4.3 contains a diagram that visualizes the FDMA and TDMA schemes that are used. The frequencies are designated from I to VII, the antennas or cells are designated time frames from A to G and the time slots are numbered from 1 to 5. Therefore, there are 35 time slots in one frequency carrier and 245 time slots in total. The spacing of the seven frequencies is determined with the bandwidth B calculated by the Shannon-Hartley Theorem:

$$C = B \times log_2(1 + \frac{S}{N}) \tag{4.1}$$

where C is the capacity of the frequency channel in bits/s and $\frac{S}{N}$ is the signal-to-noise ratio. It can be calculated by multiplying the energy per bit over noise ratio $\frac{E_b}{N_0}$ (Equation 4.2) with the bit rate R. The Doppler shift Δf (Equation 5.1 in Section 5.1) is added twice to the bandwidth B to get the minimum spacing of the channels so that there is no interference with each other.

The reasoning for the number of antennas and time slots is given in the following sections.

4.4 Decibels: dB, dBm and dBi

In communications theory it is customary to use logarithmic notation as it simplifies the repeated multiplications of factors in logarithmic notation to simpler repeated additions. Analogous subtraction in logarithms equates to division. The notation used is the decibels (dB), decibels represent ten times a ratio to a reference level or value ($10log\left(\frac{x}{x_{ref}}\right)$). This reference value is critical to interpreting the number. It is customary to use this reference relative to 1 Watt (W). For the purpose of this report the notation dB is used to refer to dBW or decibel relative to one Watt. It is also possible to calculate the power relative to a miliwatt (mW), this would then yield dBm, which is a shortening of the full nomenclature of dBmW. Antenna gains however are not given in power but rather are the ratio between the antenna and an isotropic antenna. An isotropic radiates energy in every direction so dBi is simply the measure of how well an antenna can radiate energy in a certain direction.

4.5 Link Budget

The link budget is a necessary part to of any communication systems. At its simplest level it is a collection of losses and gains to the transmitted signal, from which the power above the noise floor can

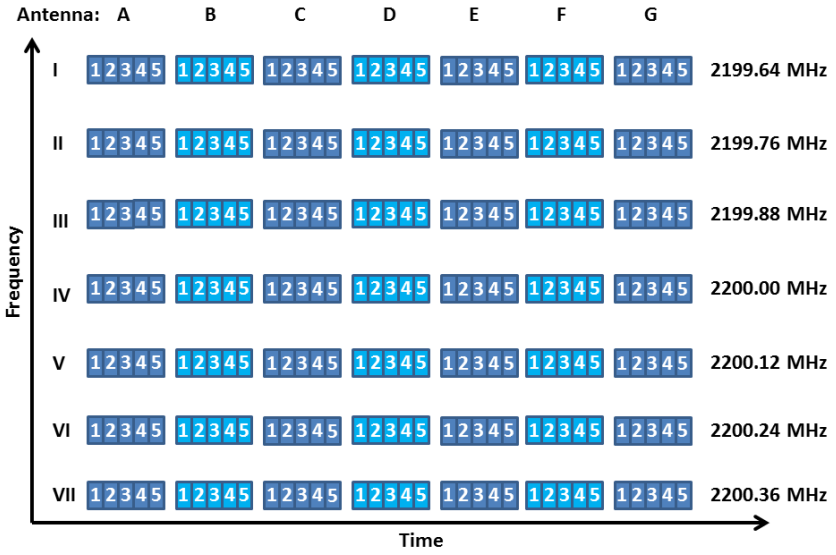

Figure 4.3: Diagram showing the FDMA and TDMA schemes used.

be determined. As the communication is digital, it is important to determine signal to noise ratio per bit, or E_b/N_0. Furthermore, the link budget can be used as a tool to get a first order estimate of the communication array power.

In communications it is usual to express gains and losses in decibels Watts. This is done to make the total calculation simpler.

The governing equation for the energy per bit, $\frac{E_b}{N_0}$, can be seen below, from literature [3].

$$\frac{E_b}{N_0} = EIRP - L_s - L_a - L_{pt} + \frac{G}{T} + 228.6 - R_b. \tag{4.2}$$

This can be found to be where EIRP is the Equivalent Isotropically Radiated Power, which is a combination of the transmission power of the satellite, the line loss of the satellite and the gain of the transmitting antenna. L_s is the free space loss, L_a is the atmospheric loss, L_{pt} is the pointing loss, $\frac{G}{T}$ is the receiver antenna gain relative to the ambient noise level and R is the bitrate of the communication. The constant number 228.6 is the the logarithmic value of all the constants for each term summed up. In the following sections, each of the these variables will be worked out further. The Effective Isotropic Radiation Pattern (EIRP) is determined using the following equation.

$$EIRP = T_x + L_l + G_t \tag{4.3}$$

The Transmission power T_x is derived from the power budget. This power does not take into account the efficiency of the antenna and is purely a measure of the radiated power.
The line loss, L_l is estimated from literature to be 3dB. This also includes amplifier back off where, each amplifier is run at less power to increase efficiency.
The gain of any antenna G_t represents the directionality of the the radiating element with respect to an isotropic antenna (which radiates in every direction). The gain of the transmitting antenna can first be estimated by the following by taking it as a fraction of a solid angle. A solid angle of $41,253$ degree^2 corresponds to a full sphere, which is akin to an isotropic antenna. As such we can write the directivity as (in dBi)

$$D_t = 10log_{10}(41,253/A_\theta) \tag{4.4}$$

This can be rewritten as

$$D_t = 46.15 - 10log_{10}(A_\theta) \tag{4.5}$$

This equation however only gives the directivity. To obtain the gain it is necessary to multiply by the antenna aperture efficiency. This aperture efficiency will be discussed further in Section 4.10.2. This

solid angle requirement will also be determined later as there is a requirement which is derived from Section 3.3 and the altitude of the satellite.

The free space loss L_s is established in literature to be [9]:

$$L_s = \left(\frac{4\pi h}{\lambda}\right)^2 \tag{4.6}$$

where h is the distance from the satellite and λ is the wavelength of the transmitting radio signal. This equation is derived from the fact that the signal will be spread over a certain volume as it is sent out over a distance, the larger the distance the larger the loss. This can be written in logarithmic form as seen in Equation 4.7.

$$L_s = 20log_{10}(\frac{4\pi}{c})(+20log_{10}(h) + 20log_{10}(f) \tag{4.7}$$

Here the first part are only constant and can be written as seen in Equation 4.8

$$L_s = 92.45 + 20log_{10}(h) + 20log_{10}(f) \tag{4.8}$$

From this we can see that higher the frequency we choose the higher the free space loss, loss which then has to be compensated by a larger the communication power. Therefore the ISL at 30GHz will experience the largest free space loss for a given distance. As the satellite is at a lower altitude and has a relatively large minimum view angle the slant angle distance of 1294km (the maximum distance from the satellite) is extremely large compared to nominal height of 500km, which increases the free space loss by about 10 dB. However, the amount of users at this distance is affected by the distribution of the users accessing the satellite. An assumption was made that the users are uniformly distributed through out the globe as such the link budget was calculated for all the users on the edge of the footprint, which is the worst case, and averaged with the best case scenario, where all the users are directly under the satellite. By averaging these two extreme scenarios it has the effect of ensuring that the users are uniformly distributed.

The pointing loss is established as a fraction of the total beam width, which was found in literature[3].

$$L_\theta = -12\left(\frac{\epsilon_\theta}{\theta}\right) \tag{4.9}$$

θ is the beam width and ϵ_θ is the pointing loss, which will be derived from the ADCS in Chapter 9,

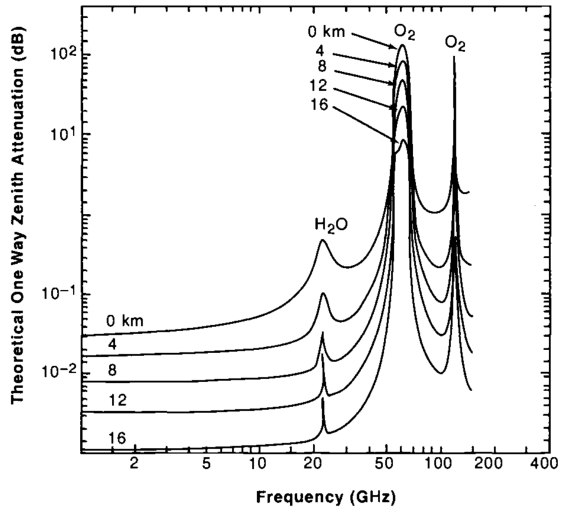

Figure 4.4: Signal attenuation due to atmospheric absorption [10].

The atmospheric loss is a function of the frequency used since the atmosphere does not absorb all frequencies evenly, as shown in Figure 4.4. ISL antennas do not have any atmospheric losses as they do

not pass through the atmosphere as such the loss are 0dB. From the figure above the loss is assumed to be 3dB for the 2.2GHz ground to user link and 7dB for the higher frequency 12GHz Ka-band Satellite to ground station link.

The gain of the receiving antenna is 0dB for the ground user as which follows from requirement 7 (Table 1.1) stating that the user has an omnidirectional antenna. This is to account for the fact that it is not known what the orientation of the phone is. For the ground station and the ISL the gain will be exactly calculated in Section 4.10.2. However for initial estimation Equation 4.10 will be used.

$$G_r = \eta_{r_{ap}} \left(\pi D_r \frac{f}{c} \right)^2 \tag{4.10}$$

Where $\eta_{r_{ap}}$ is the aperture efficiency of the receiving antenna, D_r, f is the frequency of the communication and c is the speed of light.

The system noise is simply calculated in decibels using [3]

$$N = -228.6 + T_s$$

Using this we can calculate the $\frac{G}{T}$ using

$$\frac{G}{T} = G_r - N$$

The bit rate depends on the exact coding scheme used, the amount of users simultaneously connected to the satellite and the service they bandwidth they use. The multiple access method is explored in Section 4.3.

The total amount of users is estimated in the Market analysis (see Chapter 17, Section 17.3) to be 1,000,000 users. However not all these users will be accessing the system at the same time, so the assumption is made that the maximum of 5% of the user base (50,000) will be active at one time. This assumption is based on the Iridium systems maximum capacity is 5% of the designed user base[11].

It is a top level requirement that each of the users needs should a data rate of at least 10kbps, however, on average not every user will be using the full 10kbps all the time, furthermore, the requirement for the messaging is only 1 kbpm, which equates to about 0.01667 kbps.

An assumption is made regarding the amount of traffic going through the satellite, that 80% of the users will be using text messaging at one time, while the rest will use phone or Internet. This can be assumpted due to the fact that this system will be mainly used by users in a deserted location that need to transmit a message instead of using the Internet extensively. Therefore the system only needs to provide an average speed of 2 kbps per user.

However due to the space and time division to achieve this data rate it is necessary to increase the data rate by the amount of time slots required. In this case as we have 7 antenna which are cycled through and each frequency has 5 time slots therefore the data rate needs to increase by a factor of 35, giving the final data rate that the satellite has to provide as 70kbps per frequency channel.

$$\text{Bandwidth}_{\text{total}} = \frac{\#\text{Users} \cdot 2\text{kbps}}{\rho \cdot \#\text{Satellites} \cdot \#\text{Channels}}$$

Where ρ is the code rate, the modulation scheme that will be used will be used will be QPSK with a code rate of 9/10 as other coding schemes only allowed for lower bit rates [9]. This choice of coding rate also gives us the minimum required $\frac{E_b}{N_0}$ of 3.89 dB [9]. This gives the minimum $\frac{E_b}{N_0}$ for the link to close, however there is an additional 3 dB of link margin that is added as to ensure that the link can close and serve as a safety margin.

4.6 Design of the antenna footprint

From Chapter 3 follows the requirement of the coverage area, however it is necessary to make decision on how to this area will be irradiated. In the interest of keeping the power used down rather than using one large low gain antenna a set of narrower high gain antennas was selected. To fully cover the footprint, space division multiple access was used. When designing the antenna array it is important to look at the total coverage and determine how each antenna needs to be pointed and sized. To cover the area given, its was important to trade-off the amount of antennas, hence the complexity of the antenna array, and

the weight and power benefit by having higher gain antennas. One of the most effective ways of packing a circle (which in this case represents the total ground coverage) is by placing other circles inside of it in a hexagonal pattern. However this still leaves problem of determining the exact size of each of these footprints. This section will now determine footprint of each of the antenna beams as the gain achieved by each of the antennas. Furthermore there is a physical requirement for the antenna to fit on a face of 0.6 by 0.6 face, so any excessively large antenna design should be avoided. The exact design of each of these antennas is explored in 4.10.2. The way this gain was optimized was though a program where the central beam half power beam width was entered as a solid angle, this would then create the outer footprints in such a way that there would be 100% coverage within the circle. A detailed overview of the program will be presented in appendixA.3, however using the same method as described in 3.2, with the exception that now it is necessary to account for a certain offset. From this we can see that when selecting a central antenna with a beam width of 60 degrees and a gain of 9.5dB, the optimal design is a number of external antennas with 38.5 degrees half power beam width and a gain of 23.3dB. A plot of the footprints and output of the program is given in 4.5. I assumed to give circular footprints even though in practice the curvature of the earth and the angle offset would create ellipses, however the elliptical component would only be noticeable outside of the coverage area.

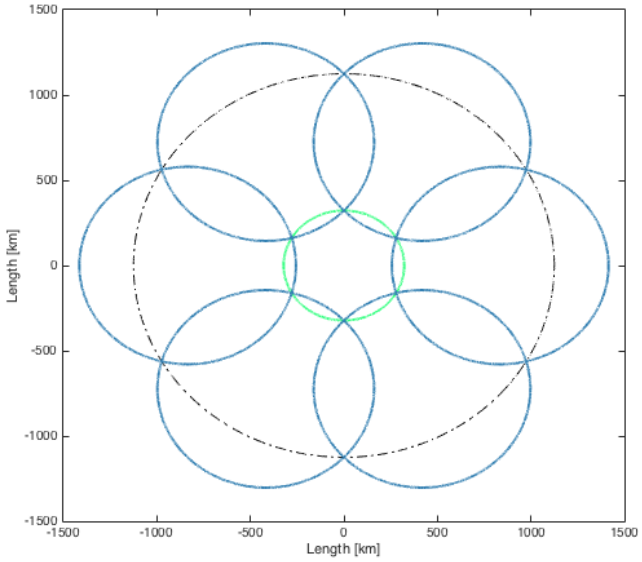

Figure 4.5: The exact coverage of the satellite plotted using the solid angles [3].

Due to the relatively high gain value required from this setup, the optimal antenna solution is to use parabolic reflectors. With the required gain the only other option would be a circular horn antenna, but it would be too long to fit in the spacecraft. A more detailed explanation will be handled in section 4.10.2.

4.7 Antenna gain footprint

In this section the exact gain pattern of each of the user antennas will be determined together with a plot with the gain plotted on the ground plane. To be able to plot the gain, it is important first to define the actual propagation of the electromagnetic waves. This is done in the following way, in polar coordinates the reference system of a sphere is defined to be where the signal originates from. From here the coordinates angles ϕ and θ can be defined. Together with this an angle of the respective electric fields of E_θ and E_ϕ can be derived. A graphical representation can be seen in the Figure 4.6 [12].

Letting E_0 (the original Electric field distribution) lie on the xy plane allows the following important definitions. When $\phi = 0$ the plane represented is the xz plane (or the plane from the satellite to the ground) and $\phi = 90$ represents the yz plane or the ground plane. It assumed that the far field radiation is modelled, so that the radiation field does not change greatly with distance.

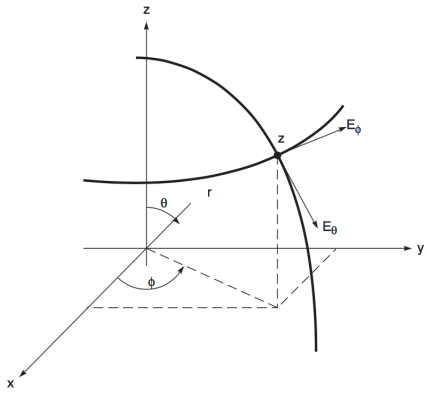

Figure 4.6: Reference frame coordinate system.

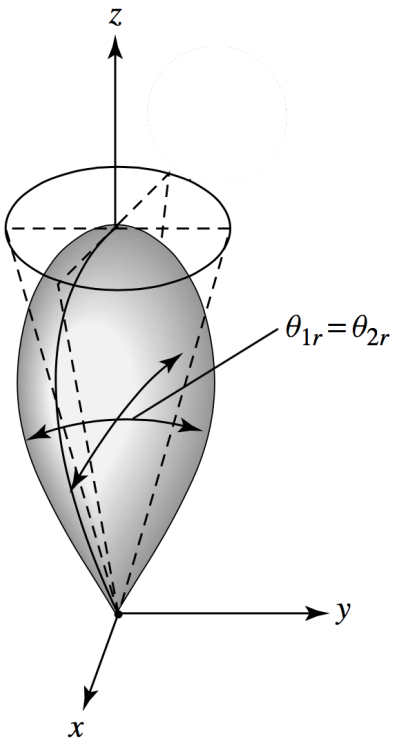

Figure 4.7: 3d representation of a rotationally symmetric beam such as that of the parabolic antenna [13].

As this the exact equations for E_θ and E_ϕ are extremely complicated, we can characterise the equation as well using the radiation intensity U we can determine the directivity of the beam on the yz plane using the the following relation.

$$D = \frac{U}{U_0} \tag{4.11}$$

Where D is the directivity of the beam and U is the radiation intensity of the antenna and U_0 is the radiation intensity of an isotropic antenna. The radiation intensity of an isotropic antenna can be given by

$$U_0 = \frac{T_x}{4\pi} \tag{4.12}$$

Recalling that the gain is simply the directivity multiplied by the aperture efficiency (see Section 4.5). Furthermore as the antenna pattern is rotationally symmetric a representation of it can be seen Figure 4.7in we can write the radiation intensity as [13].

$$U(\theta,\phi) = \begin{cases} B_0 \cos^2(\theta), & \frac{-\pi}{2} \leq \theta \leq \frac{\pi}{2}, 0 \leq \phi \leq 2\pi. \\ 0, & \text{elsewhere.} \end{cases} \tag{4.13}$$

Combining these two equations we get

$$D = \frac{4\pi B_0 \cos^2(\theta)}{T_x} \tag{4.14}$$

Where B_0 is the maximum magnetic field Realizing that $D_{max} = \frac{4\pi B_0}{T_x}$ we get the following equation for

the directivity of

$$D(\theta,\phi) = \begin{cases} D_{max}\cos^2(\theta), & \frac{-\pi}{2} \leq \theta \leq \frac{\pi}{2}, 0 \leq \phi \leq 2\pi. \\ 0, & \text{elsewhere.} \end{cases} \tag{4.15}$$

The D_max can be then determined from the equation

$$D_max = \frac{(\pi D)^2}{\lambda^2} \tag{4.16}$$

$$G(\theta,\phi) = \begin{cases} \frac{(\pi D)^2}{\lambda^2}\eta_{app}\cos^2(\theta), & \frac{-\pi}{2} \leq \theta \leq \frac{\pi}{2}, 0 \leq \phi \leq 2\pi. \\ 0, & \text{elsewhere.} \end{cases} \tag{4.17}$$

Filling in the values the following plots are achieved, which illustrate the gain pattern of the antenna on the xy plane (and since the beam is rotationally symmetric gives the whole gain from the satellite), the plot was made using the program described in Appendix A.3.

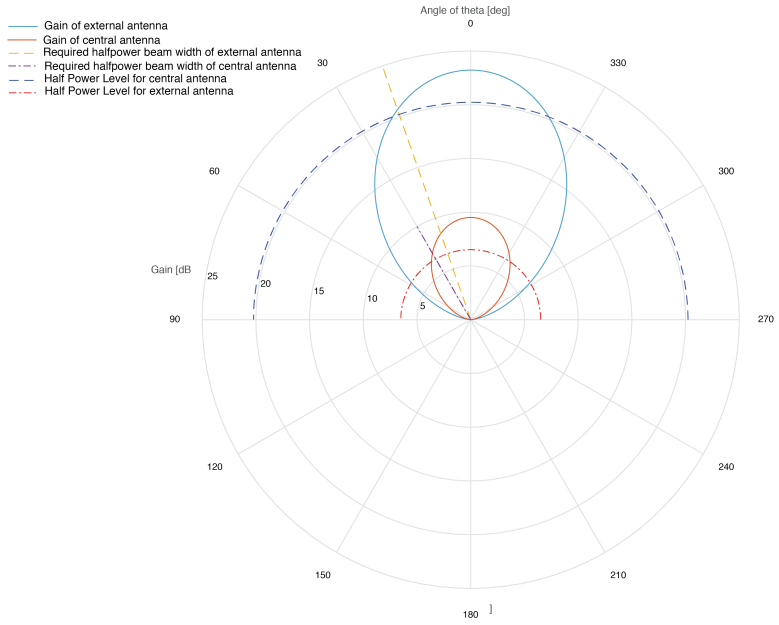

Figure 4.8: Plot of gain from the Parabolic antennas used for Satellite to User Communication.

From this plot we can see that in fact the antennas do fulfill the requirements for the half power beam width as required by astrodynamics, as the arc at -3dB (equivalent to the half power) intersects the line at a wider angle than the required angle as plotted by the straight line for both the central antenna and the external antenna.
However the problem is that the projection on the earth of this plane is not necessarily a circle and will not reflect these values as such we need to plot the projection of these gain levels on the ground. The intersection of this plot was calculated with using the method shown discussed in Section 3.2.

From the plot you see that the tilt of the antennas cause a larger area to be covered by the antenna. This would imply that the transmitting power can be lowered, as the link budget is designed in a way the link can only be established if the user is at least within the -3dB zone (relative to the center of the circle which represents the full gain of the antenna). This is however not the case as doing so would mean that full coverage would not be met within the circle required by astrodynamics (represented in Figure 4.9 by the dashed line). In the Figure 4.9 there is also the problem that the equipotential gain lines are represented as circles and not ellipses. If the gain lines would be plotted using the ellipses it would become apparent that the area on the outside of the dashed footprint would be reduced, and that the ellipses would be concentric.

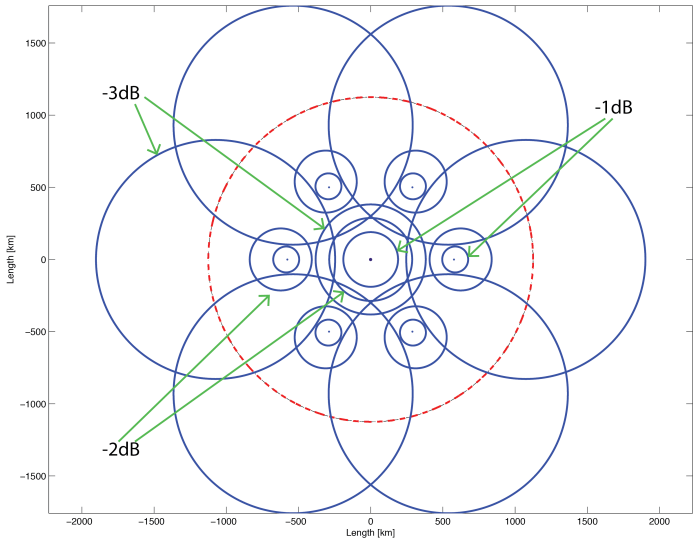

Figure 4.9: Plot of gain from the Parabolic antennas with the intersection of the line, the further out the circle form the center the lower the gain.

4.8 Ground station

The ground stations are necessary to provide the satellite with the ability to connect to the internet, although the precise design of the ground station is not part of the project. However, for the link budget an estimation was made of the configuration of the ground station. To provide the highest gain it was decided to use a 3 axis pointing directional parabolic antenna, which can point within a an accuracy of 0.5 degrees to the satellite. The antenna is parabolic as it requires a gain of 30dB, furthermore since it is transmitting at a frequency of 12GHz, the diameter of the parabolic antenna can be estimated to be 2.6m long with equation 4.19. Furthermore it can be correlated that the total data rate for each satellite down is 0.49Mbps (Section 4.3). If this is multiplied by the amount of satellites, then divided by the data rate of the satellite, the required amount of ground stations is calculated, shown in Equation 4.18.

$$\#GroundStation = Max(DataRate_satellite)\#satellites \tag{4.18}$$

From this we can see that it is necessary to operate 22 ground stations. This is on the assumption that each ground station can only service one satellite at the time. It is possible that each satellite could be serviced by more than one ground station, this would mean that less ground stations would be required.

4.9 Antenna Design

To ensure the functionality of the communication, a proper selection procedure for antenna needs to be conducted. This includes antenna type selection, initial sizing and design of the deployment mechanism; as well as plotting of the radiation pattern of the antenna. As there are three different types of communication link, three antennas need to be designed, namely the antenna for the satellite to ground communication (Satellite to user antenna), the antenna that receives requested data and TT&C (Telemetry Tracking and Command) from the ground station (Satellite to ground antenna), and finally the antenna that is in charge of the intercommunication between the satellites (ISL). When designing an antenna there are also physical constraints that need to be fulfilled, furthermore the is always a trade off to be made between the mass of the antenna and the power it uses.

4.9.1 Antenna Choice

For space missions several antennas are available, this section will provide a brief summary into the antenna choice and the motivation behind the choice.

Parabolic antennas usually have high max gain (typically around 15-65 dBi). These antennas can generate shaped beams and can also be used as a shaped array antenna. The downside of parabolic antenna is the relative small half power beam width that it has. Half power beam width is the width of the beam when the beam is 3dB less than the maximum, which is half of it. Through the concentrated beam, higher gain can be obtained. Horn antennas are simpler and directional antenna. It usually uses a metal flaring which has a shape of a horn to direct radio waves in a beam. They can provide global earth coverage at a wide range of frequency as well as a wind range of bandwidth, and they are light in terms of mass. A horn antenna usually works with frequency of 4GHz or above since they have no resonant elements. The maximum gain that the antenna is able to achieve, which is around 5-25 dBi, is generally lower than that of parabolic antenna. This is due to the fact that the parabolic antenna is able to produce a very concentrated beam.

Another option worth considering is helical antenna, it also has relatively low gain, and it has circular polarization only and it is able to provide global polarization at low frequency around 2GHz, , with a typical max gain of 5-20 dBi. The efficiency of the helix antenna drops dramatically with added turn of helix[3][7]. Due to the fact that the satellite is relatively small and flying at a relatively low orbit, the weight, cost, aerodynamics profile as well as the ease of deployment and installation are constraints. It is worth considering the possibility of using an antenna that is low profile. In this case, the microstrip antenna or patch antenna is looked into. The patch antenna are low profile, conformable on most of the surfaces and rather cheap to manufacture with the print circuit technology[13]. The downsides of the patch antenna are also very obvious. It has very low efficiency, low power, poor polarization purity and very narrow frequency range. The typical maximum gain of the patch antenna is between 6-9 dBi, which also limits the application of the patch antenna [13]. For the telemetry and telecommand application, monopole/dipole are considered to be an option[12]. Monopole antenna uses a straight rod shaped conductor, which mounts perpendicular on a ground plane, to transmit the signal. On contrary, the dipole antenna features two identical rod conductor and the signal comes from the transmitter which is located in between two halves of the antenna. The frequency used in the Telemetry and telecommand is considered to be high (Ku-Band) , thus the ground plate needed for the antenna is relatively small, which made it possible to be mounted on the satellite. In general, the size of the ground plate is in order of half of the wavelength and the antenna itself is a quarter of the wavelength[13]. The higher the frequency, the smaller the monopole antenna itself and the ground plate. If chosen as an option, antenna itself can be designed to be retractable for space saving purposes[12].

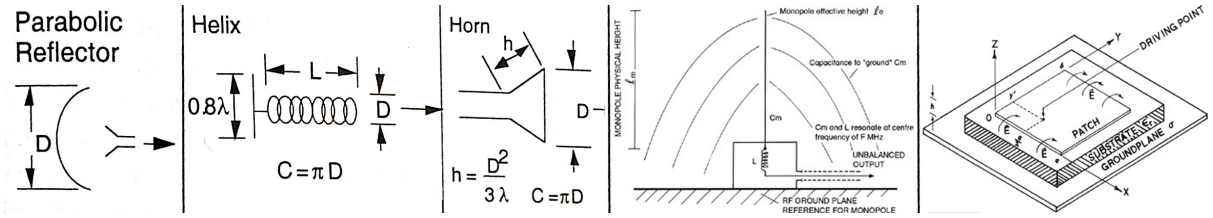

Figure 4.10: Different antenna types [3].

4.9.2 Detailed design of the parabolic antenna

In order to design a parabolic antenna with the best performance which fulfills the design requirement, different criteria are taken into account. First of all, the diameter of the reflector in relation to the half power beam width is considered (θ_{app}). Secondly, the diameter of the reflector in relation with maximum gain, with efficiency taken into account (η_{app}), is also examined. The required value of the maximum gain and the half power beam width is obtained from the link budget section. Only when the diameter fits both equations, it is then validated and can be used for further sizing. Otherwise, the link budget tool will have to be changed accordingly to minimize power usage.

$$\theta = \frac{21}{fd} \tag{4.19}$$

$$G = \epsilon \frac{4\pi}{\lambda^2} A = \eta_{app} \frac{(\pi D)^2}{\lambda^2} \tag{4.20}$$

[14]

In the second equation, D is the diameter of the antenna and A is the projection area of the parabolic reflector. From here the relationship between the gain required and the dimension of the antenna can be clearly seen. When the diameter is determined, the focal length of reflector is then found. In general,

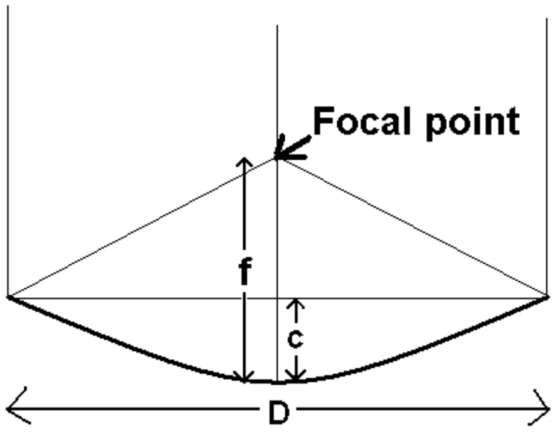

Figure 4.11: Sizing parameters of parabolic dish [15].

the focal length to the diameter ratio is between 0.25 to 0.75. When the ratio is in the lower bound of range, between 0.25 to 0.35, the feed will then be really close to the dish, thus needs to spread the beam and power at a very wide angle in order to fully illuminate the dish. This in turn makes the designing of the feed complicated. If the ratio is in the upper bound, then the feed is further away from the dish, thus the feed needs to produce a narrow and strong beam. A feed with larger diameter will be needed in this case[16]. In order to prevent the decrease in the efficiency of the reflector, overspill needs to be prevented by choosing the right focus and diameter ratio. Overspill is caused by the over design or mismatch between the feed and reflector dimension. Part of the radio wave is not being reflected, thus causing waste of power. The feed should be mounted underneath the focal point, so that there is a spread of the beam, otherwise the reflected signal is parallel to the dish. The exact distance underneath the focal point will be designed according to the design of the parabolic reflector [13].

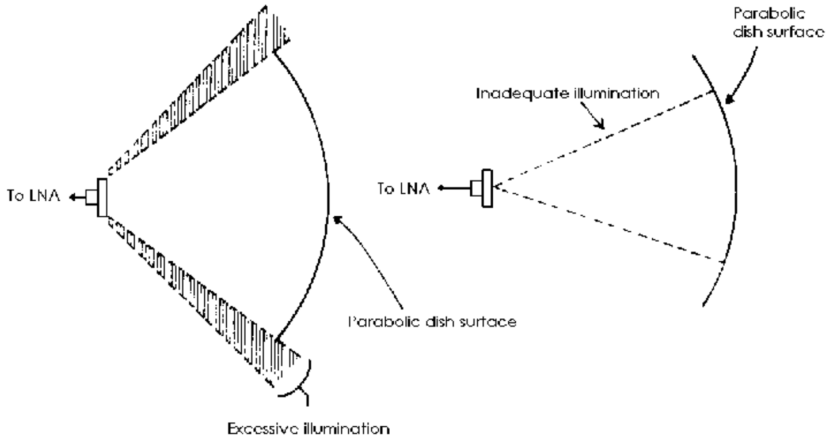

Figure 4.12: Overspill and inadequate illumination [17].

After considering all above mentioned reasons. It was decided to choose 0.45 as the ratio of focal length and diameter ratio. The depth of the parabolic dish can be calculated using the equation shown

below [16].

$$f = \frac{D \cdot D}{16 \cdot c} \tag{4.21}$$

The exact curvature of the parabolic reflector can be estimated with Equation 4.22 [18].

$$x^2 + y^2 + f^2 - 2y \cdot f = y^2 + f^2 + 2y \cdot f \tag{4.22}$$

After Simplification, the equation becomes:

$$y = \frac{x^2}{4f} \tag{4.23}$$

This equation is also used when making the sketch of the reflector with graphic software.

4.10 Parabolic Antenna Feed

Various types of the feed systems are looked at. The feed is placed at the focal point of the parabolic reflector dish and the feed is usually made of a low gain type, for example a half-wave dipole or a feed horn. Horn is decided to be used in the antenna design. It is because of by using the horn antenna, shaped beam can be generated according to the design of the parabolic reflector, thus spill over or inadequate illumination can be avoided. Spill over is when the radiation from the feed is bigger than the reflector area, thus part of the signal is not reflected. Different feed systems, which is how the radio wave is supplied to the transmitter, are also examined to order to achieve different efficiency of the parabolic reflector system . Various types of the feeding system can be axial/ front feed, off-axis/ offset feed, cassegrain and Gregorian. [13]It is done by using concave or convex reflecting lens. For small antenna, it is preferred to use the off-axis feed, because the blockage of the signal from the feed can be avoided thus to increase the efficiency. From the illustration below, it can be seen the working principle of different feed systems. [18].

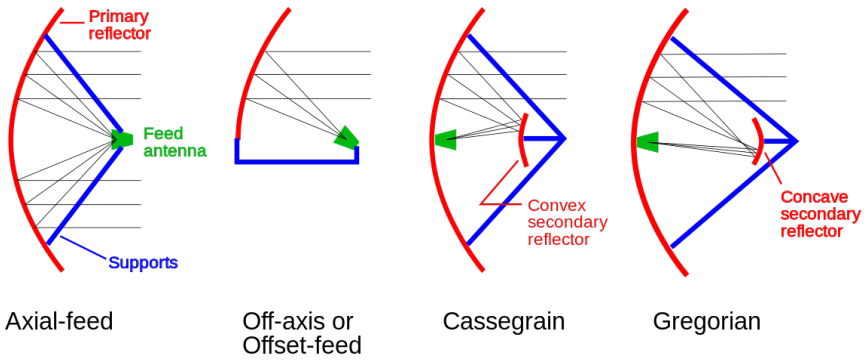

Figure 4.13: Parabolic antenna feed types [3].

There are significant downsides to these aforementioned options, that are these system suffer from the weight of the support of the feed, or reflection mirror. Thus weight and complexity are unavoidable. It is decided to use the existing self support structure for the antenna feed. This way, the weight can be minimized by eliminating the use of supporting structure and complexity of manufacturing can be avoided. With the self support structure, the aperture efficiency can be estimated to be 65 to 70 percent, which is similar to the off axial configuration, if not better.

4.10.1 Detailed design of the patch antenna

To design a patch antenna that functions as required, different design factors have to be taken into consideration. As shown in the graphs below, five different parameters are examined. They are the

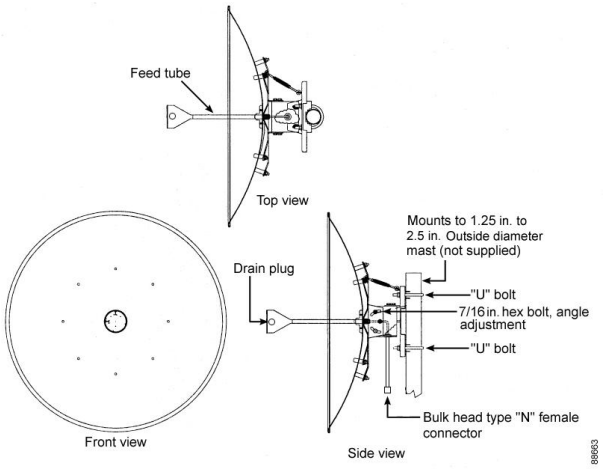

Figure 4.14: Self support structure [12].

length of the patch (L), width of the patch (W), the height of the substrate (h) in meters and the dielectric constant (epsilon) together with design of the ground plate and feeding method. These are the variables that will influence the performance of the antenna, namely the required maximum gain to insure the closing of the link budget and the half power beam width to fix the requirement from the coverage area.[12] [13]

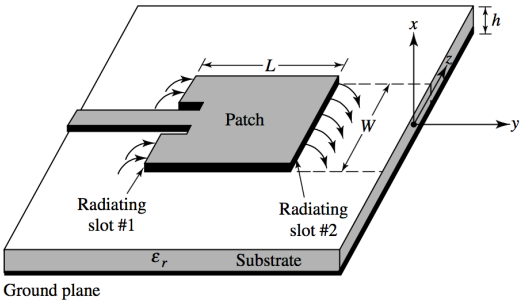

Figure 4.15: Patch antenna top view [3].

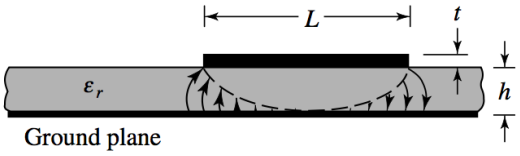

Figure 4.16: Patch antenna side view [3].

The dimension of the patch is directly related to the wavelength of the chosen signal. The longer the wavelength or the lower the frequency of the signal, the larger the antenna. The relationship is expressed as follows: $\frac{\lambda}{3} < L < \frac{\lambda}{2}$ whereas the L in this case is the length of the patch antenna. In between the patch antenna and the ground plate, there is a layer of substrate. The substrate material has direct influence on the dielectric constant. The dielectric constant describes the permittivity of signal in the material. It usually ranges between 2.2 to 12. It is preferred to choose a value in the lower bound for easier permittivity. To design a patch antenna with thick substrate with low dielectric constant, in this case better efficiency and large bandwidth can be achieved. However, sometimes a thin substrate can also be desirable due to the ability of minimize the undesired radiation and coupling. [13][12]

Feeding methods of the patch antenna also need to be considered. Four most commonly used feeding method are namely microstrip line, coaxial probe, aperture coupling and proximity coupling. By using different feeding system, bandwidth, spurious radiation and thickness of the substrate can be achieved in different values. [13]

4.10.2 Antenna choice

Since the main purpose of the mission is to provide communication to the ground, the satellite to user antenna is one of the most critical part of the communication hardware. This is because that the choice of antenna will directly affect weight of the entire communication system as well as the power consumption. More importantly the coverage area needs to be ensured. Different types of solutions are thought about, including phased array, several patch antennas which mount on a geometric angle, one patch antenna that covers the entire area, and use of several parabolic antenna as explained in the beginning of the

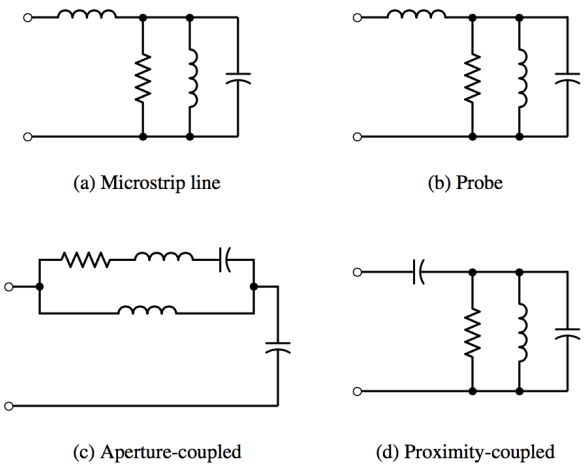

Figure 4.17: Equivalent circuits for typical feeds [3].

chapter. Phased array is first to be discarded as the high power consumption that it has. the main reason of using phased array is to be able to steer the beam electronically through constructive and destructive interference, which in turn causing the inefficient use of power and thus exceeding the power budget. Several patch antennas, which constantly broadcast signals will cause the overlapping of coverage area between each projection, as well as the relative low gain they have by nature, it will not be a good idea in terms of power consumption, considering the tight limit of the power budget. A single patch antenna was originally the choice. But during the designing, it was realized that the relative low gain it has will directly causes the higher weight in power component of the hardware. Thus it is decided to use 6 parabolic reflectors and one extra in the middle, with application of the frequency reuse. This way the power consumption can be kept low through the high gain and at the same time frequency reuse is possible to support more users. The concept is explained in the previous section.

In order to insure the inter satellite communication (ISL), a parabolic antenna is chosen. According to the requirement from the link budget tool, a gain of 25.3 dB, half power beam width of 10 degree to keep the power down and frequency of 30GHz is needed. The horn and parabolic antenna are the most power efficient antenna choices in this application since the beam produced by them are concentrated, which is required. Due to the fact that the required gain is already at the upper bound of the horn antenna gain limit and these two types of antennas have similar size. It is decided to use parabolic antenna in this case. After deployment, the antenna will be able to point forward and rotate 90 degrees to point to the side. the resason for this is to compensate the yaw of the satellite body to keep the solar panels illuminated. This way, the connection between satellite can be established at all times.

As for the satellite to ground station antenna, since the orbit of the satellite is relatively low, the required half power beam width is nearly at 120 degrees, with the gain of 8dBi at a frequency of 12GHz. In order to cover such a wide half power beam width and ensure the required gain with one antenna the only option is to design a custom patch antenna or horn antenna. The patch antenna is chosen due to its size, furthermore because the ground station has a larger antenna with high gain.

In the custom designed antenna, five layers are designed separately. At the bottom of the antenna is the ground plate. This is an important component of the antenna as the signal generated from the patch will be reflected on the ground plate then radiated. The material of the ground plate is chosen to be copper due to its high reflectivity. Afterwards, the feeding mechanism at the bottom of the antenna is looked at. It was decided not to use the common types of microstrip transmission line feeding method, due to the fact that the feed is at the same level as the antenna, thus causing the leakage of the radiation, and in turn lower the efficiency. In the custom designed antenna, it is decided to use the coaxial feeding method together with the SMA (SubMiniature version A) connector. In this way, signal loss is kept minimal since the signal is fed only alone the coaxial directed, radiation in the rest of direction is limited due to the PEC (perfect electric conductor) material. 50 ohm is used as it is the most common type of the SMA feed and it is significantly cheaper compare to the 75 ohm and 100 ohm version. Another advantage of the coaxial is the very wide range of the frequency that it is able to cope with.

On top of the feed, is the first layer of substrate. In theory, with same amount of voltage, the lower

the E (electrical field), the larger the distance between the capacitors, the easier it is for the signal to radiate. Whereas E is directly proportional to the dielectric constant ϵ_r. These relationships are expressed with equations below .

$$E = \epsilon_r \, D \tag{4.24}$$

In can be seen, in this case, in order to have a better ability to radiate the signal, the thickness of the substrate should increase while keeping the dielectric constant low. The thickness can not be increasing infinitely. Normally the ceiling of the value is quarter of the wavelength lambda. The material of the substrate directly affect the dielectric constant. It is only possible to choose the existing material available from the market. For the bottom layer of the substrate, it was decided to use the Rogers RT durold 5880, which has a substrate dielectric constant of 2.2. On the top layer of the substrate, Rogers RT durold 5870 is used.[19] It has a little worst value of dielectric constant, which is 2.3, but it fulfills the design requirement while being cheaper.

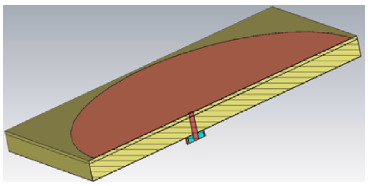

Figure 4.18: Cross-section of the antenna.

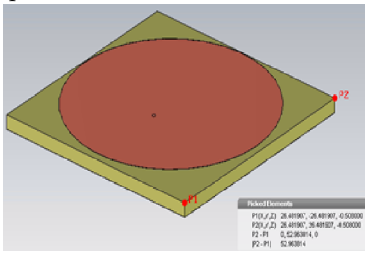

Figure 4.19: Full view of the antenna.

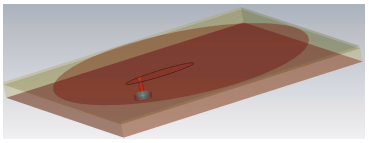

Figure 4.20: elliptical parasitic patch feed.

In between the two layers of substrates, elliptical parasitic patch feed is used. This feed functions as a transition between the patch and the feed. it provides extra matching between them. If designed properly, the reflection of the signal can be much reduced, thus more of the signal can be radiated instead of bounds back or reflected. The technique used to split the substrate layer into two and have the elliptical parasitic patch feed in the middle is called double layer PCB technology. Finally on the top of the antenna body, is the patch antenna itself. It has a shape of a circle. This is to match the required circular shape of coverage area. In order to have the feed connecting all the way from the bottom of the antenna to the patch on top, PTH (plate-through-hole) techniques is used, a hole through the antenna body while leaving the wall of the hole covered in electric conducting material. This way, the signal can be feed to the top of the antenna and then radiated.

After the antenna structure is designed, the sizing needs to be determined. The smaller the size, the wider the beam width are. On the contrary, the bigger the antenna, the higher the gain that it is able to produce. Thus it is really important to find an optimal value between them. In theory, the relationship between the frequency and the length of the antenna is given below.

$$f_c \approx \frac{c}{2L\sqrt{\epsilon_r}} \tag{4.25}$$

By trial and error method, with the help of the CST studio software, the design can be verified to see if it fits the requirement from the link budget and astrodynamics.

The final design has outer dimension 17mm by 17mm and thickness of 3.4mm. This is a rather small antenna. After the antenna is fully designed, the radiation pattern in two dimension and three dimension are plotted to show that it fits the requirement. The normalized radiation pattern of the patch is given with the equation shown below.

$$E_\theta = \frac{\sin\left(\frac{KW\sin\theta\sin\phi}{2}\right)}{(} \frac{KW\sin\theta\sin\phi}{2}) \cos\left(\frac{KL}{2}\sin\theta\cos\phi\right)\cos\phi \tag{4.26}$$

$$E_\phi = -\frac{\sin\left(\frac{KW\sin\theta\sin\phi}{2}\right)}{\frac{KW\sin\theta\sin\phi}{2}} \cos\left(\frac{KL}{2}\sin\theta\cos\phi\right)\cos\theta\sin\phi \tag{4.27}$$

After the normalized radiation pattern is known, the magnitude of the field can be found using the equation below.

$$f(\theta, \phi) = \sqrt{E_\theta^2 + E_\phi^2} \tag{4.28}$$

Using the help of the CST studio software, the detailed design specific radiation pattern can be generated. From these graphs, it can be seen whether the design fit the requirement.

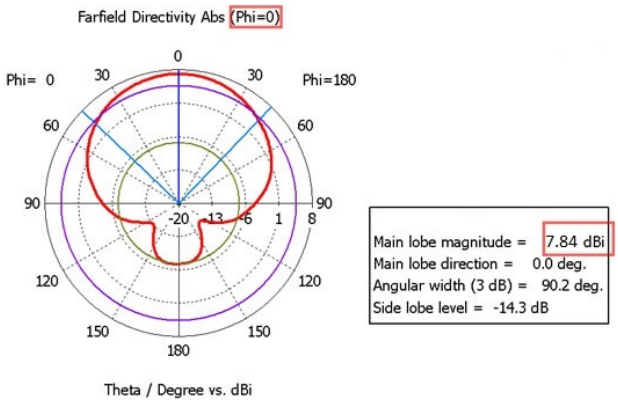

Figure 4.21: Radiation pattern of the designed antenna in 2D.

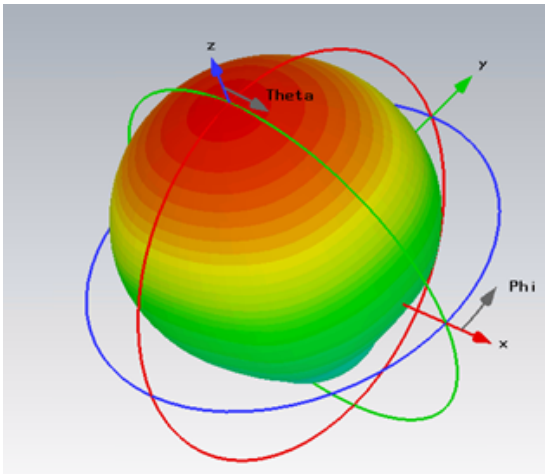

Figure 4.22: Radiation pattern in 3D.

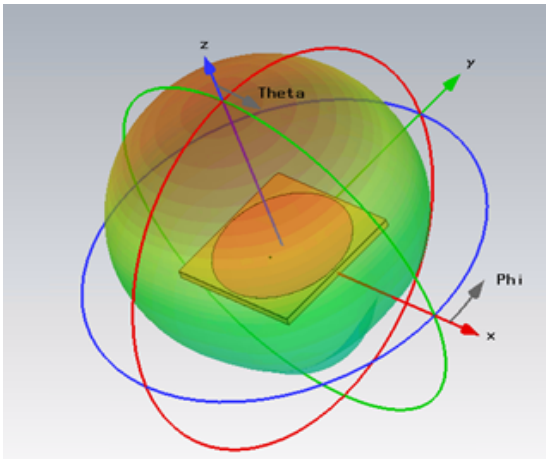

Figure 4.23: Radiation Pattern in 3D with view of antenna.

As it can be seen from the radiation plot, with current design the half power beamwidth is 113 degree instead of the 120 degrees required. A gain is also a bit lower than required. In order to further improve the performance, so that it meets the requirement, a physical modification is needed. The patch antenna will be installed on a slightly bent surface of approximately 2-3 degrees, with slightly bigger size to compensate for the bend. This way, the desired coverage and gain requirement will be met.

In the graph below, it can be seen that the return loss of the design is very low. The max value is -23dB, which indicates that only 1 percent of the signal is reflected and the rest of 99 percent of signal is radiated. Thus the design is proven to be good. And the bandwidth of the antenna can also be seen from the graph.

4.10.3 Antenna Deployment Mechanism

After the antenna is designed, the deployment mechanism is designed accordingly. For the satellite to ground antenna, 35 degrees of inclination is required between the surface and the central antenna is designed to match the required coverage area from the previous chapter. The parabolic dishes are stacked on top of each other during launching to save space,as shown in the figure below. The feed is designed to be telescopically retractable, so that prior to deployment, they would be retracted to make

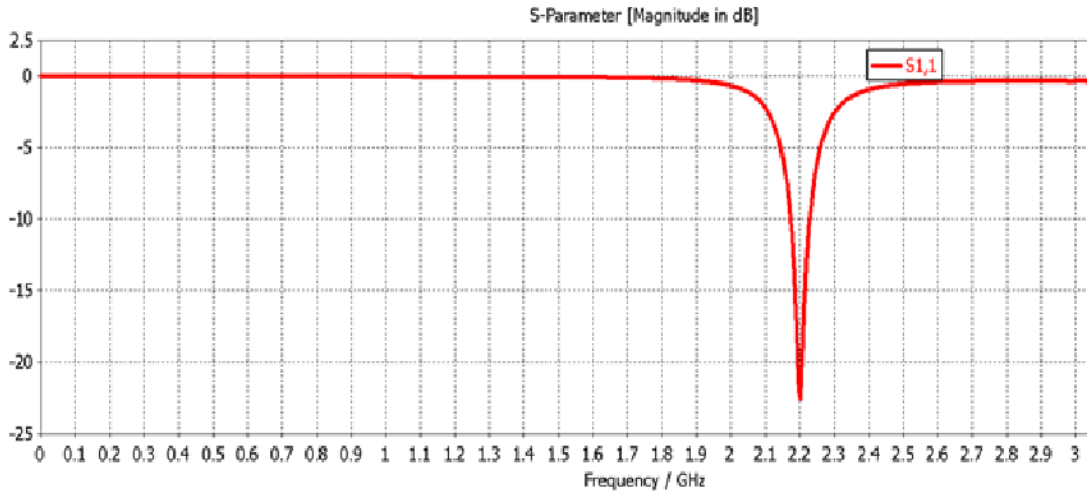

Figure 4.24: Return loss of the patch antenna and frequency.

sure that the reflectors can stack. The deployment can take place in two shifts of triangular shape. It is done this way to avoid contact between the adjacent dishes. The deployment process can be seen in the graphs below.

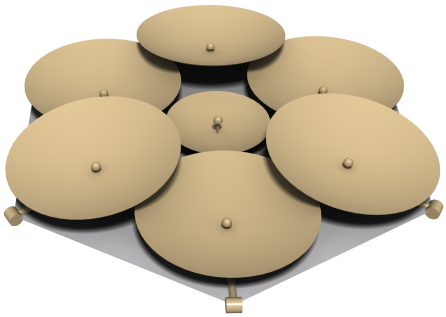

Figure 4.25: Satellite to users antenna deployment.

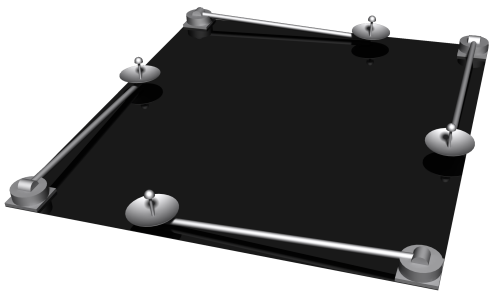

Figure 4.26: ISL antenna deployment.

For the inter satellite antenna, due to the presence of solar panels, the deployment design will have to take that into account. Before the deployment, the four ISL antennas are folded down on the top panel of the satellite in a counterclockwise fashion. It can be seen in the Figure 4.26. Once deployed, they will have pitch of 25 degrees of down to accommodate different satellite flight altitude. The 25 degrees of clearance is required to avoid the solar panels and the antenna is required. This is due to the 5 degrees for the half power beam width of the ISL antenna and 20 degrees as the antenna needs to be pointing to a satellite in the adjacent plane, which is given required the antennas to pitch down an angle of 20 degrees.Each antenna will be able to rotate from 0 to 90 degrees in yaw direction to track the neighbor satellite due to the small half power beam width that the antennas have. The extension clearance of the arm of the ISL antenna is chosen to be 40 cm to be able to avoid the solar panels completely under all circumstances.

The deployment of the satellite to ground station and Telemetry/telecommand antenna will be done with telescopic arm, which will extend through amount the satellite to user antennas. The length is chosen so that the cone shaped radiation beam from the parabolic reflector of the satellite to users antenna can be avoided completely. This can be seen in Figure 4.27. The stacked status of all the satellite during launching is shown in Figure 4.28.

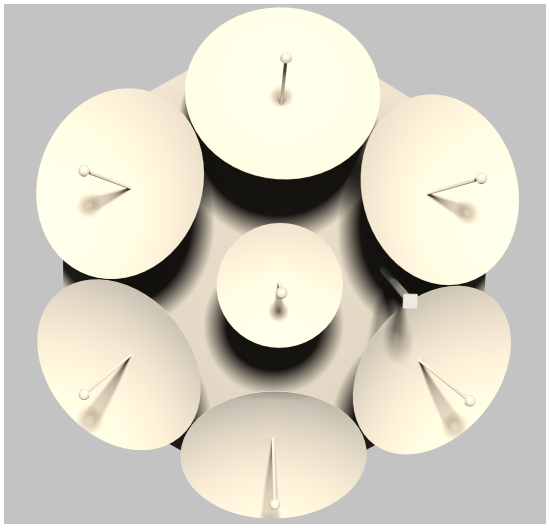

Figure 4.27: Patch antenna deployment.

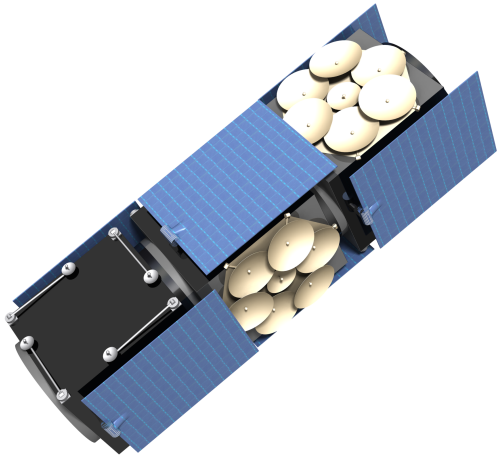

Figure 4.28: Stacked status during assembly.

4.11 Transponders

This section elaborates on the chosen architecture, its individual components and the reasoning behind the choices. The antennas are connected to transponders. A transponder is a device that receives radio signals and re-transmits them. Every transponder houses channels that are divided by different frequency bands and time slots as described in Section 4.3.

In Figure 4.29, a simplified block diagram of the communication architecture can be seen. It consists of four transponders, that are represented by the horizontal loops. The first transponder and fourth (blue) transponder are for the ISL, the second transponder (orange) is for the user link and the third transponder (green) is for the ground station and gateway link.

The **user link transponder** is connected to the seven user link antenna and is designed for S-band frequencies. As explained in Section 4.3, it has seven FDMA channels, and 7×5 TDMA slots. It operates at a nominal data rate of 490 kbps, with 2kbps per time slot. The maximum is data rate per time slot is 10kbps. Allowing users to use more time slots (maximum of five) would result in a absolute maximum data rate per user of 50kbps. The TDMA is handled within the digital processor to save size and mass in the communication hardware.

The two **ISL transponders** are connected to the four ISL antennas to connect to other satellites. They are only using TDMA and switch between the antennas to do two-way communication. They have a data rate of 700kbps each.

The **ground station transponder** directly connects to ground stations and gateways to route data between the terrestrial networks and the satellite networks and to do TT&C for satellite operation. The data rate of this transponder is 4.8Mbps. It is not always active as there is not always a ground station in sight.

4.12 Transponder Components

Every transponder has a number of standard components. Except of for the amplifiers, the references for weight and size of these components are flight-proven, reliable components taken from the Thales Alenia microwave telecom catalogue [20]:

Low Pass Filter:

The low pass filter is used to filter unwanted high frequency noise that is added to the signal during transmission.

Low Noise Amplifier:

The Low Noise Amplifier (LNA) amplifies the weak signal from the antenna to a power level where it can be easily processed by the following components.

Down Converter:

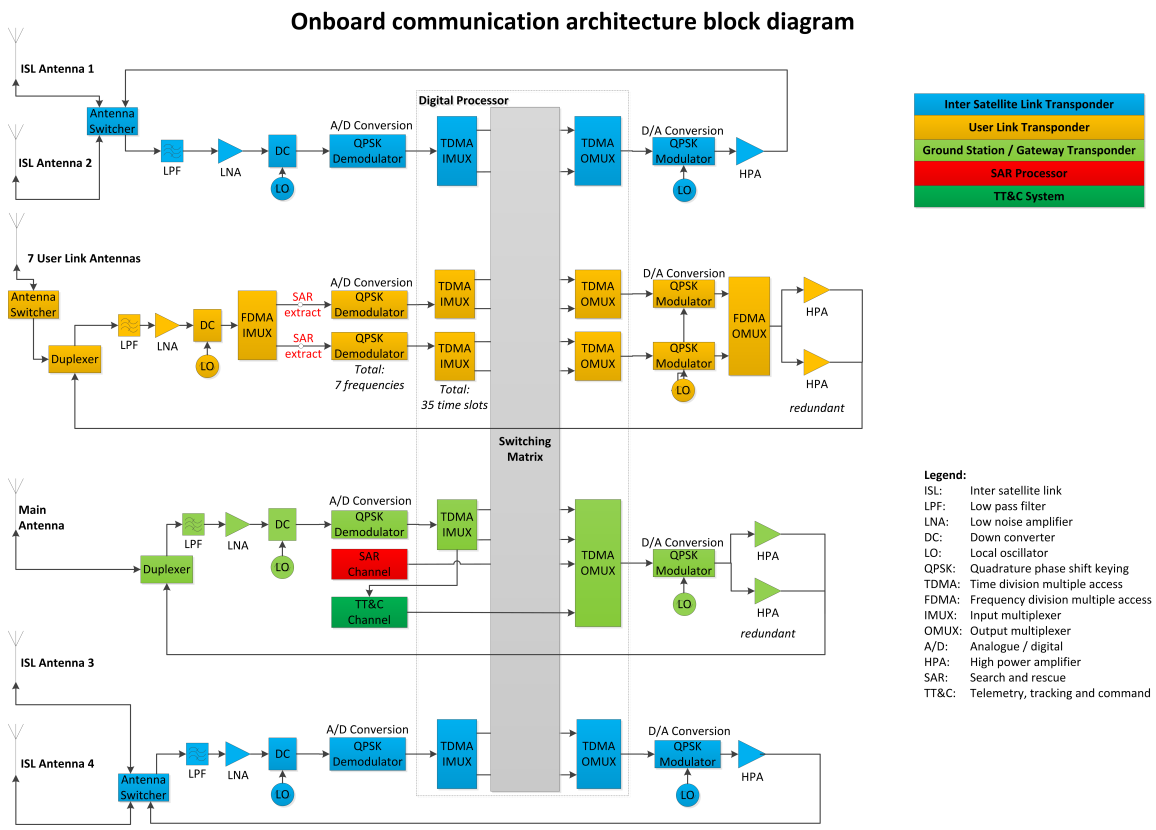

Figure 4.29: Simplified block diagram of the communication payload.

The down converter translates the signal from its carrier frequency to an Intermediate Frequency (IF) that is usually lower than the carrier frequency. Lower frequencies are easier to process and the required hardware is lighter.

Local Oscillator:

The local oscillator serves as a sine wave generator to create the IF and the subcarrier signal for the modulation.

FDMA Input and Output Multiplexer:

The Frequency-Division Multiple Access (FDMA) input multiplexer is a device that splits the main carrier into different subcarriers at different frequencies. That way it is possible to have multiple users access one satellite transponder. Each subcarrier is designated an individual hardware channel. In this case, seven subcarriers are chosen around the center frequency of 2.2Ghz (see Figure 4.3). The output multiplexer merges the the subcarriers and outputs one signal that is amplified and transmitted via the antennas.

QPSK Demodulator and Modulator:

In the Quadrature Phase Shift Keying (QPSK) modulation scheme the phase of the carrier signal is shifted after a sequence of two bits. This technique is used due to its efficient bandwidth usage (more data rate on a bandwidth, or the same data rate with less bandwidth) and its low signal-to-noise ratio requirements.

Each frequency channel has a QPSK Demodulator that demodulates the analog subcarrier signal and outputs a digital data stream. The QPSK modulator converts the digital data stream into an analog signal modulated on the subcarrier frequency.

TDMA Input and Output Multiplexer:

The Time-Division Multiple Access (TDMA) input multiplexer splits the data stream within a frequency channel into time slots, with every single one assigned to one user. The output of the TDMA input multiplexer are data packages which are processed serially. The TDMA multiplexers are not dedicated devices but are rather functions embedded in the software of the digital processor. This makes the hardware less complicated and heavy but requires more computing power from the processor.

Digital Switching Matrix:
The digital switching matrix is also a function within the processor that allows data packages to be routed from any incoming channel to any outgoing channel. The data packages contain information on their destination and are then send accordingly to a routing table that is constantly being updated by the ground station.
User Link Antenna Switcher:
The user link antenna switcher cycles through the seven user antennas. It is coupled to the digital processor so that signal routing is synchronized with the antenna selection.
ISL Antenna Switcher:
Each ISL transponder has a pair of antennas, one receiving and one transmitting antenna. To be able to send signals both ways, the ISL Antenna switcher periodically switches around receiving and transmitting antenna. An alternative to this concept is having one transponder per ISL antenna and making two-way communication possible with duplexers at each antenna. This requires more hardware but less data rate, but as the total satellite data rate is relatively low, the first concept was chosen.
Duplexer:
The duplexers are used in the user link transponder and the ground station link transponder to be able to use the antennas for both receiving and transmitting. The duplexing method used is Time-Division Duplexing (TDD), meaning that the antenna alternates between receiving and transmitting mode so that the same frequencies can be used for receiving and transmitting.
High Power Amplifier:
The high power amplifier amplifies the outgoing signal to be transmitted by the amplifier. The amplifier choice is strongly dependent on the frequency band used. However, all frequency bands have in common that they use Traveling Wave Tube (TWT) amplifiers. TWTs are vacuum tubes that contain an electron beam from which the power is taken to amplify the radio waves. They have a high gain, efficiency and a large bandwidth but for the expense of a bulky size and weight. The size scales with the wavelength, so a low frequency amplifier is larger than a high frequency amplifier. The reference hardware for size and weight estimation is taken from the L-3 Electron Technologies, Inc. (ETI) space TWTs product line [21].

- The **S-band TWTs** are used for the communication link between user devices and the satellite and are connected to the user link antenna switcher. Because the user link is critical for system functionality. There are two S-band TWTs for redundancy. Only one is active at a time and the other one serves as reserve in case the primary amplifier fails.

- The **Ku-band TWTs** are used for the communication to ground control stations and terrestrial communication gateways. As for the user link, the Ku-band TWTs are critical for system functionality and need to be redundant. Again two amplifiers are used, one active and one for spare.

- The **Ka-band TWTs** are used for the ISL. There is one amplifier per two ISL antennas, so that one antenna is receiving and the other transmitting. The antenna switcher connects the amplifier to the transmitting antenna. There are therefore two Ka-band TWTs. It was decided that no redundancy is implemented into the ISL for weight reasons. Failure of one Ka-band TWT does not cause a total loss of system functionality, it is still possible to connect to user devices, ground stations and to other satellites via the second Ka-band TWT. However, the total data rate and signal routing flexibility will be reduced.

Electronic Power Conditioner (EPC):
The electronic power conditioners supply the TWT amplifiers with the necessary power. They convert the bus voltages from the Electric Power Subsystem (EPS) into the appropriate voltages for the amplifiers. For every amplifier, there is one EPC, also for the spare amplifiers. This means that there are two inactive EPCs for redundancy.

4.13 Communication Procedures

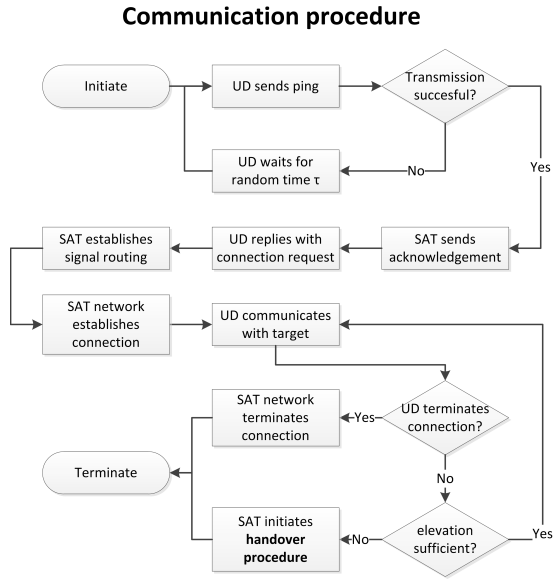

Figure 4.30: Flow diagram of the communication procedure.

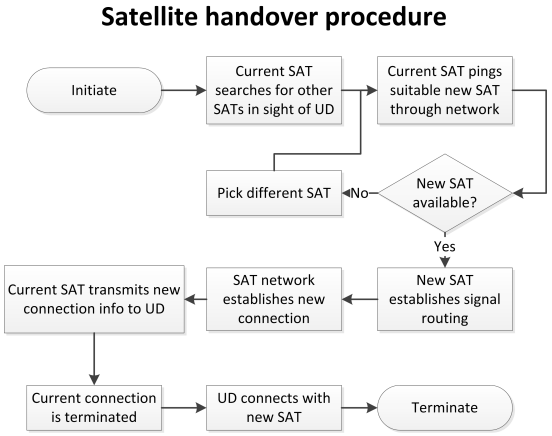

Figure 4.31: Flow diagram of the satellite handover procedure.

Figure 4.30 shows the flow diagram for the procedure of one user connecting to the satellite. The initial contact between satellite and user is made similar to the so called *aloha protocol*: The user device sends a ping signal at one of the seven frequencies. When the signal collides with another signal or no channels on the satellite are free, the user device waits for a pseudo-random time τ and selects a different frequency and retransmits the ping. When the transmission of the ping is successful, the satellite returns an acknowledgement with the time slot allocated to the user device on the same frequency. The user device now knows this and can request a connection to a target. The satellite then establishes the internal signal routing connects with either ground station or neighboring satellite. These in turn also route the signal so that the network establishes a connection between the user device and its target. The user device can now communicate with the target until one of them terminates the connection or the satellite gets out of sight. In the latter case, the satellite initiates the satellite handover procedure.

The satellite handover procedure is shown in Figure 4.31. Before the satellite gets out of sight of the user device, it searches for other satellites that are in sight of the user device. It then pings the most suitable satellite through the network, so either via the ground station or via the ISL. The new satellite can be also a neighbor with a direct ISL connection. When the new satellite is not available, the current satellite picks a different satellite and pings that one. If the satellite is available, the new satellite establishes its internal signal routing and the satellite network establishes a new connection while the old connection is still active. The current satellite transmits the new connection info (time slot and frequency) to the user device, so that the user device can immediately connect to the new satellite once the current connection is terminated. The user will therefore barely notice the handover.

Chapter 5

User Tracking Subsystem

This chapter discusses the tracking functionality of the payload. The mathematics and algorithms behind the Doppler tracking are discussed in Section 5.1. There are two kinds of applications for the tracking: The SAR application as defined in the requirements and additional scientific applications. They are described in Section 5.2 and Section 5.3, respectively.

5.1 Doppler Tracking Method

Doppler tracking makes use of the shift in observed frequency of a radio wave due to the relative motion between satellite and user. The advantage of using the Doppler shifts for SAR tracking is that the user devices are not dependent on a third party navigation service like GPS, Galileo or GLONASS. The second advantage is that only a carrier signal without any other information modulated on it is sufficient to track the device. Thirdly, the Doppler shifts are a byproduct of the communication and have to be taken into account for that anyway. Therefore, one only needs to implement the hardware that extracts, processes and transmits the frequency shifts.

To verify the SAR requirement of determining the position of a user device within 2km accuracy, a program was written which simulates a Doppler shift observation due to the relative velocity between user device and satellite and recreates the position of the user device based on the observed Doppler data. The program simulates the observed Doppler shift of a known satellite orbit and a stationary user device with Equation 5.1, where c is the speed of light, f_t is the transmitting frequency and $\frac{dr}{dt}$ is the relative velocity between satellite and user device, the so called range rate.

$$\Delta f = -\frac{f_t}{c}\frac{dr}{dt} \tag{5.1}$$

The observed Doppler shift is a function of time t, but also a function of transmitting frequency f_t and device location $\vec{x}_u$: $\Delta f = g(t, f_t, \vec{x}_u, ...)$. f_t is unknown because the user devices can have a bias in frequency generation which cannot be predicted. Hence, the deviation of the real frequency from the nominal frequency has to be estimated as well. To reduce the number of unknowns, $\vec{x}_u$ is converted into spherical coordinates with the Earth radius assumed to be constant at Re = 6371km, leaving only the latitude ϕ and longitude λ unknown. To estimate the unknown parameters f_t, ϕ and λ, a linear method is used. Equation 5.2 shows the first terms of the Taylor expansion of the function g representing the Doppler observations, where f_t, ϕ and λ are treated as variables.

$$g(f_{t0} + \Delta f_t, \phi_0 + \Delta\phi, \lambda_0 + \Delta\lambda) = g(f_{t0}, \phi_0, \lambda_0) + \frac{\partial g}{\partial f_t}\Delta f_t + \frac{\partial g}{\partial \phi}\Delta\phi + \frac{\partial g}{\partial \lambda}\Delta\lambda \tag{5.2}$$

f_{t0}, ϕ_0 and λ_0 are set to be the average of the satellite positions during the pass. They are initial guesses on the parameters and are updated with the solution of the linear system Δf_t, $\Delta\phi$ and $\Delta\lambda$. The linear system that follows from Equation 5.2 and needs to be solved is:

$$A\vec{x} = \vec{y} \tag{5.3}$$

where $\vec{x} = [\Delta f_t \quad \Delta\phi \quad \Delta\lambda]^T$ is the parameter vector and $\vec{y} = [\Delta g_1 \quad \Delta g_2 \quad ... \quad \Delta g_n]^T$ with $\Delta g = g_{obs} - g(f_{t0}, \phi_0, \lambda_0)$ is the difference between observed Doppler frequencies and estimated Doppler frequencies. The design matrix A is given by:

$$A = \begin{pmatrix} \frac{\partial g}{\partial f_t}|_1 & \frac{\partial g}{\partial \phi}|_1 & \frac{\partial g}{\partial \lambda}|_1 \\ \frac{\partial g}{\partial f_t}|_2 & \frac{\partial g}{\partial \phi}|_2 & \frac{\partial g}{\partial \lambda}|_2 \\ \vdots & \vdots & \vdots \\ \frac{\partial g}{\partial f_t}|_n & \frac{\partial g}{\partial \phi}|_n & \frac{\partial g}{\partial \lambda}|_n \end{pmatrix} \tag{5.4}$$

The partial derivatives are simply numerically determined with a central difference scheme:

$$\frac{\partial g}{\partial f_t} = \frac{g(f_{t0} + h) - g(f_{t0} - h)}{2h} \tag{5.5}$$

where h is a number larger than 0 and n is the number of observations. The linear system in Equation 5.3 can be solved with linear regression when $n > 3$. In fact, the accuracy improves when n is large.

The solution of the system is an update of the initial guess of the parameters. The updated parameters are:

$$\begin{aligned} f_{t_1} &= f_{t_0} + \Delta f_t \\ \phi_1 &= \phi_0 + \Delta\phi \\ \lambda_1 &= \lambda_0 + \Delta\lambda \end{aligned} \tag{5.6}$$

With the updated parameters, a new estimation of $\vec{x}$ can be done and the parameters are further improved. The iterations keep on going until $|\vec{x}|$ is smaller than a predefined threshold value or until the number of iterations reaches a predefined limit.

The equations are implemented in a Matlab code to simulate the on-board tracking procedure (see the Interface Control Document in Appendix A.4). The result is that two passes are sufficient to determine the position of the user within 2km radius. In fact, the standard deviation of the latitude is 2.0m and the standard deviation of the longitude is 7.9m (giving a radial accuracy of 8.1m) for two satellite passes with a maximum elevation of 33°. Therefore the SAR requirement can be fulfilled with the chosen system.

In general the tracking will become more accurate the more observation data is available, so either more passes, more satellites or a higher sampling frequency. On the other hand, less observations are needed when the number of unknowns is reduced; for example by putting a constraint on the frequency bias.

However, the analysis was made with two significant simplifying assumptions: The first one is that the users are stationary, the second one is that there is continuous contact between users and the satellite, so that the Doppler curve is complete. For a more accurate and realistic result, the motion of the users and incomplete Doppler observations have to be taken into account as well.

5.2 Search and Rescue

This section describes the design of the onboard SAR tracking subsystem. Together with the onboard communication hardware, it makes up the payload of the spacecraft. The architecture of one SAR channel in the system is shown in Figure 5.1. The SAR channel takes the frequency data extracted from each of the seven frequency channels. It has a TDMA input multiplexer that splits the sub-carrier into time slots with each allocated to one user. The signals are converted to digital domain and a Fast Fourier transformation is performed on it to extract the frequency information. A QPSK demodulator extracts the device ID. The frequency information and device ID are fed into the SAR data processor. To perform the Doppler tracking of the user device as described in the previous subsection, the SAR-data processor needs the satellite position and system time which are obtained from the ADCS system as well.

The Doppler tracking procedure is shown in Figure 5.2. The SAR system has an encryptor, a compressor and an on-board SAR memory. The data is encrypted to prevent unauthorized access of the tracking data. When the SAR data needs to be transmitted, it is channeled to the switching matrix which routes it either directly to a ground station via the Ku-band link or via the Ka-band ISL to a

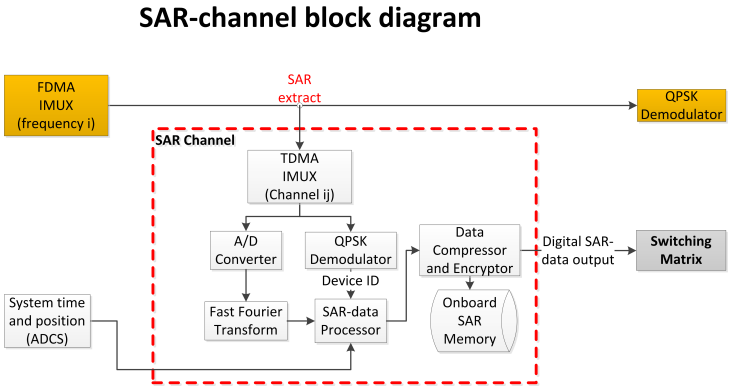

Figure 5.1: Block diagram of a channel in the SAR processor

different satellite which transmits it to a ground station. It is possible that an authorized third party, such as a governmental coast guard, wants to access SAR data of a user in distress. Figure 5.3 shows the flow diagram of a third party SAR request. First, the ground station databases are searched for recent tracking data. If that is not sufficient, the ground stations send a command to the satellite network to search for a user device. If the device ID is found on an on-board SAR memory, that data is returned, otherwise the satellite broadcasts a search command to which the user device can reply. When the user device replies, the procedure in Figure 5.2 is initiated and real-time SAR data can be returned.

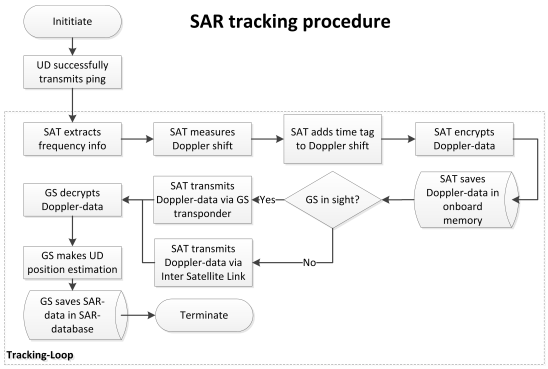

Figure 5.2: Flow diagram of the SAR tracking procedure.

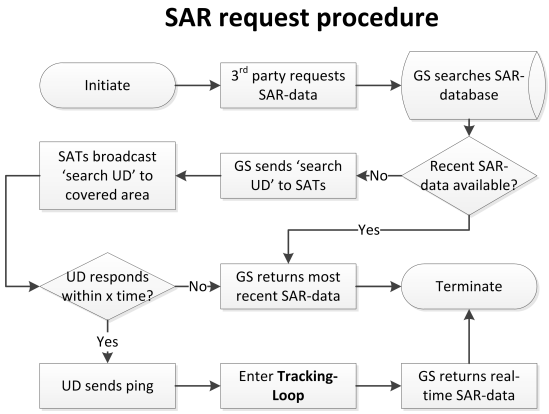

Figure 5.3: Flow diagram of a third party SAR-data request.

5.3 Additional Applications

The basis of the design is a constellation of 209 satellites orbiting the Earth in a low earth orbit and communicating with a large number of ground terminals as well as with each other using radio waves. There are several other, mainly scientific purposes that can be served with such a system. They are based on the fact that the satellites track the user terminals and the satellites in turn are being tracked by the ground stations, resulting in vast amounts of data. By letting the user devices transmit their GPS position, if available, they will serve as tracking stations, creating more data and increasing the accuracy of the orbital parameter estimation. The data that is produced this way can be used for the following scientific applications:

- Thermospheric Research: The satellites will decay due to their low altitude and atmospheric drag. Their position is constantly tracked so that the decay can be recorded. The large set of data can be used to update and refine the models of the thermosphere.
- Gravity and Magnetic Field Measurement: The orbits of the satellites are not perfect but disturbed by imperfections in the Earth's gravity field. This is caused by the non-uniform mass distribution of the Earth. Recording the disturbances can give some information about the mass distribution,

resulting in a better geological model of the Earth, where for example tectonic changes can be identified. With the magnetometers used for attitude determination (Chapter 9), the magnetic field of the Earth can be measured and its model can be refined.

The measured data could be made available for free to scientific and educational institutions, which can give the system a boost in publicity. By making the data publicly available, processing of it can be crowd-sourced and society can profit from it while reducing the cost of processing it in-house.

The applications mentioned above do not impose the need of significant additional hardware (and therefore cost) to the existing design. The processors simply have to be programmed in a way that they extract the desired information and relay it to the ground via unused bandwidth slots in the ground station links. The secondary payload therefore houses a huge potential in a scientific point of view, which is why government agencies and research institutions should be considered as partners in this venture.

Chapter 6

Telemetry, Tracking and Command

The telemetry, tracking and command subsystem is the heart of the satellite. A simplified block diagram with different command and telemetry signals for the subsystems is shown in Figure 6.1. The TT&C data from and to the ground station are transmitted via the Ku-band ground station link. The data is not routed through the switching matrix as the only destination possible is a ground station which is in sight of the satellite. It is retrieved from the TDMA input multiplexer and sent to the TDMA output multiplexer of the ground station transponder. During safe mode or during unexpected loss of antenna pointing or satellite attitude control, a monopole antenna on the opposite site of the satellite is activated to be able to still contact the satellite.
Every subsystem has its own set of commands and telemetry data for operation:
Power Subsystem: The commands for the power subsystem are a safe mode command to bring the spacecraft into safe mode, subsystem ON/OFF commands to manually control the spacecraft subsystems and solar array pointing commands to manually set the pointing direction of the solar arrays. The telemetry data transmitted by the power subsystem are battery status (charge, power output and voltage), solar array status (power and voltage output) and subsystem voltages.
Propulsion: The propulsion subsystem has only one command which is the manoeuvre command. This command simply lets the thruster fire for a certain amount of time. The telemetry of the propulsion subsystem is the tamk pressure and valve status of the thruster. The temperatures are managed by the thermal subsystem telemetry.
ADCS: The ADCS receives manoeuvre commands to realign the spacecraft in case its attitude drifted off or in case the spacecraft has to cover a certain area of interest with its antennas for example in case of a natural catastrophe. The telemetry data from the ADCS include the self determined attitude and the position from the GPS receiver to track the spacecraft and make an update of its orbital parameters.
Thermal: The thermal subsystem does not receive commands from the ground station, it only sends telemetry data about system and subsystem temperatures and status of the heater.
Communication: The communication payload receives the following commands: software updates to improve the performance of the communications processor, routing tables for the switching matrix, capacity allocation in special cases like, as mentioned above, natural disasters, subsystem diagnostics and antenna pointing commands. It can be seen that these commands, especially the software updates and routing tables can take a lot of data, which is the reason why the TT&C data is transmitted with the higher bandwidth Ku-band link together with the gateway data. The telemetry data of the communication payload are channel and amplifier status and capacity utilisation.
SAR Processor: The SAR processor receives only a 'search user device' command when an authorized third party requests to track a device. All transmissions of SAR tracking data do not go together with the other TT&C data because it has to be independent of having a ground station in sight or not. This data is routed through the switching matrix and can be transmitted via the user link or ISL transponder as well. See section 5.2 for more information about the SAR processor.

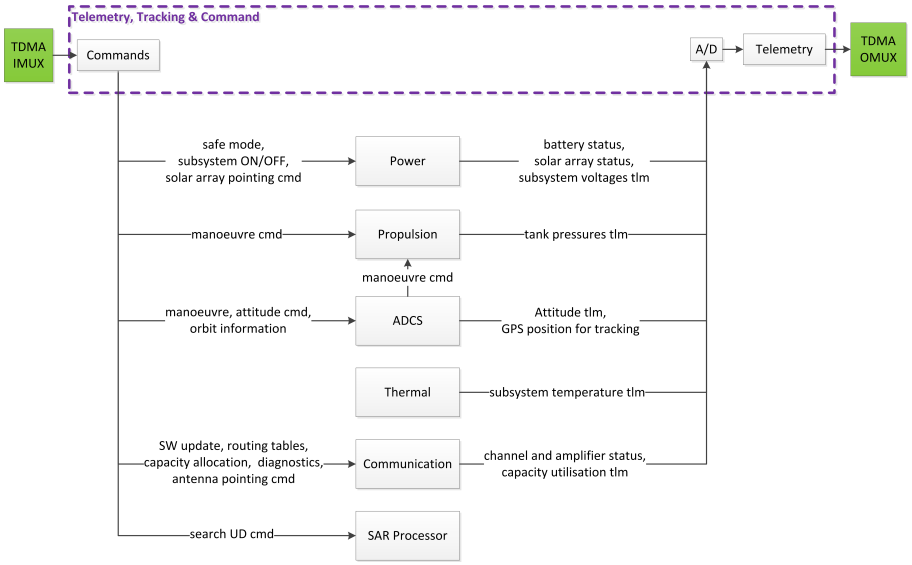

Figure 6.1: Block diagram of the TT&C data handling.

Chapter 7

Electrical Power Subsystem

In order for the spacecraft to keep orbiting throughout its lifetime and carry out its communication purpose, it needs to be powered and thus requires an electrical power subsystem (EPS). As the spacecraft passes through the daylight part of its orbital period, the EPS is responsible for getting the solar energy from the sun through the use of the solar panels. This power is distributed to the rest of the subsystems. This is the primary power source.

Furthermore, that power should also be stored in a secondary power source, which will be used during the eclipse, where the spacecraft will not be in vision of the sun and thus unable to receive solar energy. While this is the main requirement of the EPS, other requirements shall be satisfied as well by the subsystem. They are derived and shown as follows:

Req EPS 1: The EPS power delivery to the spacecraft shall be $\geq$ 102.3 W.

Req EPS 2: The EPS shall distribute the available power to the other subsystems, such as ADCS, communications, propulsion and thermal control.

Req EPS 3: The EPS shall provide switch on/off capability to the communication subsystem when the propulsion is active.

Req EPS 4: The EPS shall provide bus voltage of 12 Volts (after power loss) with margin of $\pm$ 0.1 Volts.

Req EPS 5: The EPS shall dissipate the excess power when required through the use of the power management system.

Req EPS 6: The EPS shall include a measure to prevent either under or overcharging through the use of a battery management system

Req EPS 7: The EPS shall monitor bus voltage with accuracy better than 100 mV.

Req EPS 8: The EPS shall provide the data measured by instruments to CDHS (Command Data Handling Subsystem)

7.1 Primary Power source

In order to generate enough power to satisfy Req EPS 1, the solar panel must have a large enough area to get and generate the required solar power. This area is calculated using the Equation 7.1.

$$A_{solar} = \frac{P_{tot}}{S_{in}\ \eta_{sol}\ L_d\ I_d\ \cos(\theta)} \tag{7.1}$$

The total power required is found from the power estimation of all subsystems, and the solar flux is a constant value taken to be 1366 W/m^2. The type of solar panel used for this spacecraft is chosen to be the NanoPower Solar P110-A/B type, which is a triple junction solar panel with an efficiency of 26 percent at its beginning of life and an inherent degradation of 0.77. Furthermore, it has a mass of 59 g per panel as well as the dimensions of 98.5 x 82 x 2.15 mm.

To find the inherent degradation, Equation 7.1 is used.

$$L_d = (1 - D_y)_s^L \tag{7.2}$$

The degradation for a triple junction solar cell is 0.5% per year and the satellite lifetime is known to be 10 years. This gives out a life degradation of 0.95.

Take note that the solar panel efficiency η_{sol} is only for the beginning of life, and will undoubtedly decrease near the satellite's end of life of 10 years. As the worst case need to be considered to ensure enough power through all phase of a satellite's life, the solar efficiency at the beginning need to be calculated. This is done using Equation 7.1.

$$\eta_{sol} = \eta_{BOL} L_d I_d \tag{7.3}$$

with η_{sol} being the solar efficiency at the end of life, and has the value of 19 %.

Finally, the incidence angle is something that will vary as the satellite moves along the orbital period and will depend greatly on how the panels are configured in direction of the sun. As such, several configurations are considered for this project, namely: a pointable solar array, a body mounted solar panels, a flat plate of solar panel on top of the spacecraft, and finally a deployable solar panel at an angle of 135 degrees to the nadir-pointing face (+w direction).

For a pointable solar array, a hinge mechanism will provide a rotation around the pitch axis and the ADCS will provide the yaw rotation in order to ensure that the array is always pointed directly at the sun. In this configuration, θ is the incidence angle, which is known to be 8 degrees from Chapter 3.

For a body mounted solar panel, the assumptions made is that the spacecraft is having a yaw rotation, which means that at least an average of one side will always be pointed directly to the sun. The incidence angle will then increase along the period of the daylight time, reaching its maximum at half the period.

For the flat plate configuration, it is assumed that the panels will not have any solar incidence for the first 27 degrees in the orbit. Therefore, the incidence angle will be adjusted for the 90 degrees flat angle, which will reach its maximum at half of the orbital period.

For the 4 deployable solar panels configuration, the assumptions made are that an average of two panels will be pointing the sun, while the other two panels are in the shadow. This means that the incidence angle will be adjusted for the 135 degree that the panels make with respect to the nadir-pointing face. The maximum, in that case, is reached at half of the daylight period.

Given a total power of 103.56 W, a MATLAB code is created to compute the required area of solar panels that generates the required power over the orbital period. Meanwhile, the number of panels for the obtained solar panel area is also computed. A graph comparing the power against time for each solar array configuration is made and shown in Figure 7.1.

For this graph, the y-axis is the power generated by the solar panel throughout the daylight period, with the x-axis being the incidence angle to the sun the solar panels made throughout the daylight time. As obtained in Chapter 3, the total orbital period of the 5730 seconds, with a daylight time of 3597 seconds and an eclipse period of 2133 seconds.

Furthermore, the choice of solar panels is NanoPower Solar P110-A/B, which have a dimensions of 98.0 x 82.5 x 2.15 mm and a mass of 59 g [22]. With this in mind and knowing the total required area using Equation 7.1, all the values for the four different cases are presented in Table 7.1.

Table 7.1: Solar panels area for different configurations.

Configuration	Area $[m^2]$	No of Panels
Pointable	0.8643	108
Body-mounted	4.7968	596
Flat Plate	1.3402	166
135 degree 4-panel	1.0515	260

The reason that the results for body-mounted and 4-panel configuration are much higher in comparison is because the number of panels are only counted for one side for the spacecraft. As such, they have

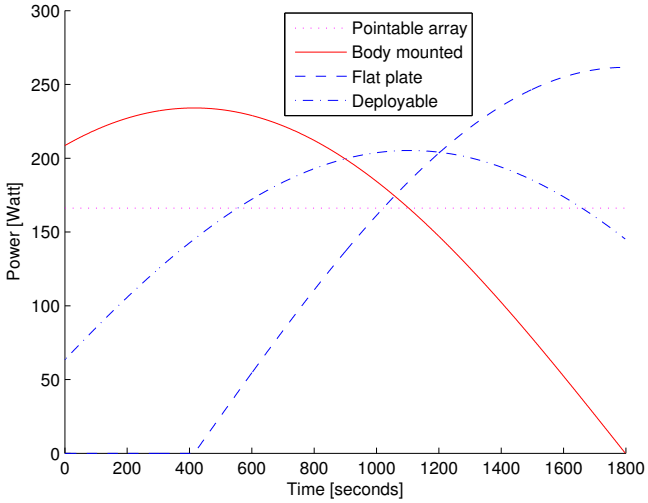

Figure 7.1: Power throughout half daytime for different solar array configuration.

to be quadrupled to ensure that the solar panel continue to generate power throughout the satellite's orbital period. Similarly, for the configuration of 4-panel at 135 degrees, the number of solar panels needs to be doubled.

Therefore, it can be seen that the pointable configuration would require the least number of panels, resulting in the least amount of mass and cost, which makes is it ideal choice. The NanoPower Solar P110-A/B has an individual mass of 59 g, so assuming a total solar panel mass of around 118 g with the structural frames attached, leads to a total solar panel mass of 12.75 kg.

With the amount and dimensions of the solar panels known, the next step is to determine how they will be deployed and operated throughout the satellite lifetime. Considering the choice of a pointable solar array, this means that the solar panel needs to be constantly rotated throughout the daytime period in order to get the incidence angle to generate maximum power. To do so, the solar panel need to be rotated around two axis, for it will have to pitch and yaw. The yaw rotation will be satisfied by the ADCS subsystem and the pitch rotation will be done by the use of an attached external motor. The choice of motor depends on the maximum torque needed, and as such the maximum torque needs to be calculated. This is calculated using Equation 7.4.

$$Tq_{sp} = I_{sp}\alpha_{sp} \tag{7.4}$$

Where Tq_{sp} is the maximum torque of the solar panel, I_{sp} is the moment of inertia of half of the solar panel, and α_{sp} is the angular acceleration of the solar panel. First, I_{sp} needs to be found using Equation 7.5

$$I_{sp} = \frac{m_{sp} l_{sp} w_{sp}}{12} + m_{sp} d^2 \tag{7.5}$$

Here, m_{sp} is half the mass of the solar panels known previously to be 12.75 kg. Furthermore, d_{sp} is the distance from center of solar panel to the motor, which would be half of the length of one side of the solar panel. Finally, the l_{sp} and w_{sp} are the length and width of one side of the solar panel and the dimensions of an individual solar panel are 98.5 x 82.5 mm. As such, plugging in all the numbers gives out the I_{sp} of 2.47 kg m^2.

The next step is to calculate α_{sp}, which can be done using the following Equation 7.6.

$$\omega_{sp} = \alpha_{sp} t_{sp} \tag{7.6}$$

To do this, the angular velocity ω needs to be obtained. This is done in Chapter 8, which gives an angular velocity of 0.07 degree/second. As such this angular velocity is integrated to obtain the required angle, calculated using Equation 7.7.

$$\theta_{sp} = 0.5\alpha_{sp}\ t_{sp}^2 + \omega_0\ t_{sp} \tag{7.7}$$

Furthermore, the are two different considerations for the required angle based on time; one will be calculated for the angle and time of the daylight period and another for the eclipse period. After plugging both variation to get the required angular acceleration α_{sp} and consequently the torque Tq_{sp}, the two are compared and the higher one is the maximum torque needed.

From the previous part, it is known that for the daylight period the angle would be 234 degrees and the time is 3597 seconds. Similarly, in the eclipse period the angle is 126 degrees and the time is 2133 seconds. Note that in order to calculate Tq_{sp}, the angle needs to be in radians. Putting all the known variables in the equations gives out a torque of 1.52×10^{-6} Nm for the daylight period, and 2.34×10^{-6} for the eclipse period. As the second one is bigger, this will be the maximum torque that needs to be supplied by the motor.

In general, there are three types of motor that is typically used, which are DC brushed motor, servo motor, and stepper motors. The DC brushed motor typically has lower lifetime which isn't suitable for this mission with 10 years lifetime, and the servo motor will not provide good enough accuracy in its revolutions. The stepper motor will be suitable for this purposes, and smaller micro stepper motors will easily fit the size requirement for a small satellite. As such, for this satellite the type of motor chosen would be the AM 1224 micro stepper motor [23]. This is because this motor have a very small design with minimal weight and size, yet still being able to provide 0.027 Nm of torque, which is much more than the solar panels require.

However, this is done considering the best case scenario and for design purposes a worst case scenario must be considered in order to ensure the necessary power is always generated. For example, as the satellite escapes the eclipse period and goes into the daylight time, it has to quickly rotate itself to get the most efficient incidence angle. In order to get a good baseline of how fast the solar panels should be able to rotate, the torque available from the ADCS is used. The reason for this is because the ADCS torque serves as the maximum limit of the torque that the motor should not exceed.

Looking at the ADCS chapter gives out a value of $5.5 \times 10^{-4} Nm$, and by using the previous formula the worst angular acceleration is found to be 0.0125 degree/second. Consequently, this means a rotation speed of 45 degree per minute, which enables it to complete a 180 degree rotation in four minutes. Considering the total period time of 95.5 minutes, this is a reasonable value to have as a maximum limit. Furthermore, as the motor can provide 0.027 Nm of torque, there's still a good safety factor to ensure the solar panel continues to be rotated for the best incidence angle even in its worst case scenario.

In addition to the motor, a gearbox or gearhead might also be attached to the motor. Since the regular motor already satisfies the maximum torque requirement, using the gearbox will decrease the torque in order to increase the shaft speed and decrease the current. The gearbox will be chosen in accordance to the small size of the micro stepper motor, which gives 22/2 Spur Gearheads to be the final choice. [24]

A CATIA illustration of this can be seen in the following figure 7.2, showing how the solar panel is connected to the satellite.

7.2 Secondary power source

While the solar panels generate power during the daylight time, they will not be able to be directed to the sun at all during the eclipse period. As such, a secondary power source is needed during this time, and this power will be supplied by batteries. These batteries will be charged by the power generated during the daylight period, and will discharge the power for the rest of the subsystems in turn during the eclipse period. An Electrical Block Diagram shows how the generated power will be distributed within the satellite and is shown in Figure 7.3.

From the diagram, the solar panels will generate enough power to power the system, as well as charging the battery to full capacity during the daylight period. This power will first go into the power management unit, which will regulate the power and distribute it appropriately, with some going to charge the batteries and the rest being used to power the other subsystems in the spacecraft. The power management unit will also be similarly used for the power generated by the battery, as the power management unit will regulate the power distributed for all the different subsystems, each with its own voltage requirements. There is some power dissipated through this process, and thus the power management unit will have its own efficiency as well. The power management unit chosen to be used is the Smallsat Power from ClydeSpace [25], and the efficiency for this is 95%.

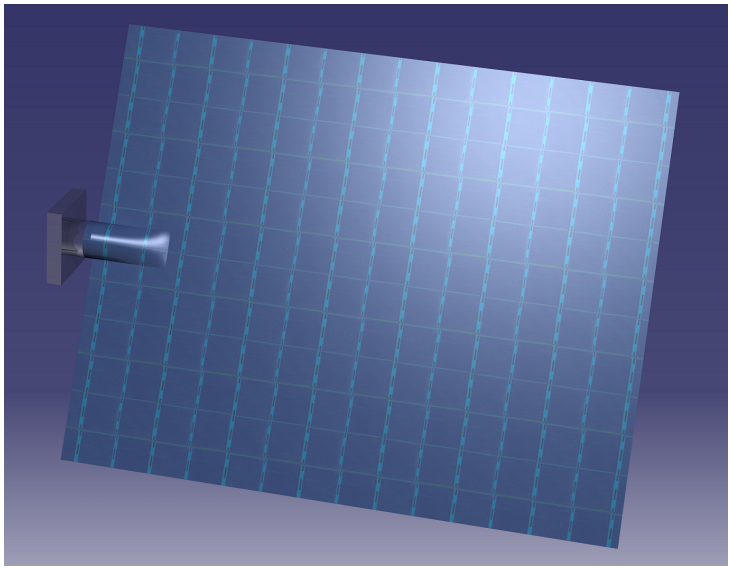

Figure 7.2: Illustration of motor and gearbox of solar panel.

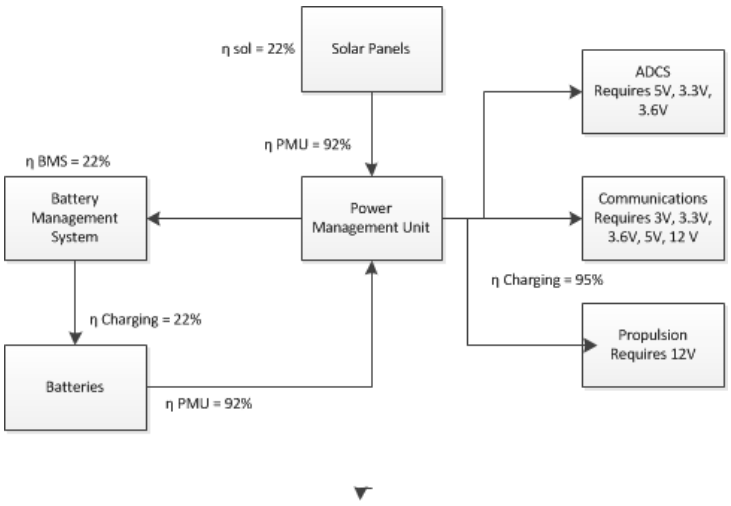

Figure 7.3: Electrical Block Diagram.

Another important part shown in the electrical block diagram is the battery management system. The purpose of this system is to manage the battery, to identify how much each battery has been charged to prevent either undercharging or overcharging the battery and distribute the charging power appropriately. The battery management unit used here is the Orion Extended Size, with an efficiency of 95%. All these efficiencies take into account the power dissipated as it goes through the different components. Calculations are made to accurately know the necessary power to charge the batteries and power the other subsystems.

Therefore, the criteria for choosing the battery is that not only does it must provide enough voltage to other components of the subsystem, it must also have enough capacity to provide enough power for the entire satellite during the eclipse period. Furthermore, enough batteries are needed to be able to last throughout the 10 years lifetime of the satellite.

The battery chosen for this is the LiFePO4 Nanophosphate, which are chosen as it's able to generate the necessary power while still having a very good lifetime compared to other batteries of its size. The batteries needs to supply about 108 W (after all the efficiencies are considered) throughout the eclipse time of 2133 seconds, which means it needs to be able to deliver 64Wh. Considering that the Nanophosphate battery has a voltage of 3.2 V and a capacity of 2.5 Ah, this leads to 8 Wh per battery, which means a total of 8 batteries is needed.

Looking at the power budget, 12 Volts are the highest required voltage for the components and as such the configuration for the 8 batteries is two sets of 4 batteries in series that will be put into parallel. Considering the 10 years total lifetime of the battery, a single set of batteries will not be enough and at least seven sets are needed. Finally, a redundancy factor needs to be considered as a safety measure for the risk management in case some of the batteries fail. A redundancy factor of 2 is chosen, which means that a total of 112 batteries need to be on board. Taking into account the battery case needed to contain 122 batteries, as well as the battery management unit, all add up to a total of 11 kg for the battery component of the power subsystem.

Chapter 8

Attitude Law for Solar Array Pointing

In order to generate sufficient power for the satellite, the solar panels need to be pointed towards the sun at all times as stated in Chapter 7. Since the solar panels are only able to pitch, the satellite will need to perform the yaw motion to maintain sun pointing solar panels. Keeping the fact in mind that the satellite needs to be nadir pointing all the time, the required yaw rate of the satellite and the required pitch rate of the solar panels have to be determined. This is done for one day during the SKY-FI mission in this chapter. A Matlab code is written which determines and plots the satellite angles relative to the ECI reference frame using a date and a choice of the orbital plane as an input. By using the plot, the maximum required yaw rate of the satellite and pitch rate of the solar panel can be determined. These values will be used to determine whether the ADCS and the motor in the solar panels are able to cope with the required turning rate. If the design is not sufficient, a bigger motor will be needed, otherwise the power generated will be lower than the estimation.

8.1 Pointing and Rotation Theory

For an illustration of the angles and the coordinate system, refer to Figure 8.1. The x, y and z axis correspond to the ECI reference frame. All rotations are positive counter clockwise in accordance with the right hand rule. A negative rotation around the z-axis β (not in the graph) corresponds to the orbital drift. The argument of perigee ω is chosen to be 0 in this case. Technically, it is irrelevant due to the orbit being circular (hence not having a perigee) but this way the mean anomaly θ is the angle between satellite and the equator along the orbital plane, which simplifies computations. The initial value of θ at the start of the simulation is also 0. The right ascension of the ascending node Ω changes throughout the day due to the orbital drift β and has an initial value according to the orbital plane chosen for examination. The orbital inclination corresponds to i. The satellite's reference system is initially aligned with the orbital reference frame defined as the u-axis being initially pointed in flight direction, the w-axis pointing towards nadir and the v-axis completing the right hand system.

The local orbit reference frame (u,v,w) will undergo a series of rotations until its u-axis coincides with the x-axis of the ECI frame, the v-axis is parallel with respect to the y-axis and the w-axis is parallel with respect to the z-axis. From there on the location of the sun relative to the earth is determined and its latitude and longitude with respect to the ECI will yield the necessary satellite yaw and solar panel pitch. Plotting this over time will result in the yaw in pitch rate over an entire day. Equation 8.1 shows the rotations performed and Equations 8.2, 8.3 and 8.4 show the rotation matrices around each satellite axis (Roll, Pitch and Yaw, respectively). Day 0 is chosen to be the 1^{st} day of spring, or vernal equinox, as the ECI frame's x-axis aligns with the x-axis of the sun's inertial reference frame on that day and all time dependent deviations will be determined from there.

$$\begin{pmatrix} u' \\ v' \\ w' \end{pmatrix} = R_v(90)R_u(\beta)R_w(i-90)R_v(\theta) \begin{pmatrix} u \\ v \\ w \end{pmatrix} \tag{8.1}$$

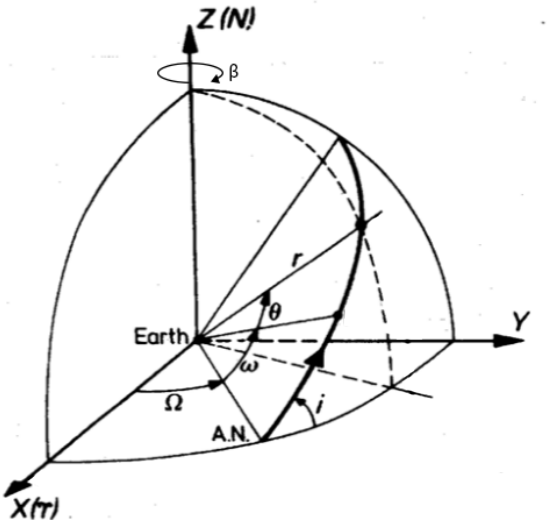

Figure 8.1: Illustration of Orbit Angles and ECI Coordingate System.

$$R_u(\gamma) = \begin{bmatrix} 1 & 0 & 0 \\ 0 & cos(\gamma) & -sin(\gamma) \\ 0 & sin(\gamma) & cos(\gamma) \end{bmatrix} \quad (8.2)$$

$$R_v(\gamma) = \begin{bmatrix} cos(\gamma) & 0 & sin(\gamma) \\ 0 & 1 & 0 \\ -sin(\gamma) & 0 & cos(\gamma) \end{bmatrix} \quad (8.3)$$

$$R_w(\gamma) = \begin{bmatrix} cos(\gamma) & -sin(\gamma) & 0 \\ sin(\gamma) & cos(\gamma) & 0 \\ 0 & 0 & 1 \end{bmatrix} \quad (8.4)$$

Note that the angle γ is in this case just place holders and has no meaning or value. After the rotation of the reference frame, the angles between the the satellite body axes at a certain time and the ECI frame axes can be determined using Equation 8.5. From these angles, pitch, roll and yaw of the satellite at a specified point in time are determined.

$$\vec{a} \cdot \vec{b} = |a||b| \cos \gamma \quad (8.5)$$

8.2 The Program

This section introduces the Matlab code developed to determine the yaw and pitch rate needed for the maximum generation of solar power. An Interface Control Document (ICD) can be found in Appendix A.10.

In order to make a plot with respect to time, a time vector is set up, which runs through the entire day in steps of one minute. The mean anomaly and the drift are computed as a function of time. The last input is the inclination, which is assumed to be constant with $i = 82°$. To get the body reference frame of the satellite to the ECI frame, several transformations need to be conducted. These transformations are visualized in Figure 8.2. Note that the satellite will not actually translate to a different position. First of all, the satellite frame is rotated θ degrees around its v-axis to get the satellite travel down its orbit to arrive at the equatorial plane. Afterwards, the reference frame is rotated around its w-axis to account for the inclination of the orbit. The exact angle is defined as $i - 90°$, in this case it is an 8° counterclockwise rotation. Now the reference frame is rotated around its u-axis by β degrees to account for the orbital drift. Angle β in this case is defined as $360 - \Omega$. Finally, to align the vehicle frame of the

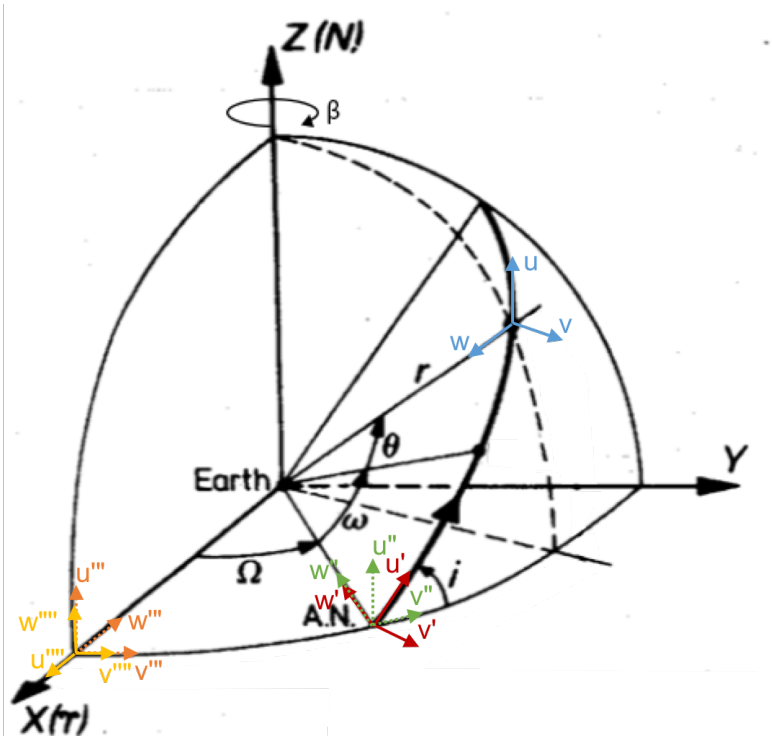

Figure 8.2: Reference frames and rotations for reference frame transformation.

satellite with the ECI frame, one last rotation is performed, causing the satellite to point exactly towards the sun on the vernal equinox. The rotation is done around the v-axis, rotating 90° clockwise. After the series of rotations, the satellite vehicle frame is aligned with the ECI, as explained in the Section 8.1.

The angle required for the yaw motion of the satellite can be found through the arc cosine of, and the angle needed for the roll motion will be the. After finding the angles with respect to time, the angular speed can be found by finding the gradient of two consecutive points on the plot. The maximum values on the graphs are the values that need to be checked against the specification of solar panel motor and the ADCS systems.

8.3 Verification and Validation

Validation is done on the code to ensure that it delivers the correct results. The simulated day is the vernal equinox, at which, by definition, the ECI frame's x-axis is aligned with the sun's inertial frame x-axis. The vernal equinox is one of 2 days of the year on which the sun is exactly above the equator, which is usually not the case due to the inclination of the earth. Assuming an orbital inclination of 90 degrees implies not orbital drift. Setting the (now constant) right ascension of the ascending node equal to 90° should result in both a constant yaw and a constant pitch angle with a linearly changing roll angle due to the nadir pointing requirement. The results of the simulation can be examined in Figure 8.3.

It can be seen that both yaw and pitch are fixed at a constant angle whereas the angle between the ECI z-axis and the w-axis of the satellite varies between 0 and π. Due to the w-axis pointing towards nadir, the offset angle is equal to π when the satellite is exactly above the earth which means the w-axis is pointing in the opposite direction of z-axis.

The maximum roll rates are then computed by simply taking the difference of 2 consecutive angles from the previous plot and dividing it by the time step. For the simple case used to validate this code, yaw and pitch velocity should be 0 and the roll velocity should be $\frac{360}{95.5 \cdot 60} \frac{^\circ}{s}$. This is the case with the computed roll velocity being equal to $0.062827 \frac{^\circ}{s}$.

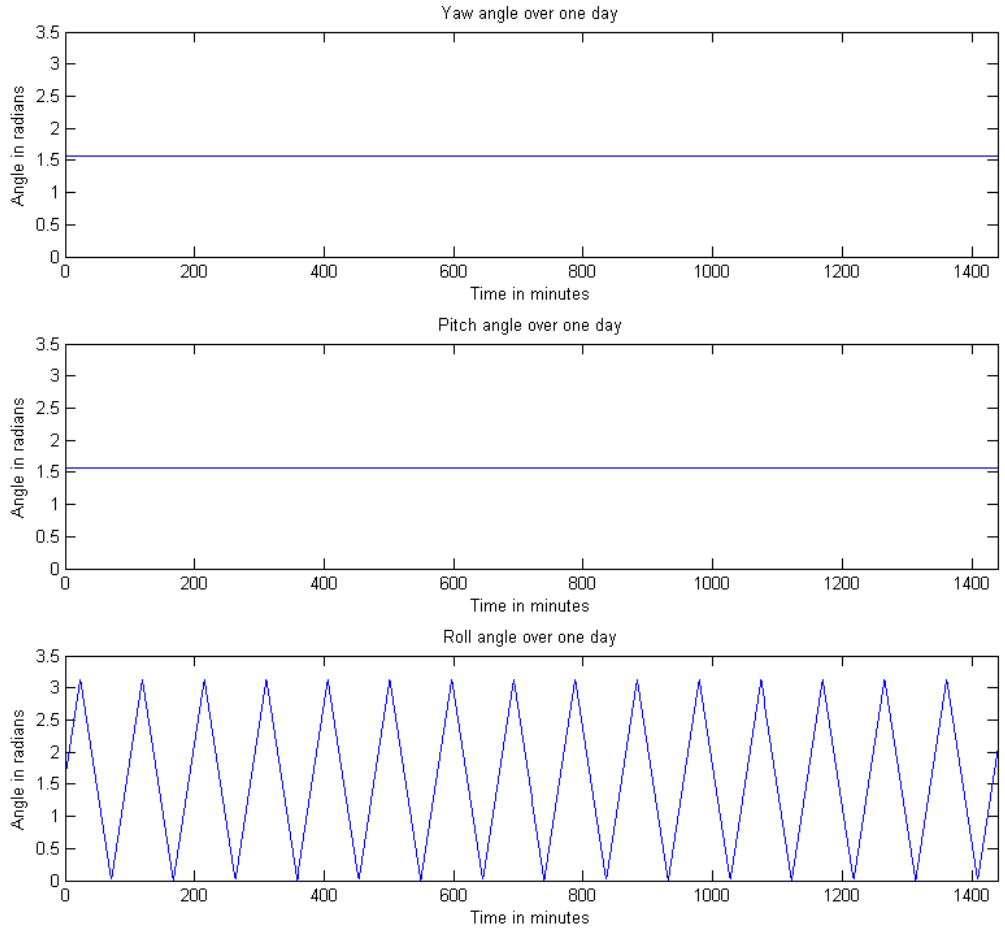

Figure 8.3: Satellite angles relative to the ECI frame over one hypothetical mission day.

8.4 Results

Using an initial satellite position on the ECI frame x-axis at the day of the vernal equinox results in Figure 8.4. These are roll, pitch and yaw of the satellite, required to maintain both earth pointing antennas and sun pointing solar panels. Yaw and pitch need to be accounted for by the ADCS while the pitch needs to be countered by the solar panel rotation.

Computing the maximum pitch velocity for the solar panels yielded $0.063415\frac{^\circ}{s}$. Relevant for the ADCS are the maximum yaw rate, which is $0.0041304\frac{^\circ}{s}$ and the maximum roll rate, which is $0.062216\frac{^\circ}{s}$. It can be concluded that the ADCS system and motors on the solar panels can cope with these rates.

8.5 Eclipse

Knowing that the satellite will spend a significant amount of time in the shadow of the earth, energy can be saved by discontinuing the solar panel pitching motion upon entering the eclipse and reorienting the panels shortly before orbiting into the sunlight again. Using the lowest possible altitude and an orbital plane aligned with the sun vector results in the largest possible eclipse time for the satellite. It will be in the shade for 37.78% of the orbit, which corresponds to 36.08 minutes or 136.01°. Figure 8.5 illustrates how this was derived. In the figure, R is the earth radius (thick circle) and R+h is the orbit radius (thin circle). From Chapter 7, information regarding the solar panel pitch motors can be obtained. They can perform a 180° rotation in 4 minutes, which means a 136.01° rotation in 3 minutes. Hence the solar panel

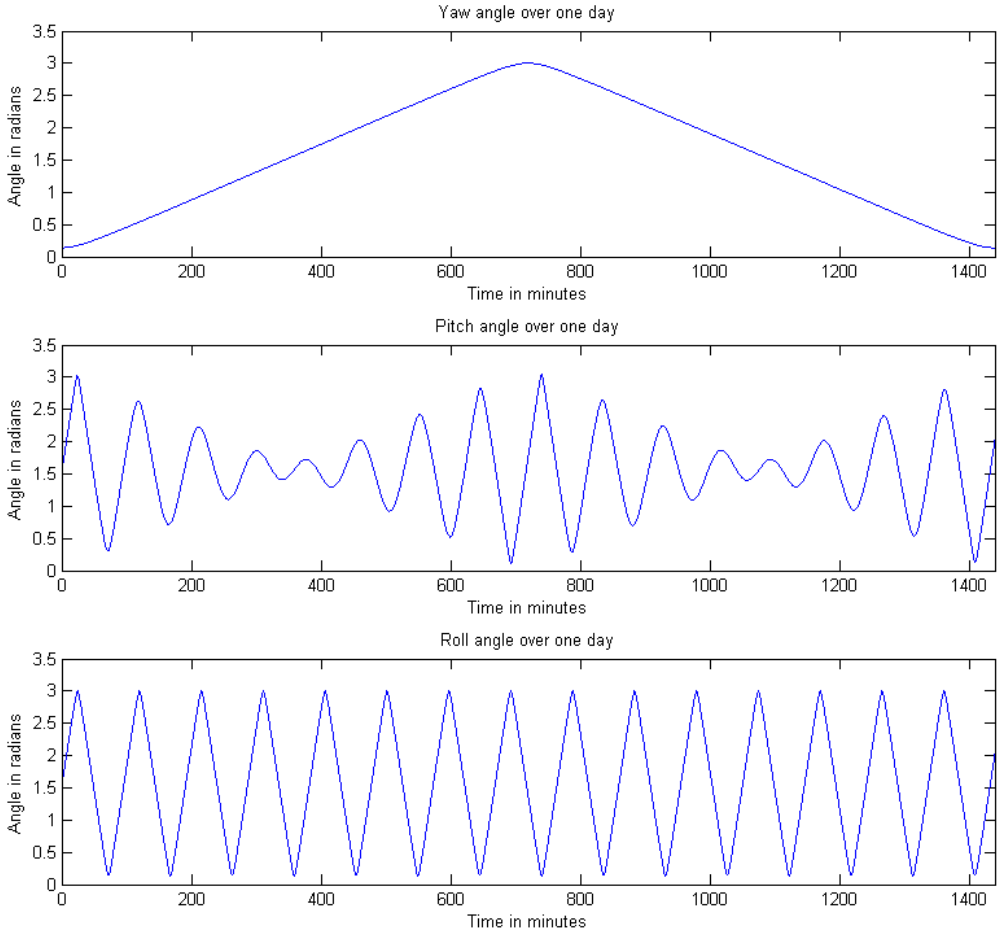

Figure 8.4: Satellite angles relative to the ECI frame over one actual mission day.

motors can be turned off for 33 minutes during eclipse to save power and can then be turned back on again 3 minutes before exiting the shaded orbit section. This is the worst case scenario, different orbits will have different eclipsing time and angle that the solar panels have to turn. But they can be calculated in a similar fashion. The ADCS has to cope with the additional rotation exerted on the satellite body to maintain a nadir pointing attitude. The yaw motion will not not change in the eclipse because the ADCS has to be active throughout the entire mission anyways.

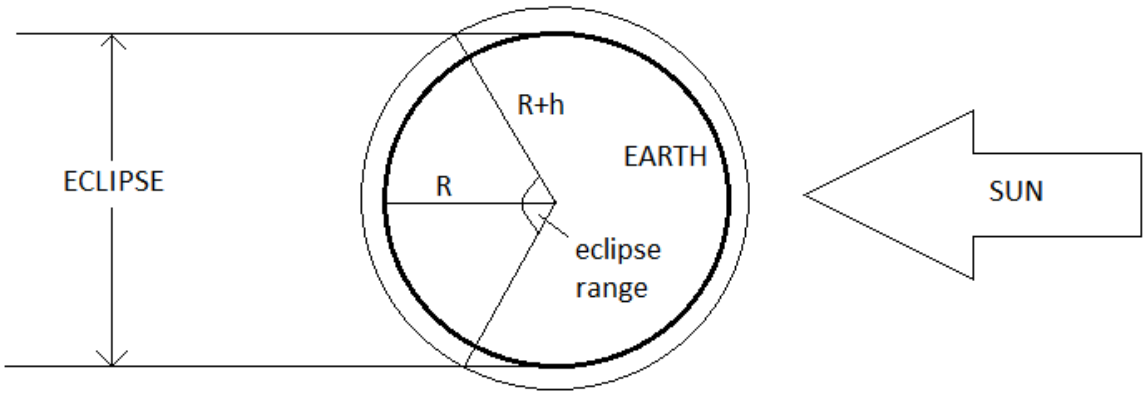

Figure 8.5: Geometric approach on determining the maximum possible eclipse time.

Chapter 9

Attitude Determination and Control System

In order to perform its mission sufficiently, the satellite needs to maintain a certain attitude in space. Various functionalities of subsystems depend on knowing and maintaining a certain attitude. In this chapter, subsystems which have an attitude requirement are identified, the required pointing and control accuracy of the satellite is determined and, consequently, an Attitude Determination and Control System (ADCS) is designed which can fulfill these requirements. It is part of the satellite Attitude Orbit and Control System (AOCS) together with the propulsion subsystem treated separately in Chapter 13.

9.1 Attitude Requirements

Multiple subsystems will not be able to fulfill their purpose if, for example, the satellite points into the wrong direction or rotates freely in space. A safe hold mode will be activated once the satellite is in the correct orbit. What this mode needs to account for will be discussed in this section, whereas the hardware will be discussed in the next two sections.

One of these subsystems is the communication subsystem. If the antenna does not point towards the earth correctly, the designed coverage cannot be achieved. The satellite has to point directly aligned with the nadir vector or else the footprint of the satellite has an offset. Theoretically communication is possible in that area, however the system can no longer guarantee it as the signal power requirement might not be fulfilled. A Matlab code "pointingaccuracy.m" A.5 was written to compute the required pointing accuracy at a certain satellite altitude given an allowable coverage area loss. Note that this computation only regards the coverage of one satellite. Due to the overlap of footprints of each satellite, the total coverage of the system is not affected equally severe. The allowable coverage area loss is correlated with the general coverage and connectivity requirement. If the coverage area of each circle may vary by 2% then the highest required pointing accuracy is 5.51°. This is easily achievable by modern ADCS systems and even passive stabilisation like gravity gradient stabilisation on big satellites [3]. Hence, the satellite coverage was designed with a tolerance of 3% to accommodate pointing errors.

Another requirement comes from the beam width of the ISL antennas. That requirement, however, is not a driving one as it only requires a pointing accuracy of 30°.

If the solar panels are supposed to be oriented towards the sun, they will also impose a pointing accuracy requirement on the system in order to optimally generate power. The effective solar radiation affecting the solar cell is the cosine of the angle under which the sunlight meets the solar cell. Since $\cos 5 = 0.996$, almost no power is lost (0.4%) due to an incidence angle of 5° so the pointing requirement of 5° is still applicable. Note that an incidence angle of 0° means that the sunlight hits the solar cell orthogonally.

A last requirement regarding pointing is the direction to which the satellite is oriented. At all times shall the satellite be nadir pointing in order to maintain coverage.

From the above mentioned requirements, the binding ADCS requirement "Req-Sub-ADCS-1" was derived.

A non-pointing-accuracy related requirement is a long lifetime of the subsystem due to the satellites performing their mission for 10 years, which eventually exceeds the lifetime of certain ADCS components.

Additionally, the ADCS should be as light, power efficient and compact as possible as these factors all affect the budget directly.

9.2 Attitude Determination

Once it is known how accurately the satellite needs to maintain attitude, sensors are chosen which can detect any deviations from it.

One option is the sun sensor. There are coarse sun sensors which are commonly integrated in solar cells in order to be able to optimally point it towards the sun. They measure the current provided by the solar cell and compare it to the maximum possible current which could be generated at an optimal angle. The accuracy of these sensors varies from 1° to 0.1° [26]. More accurate sun sensors use cameras and find the suns location relative to the spacecraft with an accuracy of up to 0.1° to 0.005° [27]. The variation of accuracy depends not only on the quality of lens and processor but also on the field of view angle. Sun sensors generally require little power and are significantly less heavy than star trackers, however during the eclipse time of an orbit they are completely useless.

Especially suited for low earth orbit operations are magnetometers. Using the Lorentz force, they measure the direction and magnitude of the earths magnetic field at the satellites location. Due to the earths magnetic field being well known and defined, the spacecrafts attitude can be derived from them. Additionally, they provide information on how much power the magnetorquer needs in order to perform a certain attitude manoeuvre, assuming the satellite uses magnetorquers of course. The low mass and power consumption makes magnetometers attractive but once the orbital radius of the mission becomes too large, they are inaccurate or even useless.

Devices like gyroscopes take a different approach when it comes to attitude determination. They measure the attitude change rate and can compute the current attitude by integrating the collected data. This can be done quite accurately using little power and, in case of Microelectromechanical System (MEMS) gyroscopes for example [28] [29], adding virtually no mass to the satellite. However a gyroscope can usually not fulfill attitude determination requirements by itself. It cannot perform initial attitude determination and measurement errors add up over time, resulting in the need to reset the gyroscope frequently using additional attitude determination devices i.e. sun sensors or star trackers. The data noise can be decreased using a Kalman filter, which uses previous data points and the linear quadratic estimation method to make estimations containing less inaccuracies than just a single measurement. Together with sun sensors for example, the gyroscope can be used during eclipse time and then be reset with the information provided by the sun sensors during day time.

9.3 Attitude Control

In order to comply with all requirements, a Design Option Tree (DOT) was made for the different control options 9.1. For this mission, 3-axis stabilisation is required. Attitude control options which can provide the necessary stabilisation are introduced in this chapter and one of them is chosen for the final ADCS design in Section 9.4.

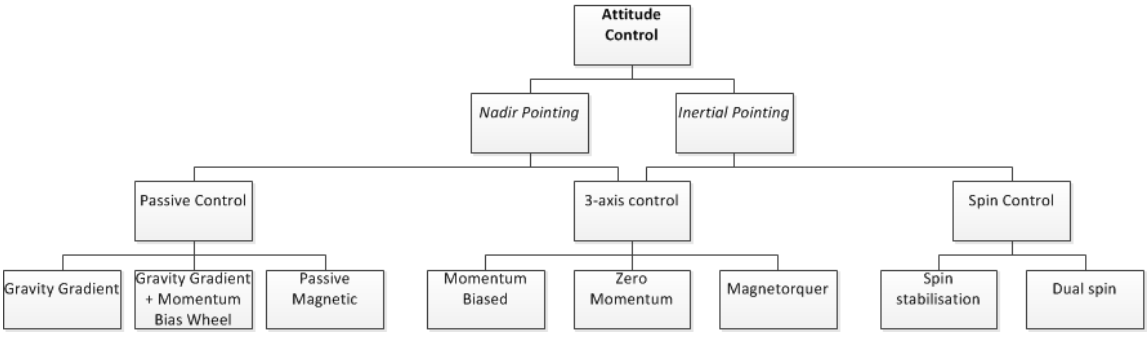

Figure 9.1: Design Option Tree for Attitude Control.

Stabilisation using momentum or reaction wheels is the most accurate way of maintaining or recovering a satellites attitude, assuming the lifetime of the wheel bearings are sufficient. Such wheels can fulfill accuracy requirements of up to 0.001° by either providing a momentum bias or by taking up the satellites momentum as a reaction to a disturbance, providing 3-axis stability for any desired attitude. They are depending on a secondary system for moment dumping (i.e. magnetorquers or thrusters), are generally heavier and consume more power than less accurate systems which might suffice for this mission.

Another option for 3-axis stabilisation are magnetorquers. Placing 3 of them orthogonally with respect to each other, they can interact with the earths magnetic field and cause the satellite to rotate. They are not as powerful or as accurate as momentum wheels, however they use significantly less power and can be designed to weigh only a few grams when it comes to small satellites like CubeSats. If a mission does not require fast manoeuvres in terms of attitude, they are a viable alternative for momentum wheels in low earth orbits, where the earths magnetic field is the strongest.

9.4 Detailed Design and Sizing

This section explains which design options are chosen and the process of determining the required ADCS performance and its sizing in more detail.

The ADCS will consist of the following parts:

- 4 Magnetorquers
- 1 3-axis Magnetometer
- 1 3-axis Gyroscope
- 5 Sun Sensors
- 2 Coarse Sun Sensors

The magnetorquers are the actuators enabling the satellite to pitch, yaw and roll. Preliminary calculations showed that they suffice to cope with any external torques which might act on the satellite and a more complex, heavy or energy consuming system (i.e. momentum wheels) is not needed. The magnetometer will function as the primary attitude determination as well as provide the input on the current magnetic field strength for the magnetorquer. There are 4 torquers in a pyramid configuration to provide redundancy. If one torquer does not function anymore for some reason, the other 3 will still be able to exert the necessary torques. The coarse sun sensors are implemented within the 2 solar panels of the satellite in order to enable an optimal orientation. The sun sensors are an effective and fast method for obtaining the initial satellite attitude after launch and will serve as a redundancy attitude determination system together with the gyroscope. There is one on each side except the "bottom" of the satellite, which is where the antennas are located.

Momentum wheels have been discarded as an option due to their mass and power consumption disadvantage. Their high accuracy is not of any advantage to this mission as the pointing requirement is relatively lenient.

The sizing of the magnetorquers depends, among other things, on the external torques that the satellite experiences throughout its mission. In order to determine the maximum possible disturbance torques which can occur, the SMAD [3] book was used as it provides the formulas for torques due to the gravity gradient, solar radiation, magnetic fields and aerodynamic drag. These formulas are Equations 9.1, 9.2, 9.3 and 9.4, respectively. Using the spacecraft dimensions/shape, total mass, residual dipole, surface reflectivity and operational altitudes as inputs, these torques can be computed and a minimum performance requirement for the attitude control system can be determined. This leads to a magnetic moment requirement for the torquer. From supplier lists, a torquer with sufficient performance can be used for mass and power budget as well as volume estimations. Torquer data from ZARM [30] is used as a reference.

$$T_{gg} = \frac{3\mu}{2R_E^3}|I_w - I_u|sin(2\theta_{nadir}) \tag{9.1}$$

μ is the earth's gravitational parameter, R_E is the earth's radius, θ is the maximum deviation from the nadir vector and I_w and I_u are mass moments of inertia [31] of the satellite, the subscript denoting the respective body axis.

$$T_{sp} = \frac{F_s}{c} A_s(1+q)cos(i_{sun})(c_{ps} - cg) \tag{9.2}$$

F_s is the solar constant, c is the speed of light, A_s is the satellite surface area hit by solar radiation, q is the reflectance factor, i_{sun} is the inclination angle with respect to the sun, c_{ps} is the center of solar pressure location and cg is the center of gravity location.

$$T_{mf} = D\frac{2M_{earth}}{R_E^3} \tag{9.3}$$

D is the residual dipole of the satellite, M_{earth} is the magnetic moment of the earth and R_E is the radius of the earth.

$$T_{ad} = 0.5\rho C_D A V^2 (c_{pa} - cg) \tag{9.4}$$

ρ is the local density, C_D is the drag coefficient, A is the satellite surface area in flight direction, V is the satellite's orbiting velocity, c_{pa} is the center of aerodynamic pressure location and cg is the center of gravity location.
For the residual dipole and the surface reflectivity, assumptions have to be made. However, even when clearly overestimated, the solar radiation and magnetic field induced torques are usually smaller than the torques due to aerodynamic drag (or the gravity gradient for large satellites). Below, in Table 9.1 these values are shown as well as the details on the magnetorquer which can provide the torques needed and the maximum manoeuvre duration.

The maximum manoeuvre duration is based on how fast the satellite can perform a 180° rotation starting and ending with no angular velocity. The calculation for this was performed for each axis and the largest value was selected. Due to the longest rotation time referring to the rotation around the z-axis in this case, this manoeuvre is called the yaw flip. For this computation, Equations 9.5 and 9.6 were used. The yaw flip will only be required if the satellite needs to decelerate, hence point the thruster in flight direction. A yaw flip might seem necessary because the solar panels cannot rotate endlessly due to the fact that they are connected to the electronic system by cables; however, the solar panels can simply "unwind" themselves each orbit by rotating back to their original position each time they enter the eclipse.

$$\alpha = \frac{T_{mt}}{I} \tag{9.5}$$

$$t = 2\sqrt{(\frac{\pi}{\alpha})} \tag{9.6}$$

9.5 Verification and Validation

The ADCS torque computations and torquer sizing do not require complicated coding or functions. The sole use of Matlab during the ADCS development was to speed up computations so a redesign could be done without much effort. Formulas used in the code were directly obtained from literature and each of them were verified.

Table 9.1: Disturbance torques, Magnetorquer Specs and ADCS Specs.

Torques	**Value**	**Unit**
Gravity Gradient	$1.4864 \cdot 10^{-6}$	Nm
Solar Radiation	$1.1155 \cdot 10^{-6}$	Nm
Magnetic Field	$2.4011 \cdot 10^{-5}$	Nm
Aerodynamic Drag	$3.8777 \cdot 10^{-6}$	Nm
Magnetorquers		
Torque on the Satellite	$3.1197 \cdot 10^{-4}$	Nm
Magnetic Dipole	6	Am^2
Mass per Torquer	0.3	kg
Power per Torquer	0.5	W
Voltage Required	5	V
Length	0.325	m
Diameter	0.0145	m
Complete ADCS		
Total ADCS Mass	1.9	kg
Total ADCS Power Use	3	W
Maximum Manoeuvre Duration	727	s

Chapter 10

Thermal Control

The temperature range in space varies from 2.7K, due to cosmic microwave background radiation, to very high temperatures which are due to exposure of the spacecraft to intense solar radiation. In addition, the spacecraft produces internal heat due to power dissipation of subsystems. This chapter will provide an analysis of the heat propagation through the spacecraft and a design will be made to make sure the components of the satellite are within their operation temperature.

10.1 Thermal Requirements

Requirements on the thermal control subsystem flow from system and subsystem level. The mission itself does not put any constraints on temperature ranges, only on cost and time. Subsystems set their operating temperature for their elements and this gives a range of operational temperatures that the thermal control subsystem needs to accommodate. These ranges are shown in Table 10.1.

Table 10.1: Requirements on Thermal control from different subsystems.

Subsystem	**Component**	**Operating Temp.** (C°)
ADCS	Coarse Sun Sensor	-40 to 85
	SSOC-A60 Sun Sensor	-40 to 85
	3-axis Magnetometer	-35 to 75
	Magnetorquer	-50 to 85
	ADCS CPU and circuit board	-10 to 70
EPS	Triple junction Solar Cells	-40 to 85
	$LiFePO_4$ battery	0 to 55
	Micro-stepper Motor	-35 to 70
Propulsion	Hydrazine (diazane) system	5 to 70
Payload	Main Patch Antenna	-50 to 65
	Cross-link Horn antenna	-50 to 65
	Down converter	-20 to 71
	Low-Noise Amplifier	-15 to 65
	Input Multiplexer	-25 to 70
	Output Multiplexer	-40 to 85
	TWT Amplifier	-54 to 100
	Electronic Power Conditioner	-20 to 70
Data Handling and Storage	Electronics	-20 to 70

It is evident from Table 10.1 that the most critical temperature ranges in the system are the battery and the Hydrazine propulsion system. Only operating temperatures are shown as survival temperatures show broader ranges. These components will dictate whether an active or passive technique of thermal control is used, while top-level constraints concerning cost and schedule make it difficult to achieve an ideal thermal interface [32].

10.2 Thermal Analysis

There are three essential modes of transferring heat with the system and surroundings and they are: Conduction, Convection and Radiation. Radiation will represent the main form of heat transfer between the spacecraft and environment. Conduction will be discussed in Section 10.3, while the only external environmental heat inputs come from Sun and Earth. Since radiation is the main mechanism of transferring heat to the spacecraft, the equation for radiated energy is given by Equation 10.1.

$$Q_{ij} = A_i F_{ij} \sigma (T_i^4 - T_j^4) \tag{10.1}$$

Based on the first law of thermodynamics, the steady-state temperature is based on equating the external and internal heat and setting the variation of temperature with time equal to zero.

Therefore the thermal balance is given by Equation 10.2, where the only sources of radiation are the Sun, Albedo and Earth Infra Red.

$$\varepsilon_{IR}\sigma(T_{sc}^4 - T_s^4)A_{sc} = \alpha \sum_{ij}^{k} F_{i-j} A_i q_s + \alpha \sum_{ij}^{k} F_{i-j} A_i \rho_{alb} q_s + \varepsilon_{IR} \sum_{ij}^{k} F_{i-j} A_i q_{IR} + Q_{int} \tag{10.2}$$

Equation 10.2 indicates that the total temperature of the spacecraft is obtained by summing the view factors of each face with their respective face area. For instance, the view factor for Solar radiation absorbed on an area is directly proportional to the cosine of the incidence angle that a surface normal makes with the sun vector. This incidence angle changes from 0 to 90 degrees. For the albedo and Earth Infra Red radiation, the view factor between two bodies (in this case: Spacecraft's nadir face and Earth) is given by Equation 10.3.

$$F_{sp-ert} = \frac{1}{A_{sp}} \int_{A_{sp}} \int_{A_{ert}} \frac{cos\lambda_{sp} cos\lambda_{ert}}{\pi s^2} dA_{sp} dA_{sun} \tag{10.3}$$

For the satellite we have that the maximum deviation from the nadir axis is equal to 5.1 degrees, as determined in Chapter 9. This value is for the λ_{sp}, while assuming that the part of area on Earth is always perpendicular when looking at the spacecraft, $\lambda_{ert} = 0°$. Therefore, we get for the Earth-facing surface (+w side) that the view factor is 0.736.

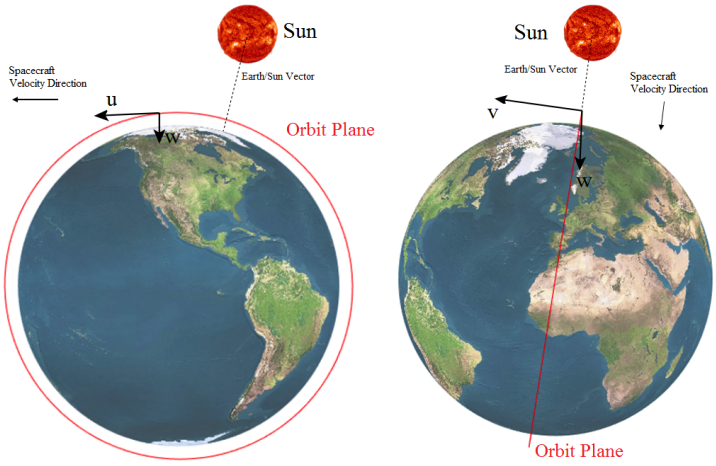

Figure 10.1: Depiction of change in angle β in two extreme cases: Hot - $\beta = 90°$ (left) and Cold - $\beta = 0°$ (right).

Two cases that represent the upper and lower bounds of the spacecraft temperature range are distinguished. They are named the Hot and Cold cases. They are defined by the minimum angle between orbit plane and sun vector β that ranges from -90 to 90 degrees. Spacecraft's polar orbit is such that it will experience all the angles in this range over its lifetime. Therefore, during the cold case ($\beta = 0°$), the

solar flux is at its maximum of 1300 W/m^2, while during the hot case ($\beta = 90°$), it has a maximum value of 1400 W/m^2. The cold case orbit has 52% of sunlight, while the hot case has 100% sunlight exposure. This is shown in Figure 10.1. Also the albedo factor is taken to be 0.4 hot and 0.24 cold (maximum values during both cases). Furthermore, the Earth infrared flux is 270 and 220 W/m^2 for hot and cold case respectively.

As the design of the spacecraft necessitates having one side always nadir pointing, we can define that face as +w. Given the fact that a body-fixed reference frame is used, the +u face is in the orbital velocity direction and +v is in the negative orbit normal direction. These axis definitions are with compliance with Section 8. All the received energy on each one of these faces, by all sources of radiation is compiled for both the cold and hot case and shown in Table 10.2. What can be seen from this table is that the hot case has constant values of radiation over the entire orbit. These values are expected since that orbit is completely facing the sun. Since in the Cold case, large variations between full solar illumination and eclipse are evident, the following thermal design will deal with only the cold case. Figure 10.2 shows the absorbed energy from the sun, albedo and Earth's Infra Red radiation on the entire spacecraft over an orbit, assuming a black body with solar absorptivity over IR emissivity of $\alpha/\varepsilon_{IR} = 1$. In Figure 10.2, thermal averages are taken for all sides of the spacecraft and their respective heat fluxes. These are calculated using Equation 10.4. They can either been taken with respect to time or angle and in this case it is angle.

$$q_{av} = \sum_j q_j \frac{(\theta_{j+1} - \theta_{j-1})}{360°} \tag{10.4}$$

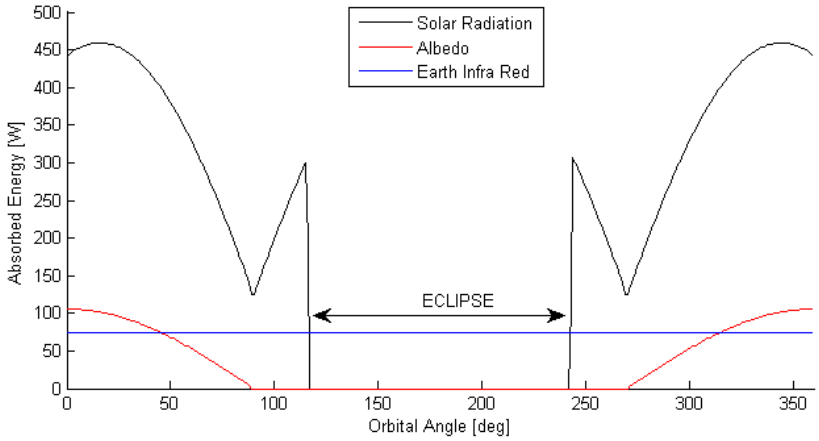

Figure 10.2: Environmental energy sources decomposed to solar heat, reflected albedo radiation and infrared light.

Table 10.2: Solar, albedo and IR heating on each face of the spacecraft over incidence for both the cold and hot case. Eclipse values same between 120-240 degrees. Hot case values constant over all angles.

θ [deg]	u^+ [W/m^2]	u^- [W/m^2]	v^+ [W/m^2]	v^- [W/m^2]	w^+ [W/m^2]	w^- [W/m^2]
			Cold Case			
20	118,5	541,7	118,5	118,5	379,0	1229,2
40	106,4	924,5	106,4	106,4	340,4	1010,3
60	87,6	1201,9	87,6	87,6	280,2	669,5
80	64,3	1340,4	64,3	64,3	205,7	248,1
100	50,6	1334,6	50,6	50,6	365,3	0
120-240	50,6	50,6	50,6	50,6	161,9	0
260	1326,7	50,6	50,6	50,6	410,0	0
280	1345,8	61,8	61,8	61,8	197,8	203,4
300	1222,4	85,4	85,4	85,4	273,2	630,3
320	957,6	104,8	104,8	104,8	335,2	981,1
340	583,5	117,6	117,6	117,6	376,3	1213,7
360	145,0	122,3	122,3	122,3	391,5	1299,8
			Hot Case			
0-360	62,1	62,1	1462,1	62,1	198,7	0

10.3 Thermal Conduction

This section will first present the heat equation. This equation will then be worked out to a finite difference approach over a two-dimensional plate. The plate represents a body plate of the spacecraft. Subsequently, the boundary condition will be discussed and applied. The analysis results in a simulation of a face of the spacecraft that is connected to a very hot plate which is in the sun and the other side of the plate is connected to a plate in the shadow. Resulting is an approximation of the time required to reach steady state and a material selection can be made.

10.3.1 Heat Equation

The heat equation for a two-dimensional grid of x and y coordinates is expressed as

$$\frac{\partial u}{\partial t} = \kappa \left(\frac{\partial^2 u}{\partial x^2} + \frac{\partial^2 u}{\partial y^2} \right) \tag{10.5}$$

where u is the temperature $[K]$, κ is the thermal diffusivity $[m^2/s]$ and x and y are the coordinates in $[m]$ [33].

The solution to the heat equation is dependent on two spatial dimensions and time, thus $u = f(x, y, t)$. To analyse the heat conduction of the spacecraft body plate, the spatial dimensions and time must be discretized.

Let the continuous, exact, solution to the heat equation be denoted as $u(x, y, t)$ for $0 \leq x < L_x$, $0 \leq y < L_y$ and $0 \leq< T$. Now discretize all dimensions: in N_x, N_y and N_t points, respectively. The discrete temperature parameter can now be expressed as

$$U_{i,j}^n \quad \text{with} \quad 1 \leq i \leq N_x, \quad 1 \leq j \leq N_y \quad \text{and} \quad 0 \leq n \leq N_t - 1. \tag{10.6}$$

Now the discrete temperature derivatives can be approached with a Taylor series. An explicit method is applied, forward difference in time and second order central difference for both the spatial dimensions. A numerical representation of the heat equation is obtained when substituting these Taylor approximations into the heat Equation, 10.5. The expression now reads

$$U_{i,j}^{n+1} = U_{i,j}^n + \kappa \Delta t \left(\frac{U_{i+1,j}^n - 2U_{i,j}^n + U_{i-1,j}^n}{\Delta x^2} + \frac{U_{i,j+1}^n - 2U_{i,j}^n + U_{i,j-1}^n}{\Delta y^2} \right) \tag{10.7}$$

with a truncation error due to the Taylor approximation in the order of $\mathcal{O}\left(\Delta t + \Delta x^2 + \Delta y^2\right)$.

10.3.2 Stability

Equation 10.7 is only stable if the factor of the mesh ratio and the diffusivity, μ, satisfies

$$\left(1 - 4\frac{\kappa \Delta t}{h^2}\right) \geq 0 \tag{10.8}$$

$$\mu = \frac{\kappa \Delta t}{h^2} \leq \frac{1}{4}. \tag{10.9}$$

10.3.3 Convergence

Reliable results can only be obtained if the sought-after solution converges to a value. Firstly, the error is expressed as

$$\epsilon = \frac{\max\left(\max\left(U^{n+1} - U^{n}\right)\right)}{\Delta t} \tag{10.10}$$

This equation evaluated the ratio of each new solution with respect to the previous time step. The steady state solution is reached when the error is below a threshold value. The threshold value assumed in this case is

$$\epsilon < 1e^{-2}, \tag{10.11}$$

thus whenever the error converges to this ratio, the program will be stopped and prompts the message that steady state is reached within a certain amount of time.

10.3.4 Boundary & Initial Conditions

The initial and boundary conditions used for the heat equation are based on the worst case scenario. With the material selection, made in the next section, Section 10.4, the temperature range is from -14 [° C] to 53 [° C]. The hot temperature is applied to two edges and the cold temperature is applied as initial condition and to the two remaining edges:

$$u(x, y, 0) = 256 \text{ [K]} \tag{10.12}$$

$$u(L_x, y, t) = u(x, L_y, t) = 259 \text{ [K]} \tag{10.13}$$

$$u(0, y, t) = u(x, 0, t) = 326 \text{ [K]} \tag{10.14}$$

10.3.5 Verification

The program is verified by analyzing the error and comparing the time to reach steady state for different time steps.

The time to reach steady state should be constant and independent of the time step as long as the mesh grid is stable, see Equation 10.9. Figure 10.3 shows the time to reach steady state with respect to the time step. The time to reach steady state is not exactly constant, but varies slightly. The variation can stem from the truncation error, as the deviations are in the order of the time step. Moreover, round off errors can also slightly change the solution. The stability is therefore verified since the time to reach steady state stays constant within the truncation error range.

To reach steady state, the convergence of the solutions is a necessary requirement. Figure 10.4 depicts the temperature change per time step. The figure shows that the solution is converging and stops when the threshold value, as specified in Equation 10.11.

10.3.6 Results

Execution of the program plots the final steady state answer, found in Figures 10.5 and 10.6. The steady state is reached within 671 seconds. This fast heat transfer is due to the thermal diffusivity of aluminum. Moreover, because the steady state is reached within 11 minutes, the spacecraft will reach its steady state temperatures during its orbit.

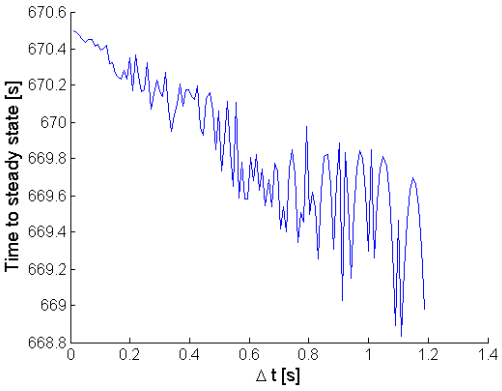

Figure 10.3: Time to reach steady state of heat equation versus time step size. $N_x = N_y = 30$, $0.012 \leq \Delta t \leq 1.1882$ and $0.0025 \leq \mu \leq 0.2475$.

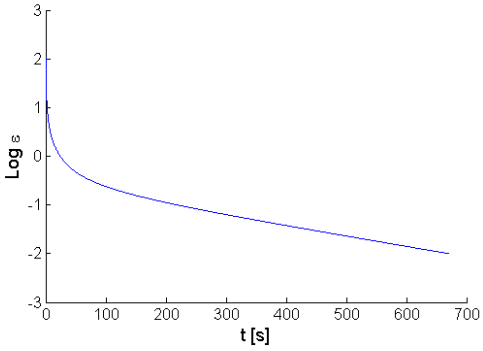

Figure 10.4: Convergence of heat equation with $N_x = N_y = 150$, $\Delta t = 0.0273$ and $\mu = 0.15$.

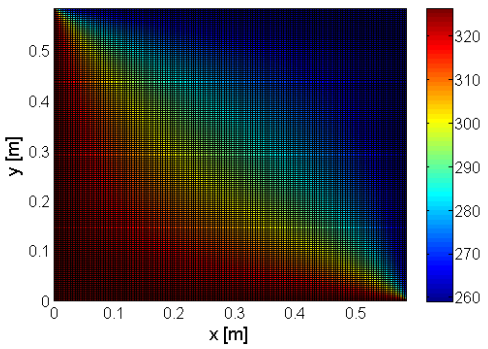

Figure 10.5: Surface plot of heat equation solution, initial and boundary conditions of 10.12, 10.13 and 10.14, with $N_x = N_y = 150$, $\Delta t = 0.0273$ and $\mu = 0.15$, converges after 671 seconds.

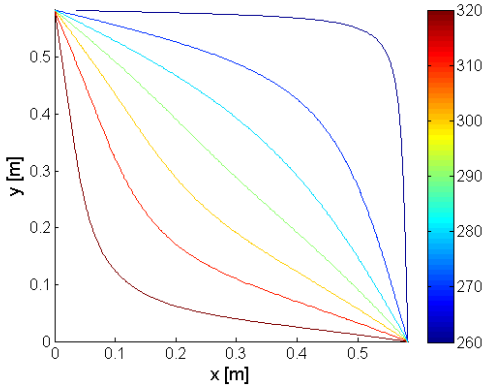

Figure 10.6: Contour plot of heat equation solution, initial and boundary conditions of 10.12, 10.13 and 10.14, with $N_x = N_y = 150$, $\Delta t = 0.0273$ and $\mu = 0.15$, converges after 671 seconds.

10.4 Thermal Design

Based on the Requirements and Analysis preformed in Sections 10.1 and 10.2, the most critical components that need thermal control are the battery and propulsion system. Following the Design Option Tree, shown in Figure 10.7, a combination of passive and active thermal control system is used, as it is more efficient way of providing instantaneous heat to individual sections, such as the hydrazine tank. These active elements will be explained in the following sections, individually for components that need them.

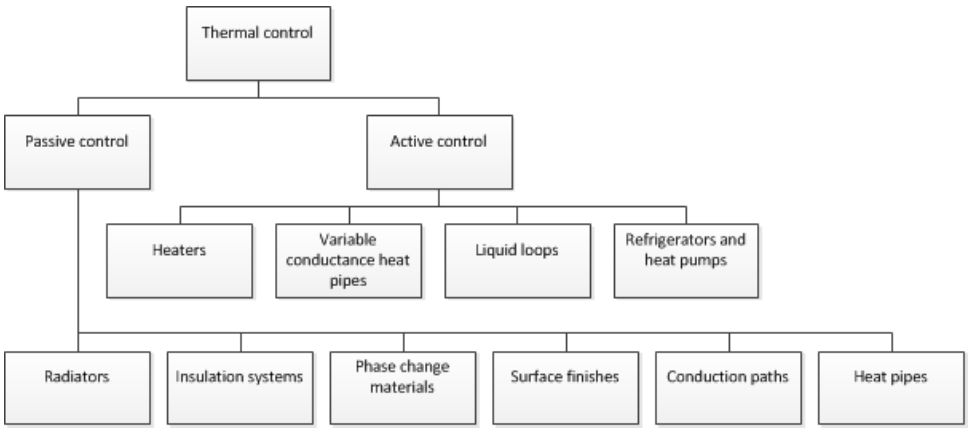

Figure 10.7: Design option tree for Thermal Control.

10.4.1 Surface Coating Analysis

One of the ways to control the thermal balance inside the spacecraft, given by Equation 10.2, is to vary the absorptivity over IR emissivity of α/ε_{IR} ratio. There exist a variety of coating applicable on the surface of the material. Ten of the most common and widely used coatings applied on the satellite's thermal environment, along with the thermal ranges they provide, are shown in Table 10.3 and plotted in Figure 10.8. For a better indication of temperature ranges, the maximum and minimum temperatures, have been indicated in Table 10.3.

Table 10.3: Average energy absorbance per face, minimum and maximum temperature of spacecraft for 11 different coatings.

Material	$\frac{\alpha}{\varepsilon_{IR}}$	T_{min} [K]	T_{max} [K]	Internal Spacecraft Temp. [C°]
Black body	1	108	213	-165 to -60
Polished aluminum	2,67	259	341	-14 to 68
2mm aluminized teflon	0,15	120	161	-154 to 113
S13G-LO	0,24	112	164	-161 to -109
Chemblaze Z306	1,03	111	215	-162 to -58
Aluminized capton 0,5mm	0,62	125	199	-148 to -74
Aluminized capton 1mm	0,57	119	193	-154 to -80
Aluminized capton 2mm	0,55	116	190	-157 to -83
Aluminized capton 5mm	0,53	112	188	-161 to -85
Bare aluminum	3,00	259	344	-14 to 71
Astro quartz	0,28	114	169	-159 to -105

What can be seen from Table 10.3 is that Polished Aluminum has a pretty high $\frac{\alpha}{\varepsilon_{IR}}$ ratio, which makes it to heat up quite rapidly. However, since the spacecraft has an orbit that is almost half of the time in eclipse, there is a need of a material that heats up rapidly, since most of the paint finishes get to temperatures below -100 $C°$.

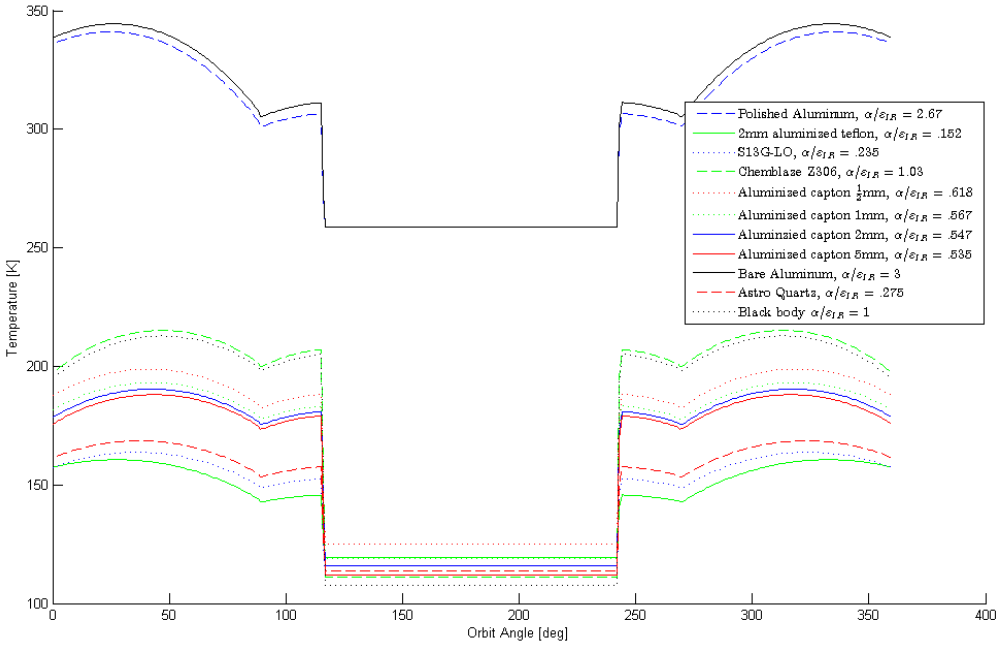

Figure 10.8: Temperature of cold case over whole orbit with 10 different materials compared.

10.4.2 Insulation of spacecraft components

The most favourable temperature range was found for polished aluminum. The minimum temperature of the spacecraft during eclipse was found to be $-14°C$ and the maximum temperature during day time is $53°C$. This temperature range is within the operating range of most of the components, listed in Table 10.1, except for ADCS CPU and circuit board, $LiFePO_4$ battery and Hydrazine tank. Therefore, an additional design for these components is needed in order to prevent freezing or overheating.

In order to preserve internal heat of the spacecraft and to make heating more efficient, these critical components need to be compartmentalized by means of Multi Layered Insulation (MLI) blankets. The effective emissivity of the MLI blanket is calculated by using Equation 10.15.

$$\varepsilon_{eff} = \frac{Q_{ins}}{A_{ins}\sigma(T_{ins}^4 - T_{nins}^4)} \tag{10.15}$$

Based on Equation 10.15, it is possible to modify the emissivity to suit the thermal control needs. Knowing the internal power dissipated by components, and the required internal temperature to prevent freezing, the effective emissivity is calculated for each critical component, which also constrains the material used for the MLI.

ADCS Electronics

In order to keep the electronics working for the ADCS, it is required to have the CPU packed with a MLI to insulate the internal heat dissipation. A MLI made of layer of 1/4 mil Aluminized Mylar and a layer of MAXORB is being used. The effective emissivity in this case is computed by Equation 10.16.

$$\varepsilon_{eff} = \frac{A_{mylar}\varepsilon_{mylar} + A_{maxorb}\varepsilon_{maxorb}}{A_{mylar} + A_{maxorb}} \tag{10.16}$$

Since the plates will be placed next to each other in a stripped pattern and are the same area, the effective emissivity results in the value of 0.22. The internal dissipated energy of the ADCS is 200 miliwats. The minimum bound of the temperature can be computed with Equation 10.17. This results in a minimum operating temperature of 2.6 C°.

$$T_{ins-adcs} = \sqrt[4]{\frac{Q_{ins}}{\sigma \varepsilon_{eff} A_{adcs}} + T_{nins}^4} \tag{10.17}$$

Battery Module

The $LiFePO_4$ battery is already packed in an aluminum box. The battery has to continuously deliver a 100 Watt of power to the spacecraft, out of which 10 Watt dissipates into heat. The battery needs to be insulated and designed to reach 0 C°. This is done by having an emissivity of 0.55 for which a coating of 1/2 mil. Aluminized Kapton is being applied.

$$T_{ins-bat} = \sqrt[4]{\frac{Q_{ins}}{\sigma \varepsilon_{eff} A_{bat}} + T_{nins}^4} \tag{10.18}$$

Propulsion Tank

The propulsion tank must be between $5^{\circ}C$ to $70^{\circ}C$. The lower bound ensures the propellant will not freeze. This is achieved by insulating the tank with Multi Layered Insulation with a characteristic emissivity coefficient of $\varepsilon = 0.05$. Additionally, two patch heaters, one for redundancy, will be mounted to be able to increase the temperature appropriately. The required energy to do so during eclipse is 0.4 Watt to keep the temperature above $3^{\circ}C$, obtained with Equation 10.19.

$$T_{ins-prop} = \sqrt[4]{\frac{Q_{ins}}{\sigma \varepsilon_{eff} A_{prop}} + T_{nins}^4} \tag{10.19}$$

Antennas

The antennas operating temperature is within the boundaries of the spacecraft temperature. However, the antennas are mounted outside the spacecraft and should therefore be well insulated. The insulation material should not interfere with the radio waves. Thus, for example aluminized capton cape shall be avoided. A MLI of astroquartz or white-painted capton cape are often used for the antennas [34].

The antennas will be made of aluminum. The bare aluminum already has low emissivity properties. Additionally, the antenna will be covered with white painted, Chemblaze A276, capton tape. The Chemblaze A276 has a solar absorptivity α between 0.22 – 0.28 and an emissivity of $\varepsilon = 0.88$. This insulation strives to keep the temperatures to an acceptable level. Component level validation shall verify the chosen protection.

Solar Panels

The solar panels are mounted outside the spacecraft. The efficiency of the solar panels decreases as the panels heat up. Hence, it is best practise to keep the solar panels as low as possible. Hence, the back of the array will be treated with a high emissivity coating. Since the spacecraft is flying at low altitudes, the albedo radiation adds a significant contribution [34]. Therefore, the back of the solar panels will be painted white with Chemblaze A276 paint. Now the heat trapped by the solar panels can radiate to the space environment through the back of the panels. The solar panels will still undergo higher temperature ranges than the rest of the spacecraft, but should be able to withstand the environment.

Temperature Instruments

Given the fact that patch heaters are part of an active system, in order to monitor the heat, temperature monitoring sensors need to be placed inside the spacecraft and on the solar panels. Given the temperature ranges that the satellite will experience over its nominal mission, there are two types of sensors that can be used: thermistors and platinum resistors. Thermistors work in lower temperature ranges than resistors and will be applied on the propulsion subsystem and in sections where temperature sensitive electronics are placed. Platinum resistors are placed on solar panels as the panels will face constant and full solar illumination.

10.4.3 Thermal Design Results

Table 10.4 shows the components that contribute to the thermal design of the satellite. Types of the specific MLI per component along with the effective emissivity are indicated. The problem with MLI's is that their density is hard to obtain analytically and is usually performed experimentally. The largest percentage of the thermal control mass is the insulation and since the density at this point is unknown, the initial estimate of 5 kg is used.

In terms of power usage, the power dissipation of $LiFePO_4$ and ADCS electornics of 10 and 0.2 Watts, respectively, are not part of the thermal subsystem budget, therefore the total power that thermal control needs is 0.4 Watts (as two patch heaters are used, one for redundancy).

The temperatures were designed for only the lower limit of the temperature range as components survive the maximum temperature. It is recommended for a further design to evaluate the actual mass of the thermal system.

Table 10.4: Thermal Design of Spacecraft's Critical Components.

Component	Effective ε	Insulation Material	Q_{ins} [W]	Designed Temperature Range [C°]
ADCS Electronics	0.22	MLI: 1/4 mil Aluminized Mylar + MAXORB	0.2	2.6 to 53
$LiFePO_4$ battery	0.55	1/2 mil Aluminized Kapton	10	6.4 to 53
Hydrazine Prop. Tank	0.05	MLI: 1/4 mil Aluminized Mylar + 2 x Anodized Aluminum	0.2	8.1 to 53
Antennas & Solar Panels	0.88	Chemblaze A276	-	n/a

Chapter 11

Structural Design

The following chapter outlines the structural environment that needs to be provided to support the payload on the given mission. Identifying the critical design loads and making sure that structural members withstand the worst-case loading is the main goal of this chapter. Furthermore, the material selection based on mass, stiffness and cost will be performed as well, completing the overall structural picture.

11.1 Requirements & Assumptions

The requirements on the structural design subsystem flow down from system level. The structural environment has to provide an adapter to the launcher. Furthermore, the structure has to withstand the largest loading coming from the launcher specifications. Additionally, the primary structure has to also withstand all the thermal loads from the illumination of the sun.

To simplify the problem and apply well known formula's to the structural design, a list of assumptions is used.

Collisions It is assumed that there are no collisions of small objects with the spacecraft.

Bodyplate load It is assumed that the spacecraft body does not bear any of the launch loads.

11.2 Critical Mission Loading

There are several types of structural loading acting on the spacecraft during its lifetime. The ones considered for the spacecraft are uni-axial tension/compression due to launcher thrusting, thermal stress caused by temperature change and dynamic loading in terms of natural frequency. As indicated in Chapter 16, the Rockot Launcher has the accelerations outlined in Table 11.1.

Table 11.1: Quasi-static loads experienced by an average payload during ascent [35].

Event	axial max, g $[m/s^2]$	axial min, g $[m/s^2]$	radial, g $[m/s^2]$
Lift-off	+ 3.6	0	± 0.7
Worst-case dynamics pressure	+ 2.8	+ 2.4	± 0.9
Peak thrust	+ 8.0	+ 6.2	± 0.5
Worst-case structural acceleration	+ 8.1	+ 6.3	± 0.5
Stage 1 shutdown	+ 8.1	- 1.5	± 0.7
Stage 2 powered flight	+ 3.0	0	± 0.4
Upper stage powered flight	+ 1.6	0	± 0.4

+ is in tension, while - is in compression

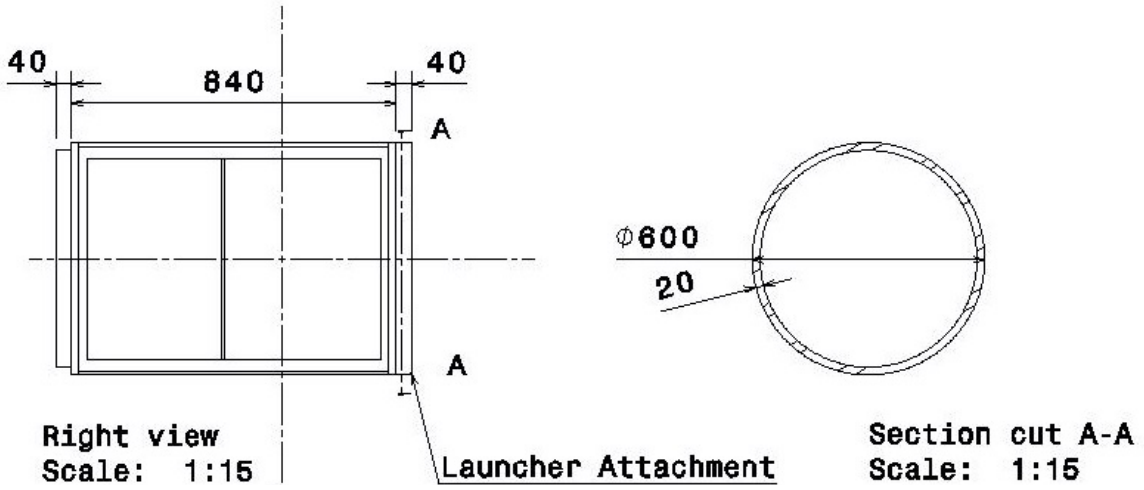

Figure 11.1: Right View of Spacecraft with Cross-section of Launcher Attachment.

From the quasi-static loads presented in Table 11.1, the worst case structural acceleration, has the highest maximum acceleration of + 8.1, while Stage 1 shutdown has minimum acceleration of -1.5. The tensile and compressive stresses are calculated by Equation (11.1) [3].

$$\sigma = \frac{P}{A} \pm \frac{My}{I} \tag{11.1}$$

where P is the launch load in $[N]$, A is the cross-sectional area $[m^2]$, M is the moment applied on the spacecraft $[Nm]$, y is the distance in $[m]$ between the moment and the load bearing part that propagates the tension and compression stresses from the moment and I is the area moment of inertia $[m^4]$ of the cross-section. This equation assumes that the thrust is a point force, which makes the mass of the spacecraft press on the Launcher attachment with a force of the mass of the spacecraft times the maximum acceleration from Table 11.1. The Launcher Attachment is shown on Figure 11.1

The natural frequency of the spacecraft mounting components should be at least two times higher than the natural frequency vibrations induced by the launcher. The launcher's natural frequency is around 100 [Hz] [35]. Thus, the launcher attachment ring and the spacecraft walls should be designed for a natural frequency of at least 200 [Hz]. The natural frequency of beam that is clammed on one side and free on the other side is [3]

$$f_n = \frac{1}{2\pi}\sqrt{\frac{3EI}{ML^3}} \tag{11.2}$$

where the natural frequency f_n is in [Hz], E is the Young's modulus, I is the area moment of inertia $[m^4]$, M is the mass of the spacecraft and L is the length of the spacecraft where the next spacecraft is mounted.

11.3 Bus Sizing

The spacecraft bus dimensions are chosen in a way such that the antenna's can be mounted on the nadir facing body plate. All subsystems and their components are added in a computer aided design program, Catia V5, and the length of the spacecraft along the nadir axis is obtained. This results in a square cross-section of 0.583 meters and a length along the nadir axis of 0.66 meters.

All of the subsystems fit inside these dimensions. The main antenna's, consisting of a hexagonal configuration of 7 parabolic antenna, are mounted on the nadir facing side of the spacecraft together with a small patch antenna for the ground link. On the other side of the spacecraft mounts four cross-link antenna's on rods of 34.5 [cm]. The launcher attachment rings are placed on both sides of the flight direction. The two remaining sides of the spacecraft contain the solar panels. The results are shown in Chapter 14.

11.4 Design & Material Selection

Spacecraft have used many different materials over the past. One of the most common materials is aluminum, from which a lot of experience is obtained from the aviation sector. Sometimes more expensive metals such as titanium are used to withstand heavy loads. However, as listed in Table 11.2, the stiffness over density ratio from the chosen titanium alloy is equal to the aluminum 7075 alloy. More recently, composite structures have become interesting as well. Composites often excel in tensile yield properties with respect to their mass. Despite these excellent properties, the knowledge of these composites is significant less than the knowledge of metals. Moreover, the composites are prone to delamination, degassing in the harsh space environment and the manufacturing cost are higher. Table 11.2 presents a list of five selected materials which are interesting to consider. Furthermore, in Appendix A.9 the interface control document of the analysis is briefly discussed.

Table 11.2: Material properties of five considered materials for the spacecraft structure [7].

Material	ρ [kg/m^3]	E [GPa]	σ_Y [MPa]	E/ρ	α [μ/m/K]
Aluminum 6061-T6	2700	68	276	24	23,6
Aluminum 7075-T6	2800	71	503	26	23,4
Titanium T1-6A1-4V	4400	110	825	25	9
KEVLAR 49 0°	1380	76	1379	55	-4
Graphite epoxy sheets GY70/934	1620	282	586	174	-11,7 (Longitudinal), 29,7 (Traverse)

11.4.1 Launch attachment ring

The launcher attachment ring, the ring that connects the spacecraft to the launch adapter ring and mounts the spacecraft vertically on top of each other as well, shall not be susceptible to vibrations. Therefore, the thickness of this ring is designed so that the natural frequency equals two times the frequencies from the launcher. Hence, the natural frequency shall be less than 200 [Hz], evaluated with Equation 11.2.

Table 11.3 presents the results, the thickness achieves the natural frequency constraint and for each material the related mass is shown. The lowest weight is achieved with the composite materials whereas the chosen metals have almost the same weight.

Table 11.3: Launch attachment ring thickness, natural frequency and mass for selected materials.

Material	t [mm]	f_n [Hz]	mass [kg]
Aluminum 6061-T6	6,9	201,30	1,40
Aluminum 7075-T6	6,6	201,32	1,39
Titanium T1-6A1-4V	4,2	201,11	1,39
KEVLAR 49 0°	6,1	200,50	0,63
Graphite epoxy sheets GY70/934	1,6	200,04	0,20

11.4.2 Body Plate Analysis

The body plates are assumed to not bear any loads. The sizing of the thickness will be done in the same analogy as the launcher attachment ring, with a frequency analysis. Besides, a plate buckling equation

is applied to analyse the critical buckling stress as well. The following equation calculates the critical buckling stress for a plate which is fixed at four sides and considers only the longitudinal launch load [36].

$$\sigma_{cr} = K_{buck} \frac{E}{1-\nu^2} \left(\frac{t}{b^2} \right) \tag{11.3}$$

where $K_{buck} = 3.35$ is the buckling coefficient based on the ratio of the width and length of the spacecraft, E is the Young's modulus, ν is the Poisson's ratio, t is the thickness of the body plate and finally b the width of the spacecraft. Again, the composites perform best regarding weight and the metals perform similarly with respect to each other.

The results are shown in Table 11.4. The graphite epoxy performs so well, a thickness of 0.21 mm can be achieved, whereas in reality a higher thickness must be applied to account for material irregularities and fabrication losses.

Table 11.4: Spacecraft outer wall sized thickness for buckling stress, natural frequency and mass.

Material	t [mm]	$\sigma_{buckling}$ [MPa]	f_n [Hz]	mass [kg]
Aluminum 6061-T6	0,87	654	200	5,42
Aluminum 7075-T6	0,84	659	201	5,43
Titanium T1-6A1-4V	0,55	675	203	5,59
KEVLAR 49 0°	0,78	671	200	2,49
Graphite epoxy sheets GY70/934	0,21	616	200	0,79

11.4.3 Internal Columns Structure Sizing

The internal columns are the main load bearing parts of the spacecraft and will undergo a yield and buckling analysis. The columns are assumed to be beams along the nadir axis of the spacecraft with a hollow square cross-section of 2 cm.

The static load analysis applies Equation 11.1 to find the Von Mises stress criteria and compares this to both the material yield properties as well as the buckling equation of a column. The buckling of a column which is hinged at both sides is [36]

$$\sigma_{cr} = \pi^2 \frac{EI}{L^2 A} \tag{11.4}$$

where E is the Young's modulus, I is the area moment of inertia, L is the length of the column and A is the cross-sectional area.

Finally, the results are shown in Table 11.5. The composites have the lowest weight although the graphite epoxy sheets have a too low thickness for manufacturing and thus should be over dimensioned.

11.4.4 Propulsion Subsystem Support

The propulsion subsystem consists of 2 propellant tank and pipes from the tanks to the thruster. The propulsion tanks must be supported by the internal structure. A design consisting of three struts is chosen and evaluated for both yield stress and buckling stress. The struts are assumed to be hinged on both sides, thus Equation (11.4) is applied for the buckling criteria. The struts consist of a square cross-sectional area with a width of 1 cm. The buckling criteria was leading for the design, the results are presented in Table 11.6.

Table 11.5: Internal columns sizing results for selected materials.

Material	t [mm]	$Y_{von\ Mises}$ [MPa]	$\sigma_{buckling}$ [MPa]	mass [kg]
Aluminum 6061-T6	1,2	69	110	0,44
Aluminum 7075-T6	1,1	74	114	0,42
Titanium T1-6A1-4V	0,7	113	171	0,43
KEVLAR 49 0°	1,1	74	122	0,21
Graphite epoxy sheets GY70/934	0,28	274	426	0,07

Table 11.6: Structural propellant tank support sizing results.

Material	t [mm]	$Y_{von\ Mises}$ [MPa]	$\sigma_{buckling}$ [MPa]	mass [kg]
Aluminum 6061-T6	0,89	84	127	0,12
Aluminum 7075-T6	0,85	88	132	0,12
Titanium T1-6A1-4V	0,55	131	198	0,12
KEVLAR 49 0°	0,8	93	140	0,05
Graphite epoxy sheets GY70/934	0,22	317	489	0,02

11.4.5 Final Design

The final material selection is based on both the structural performance analysed in this chapter as well as the thermal performance evaluated in Chapter 10. This chapter showed that composite materials have the best performance with respect to weight. However, the thermal design chapter shows that the best coating is obtained from polished aluminum. Moreover, composites are more prone to the space environment with respect to degassing and delamination. Analysis of these symptoms are still under active research. Additionally, the manufacturing of composites requires more technical inspections. Therefore, composites are more expensive and less reliable.

Titanium achieves the same performance as aluminum with less volume. The mass required to fulfill the load requirements is however the same. Furthermore, titanium is much more expensive and rare than aluminum. Therefore the aluminum 7075-T6 alloy is chosen.

This alloy is very well analyzed with respect to aerospace performance in the last 100 years. Choosing the same material for both the launcher attachment ring, spacecraft walls as well as the internal load bearing columns avoids thermal expansion problems that arise when using different materials with high temperature variations. Moreover, the aluminum body plates can be polished in such a way that the thermal parameters make is a perfect balance of incoming and outgoing heat.

The CATIA model, which is an accurate representation of the satellite model gives a total mass of 15 kg without the internal support. One third of the total mass is to be secondary supporting structure (7 kg), since it needs to carry the communications payload (41.1 kg of internal structure). Then the total mass of the satellite is 22 kg.

The design has been validated with the Finite Element Method in Catia V5. The result of the analysis is shown in Figure 11.2. The internal stress does not reach the failure criteria of the components. The design is therefore validated.

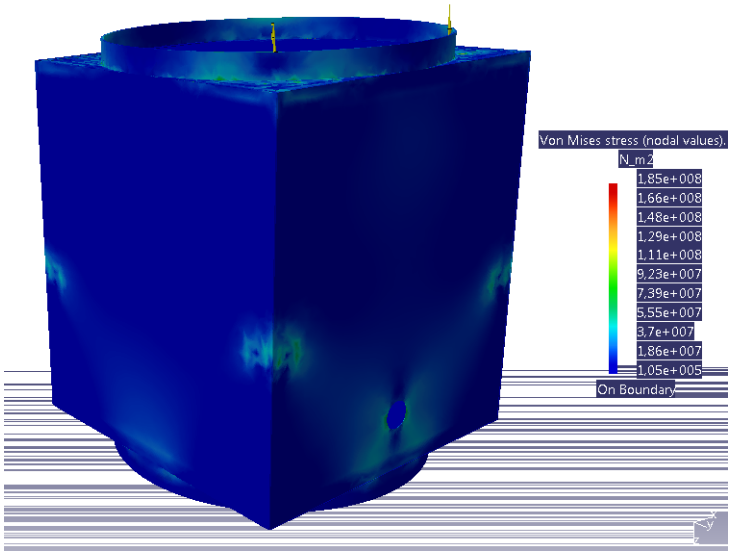

Figure 11.2: Finite element model of launch loads applied on the spacecraft body. The structure's stresses are tested on static Von Misses criteria, which represents the yielding of the material.

Chapter 12

Sustainability

Designing a sustainable mission is in the interest of everyone in the space industry. An important component of that is space debris. Due to negligence in the early days of space operations, many satellites which are not fulfilling any purpose are now orbiting uncontrollably in space, endangering other missions operating in the same orbits. A collision of satellites usually causes them to shatter into many pieces which have the potential to harm or even shatter another satellite. This can lead to an undesired snowball effect.

In order to prevent the situation from becoming worse, the United Nations Office for Outer Space Affairs [37] has introduced space law which dictates that each satellite launched shall not remain in orbit for longer than 25 years after its end of life. This can be done in 2 ways. One option is de-orbiting the satellite, which means bringing it to an altitude that is low enough so the satellite can re-enter the earth's atmosphere after 25 years or less. If this is not possible or unfeasible, nonoperational satellites may be moved to a graveyard orbit, which is located more than $300km$ above GEO. Looking at this mission and the orbital altitude at which it is initiated, it should be obvious that a graveyard orbit is not an option.

Therefore, this chapter describes how the orbital lifetime of this mission was determined and whether or not a sustainability plan is needed. If the satellite de-orbits after less than 25 years, no extra end-of-life manoeuvre needs to be accounted for.

12.1 Atmospheric Model

The orbital lifetime of a satellite depends on multiple factors. One of them is the atmospheric density at the satellites location. Unfortunately, the density in space can vary quite a lot (up to a factor > 10) due to multiple factors. Just like on earth, it varies with altitude. In addition to that, latitude, longitude, solar flux and magnetic flux affect the density as well. An atmospheric model based on mass spectrometer data and incoherent scatter radar data released by the US naval research laboratory in 2000 was used for this simulation [38]. The Matlab aerospace toolbox provides this model as a function of the aforementioned density influencing factors [39].

It uses the above mentioned factors as inputs and returns the density in $\frac{kg}{m^3}$. For simplicity, these values were averaged over latitude and longitude, so a constant density with respect to altitude was obtained which only depends on magnetic and solar flux. Historical data on magnetic and solar flux was obtained from the NOAA website [40]. It was used as an input under the assumption of equal or similar flux behaviour in the future. The averages, maxima and minima of both data sets were calculated using a simple Matlab code and then used to make various .txt files which contain a list of densities and their respective altitudes in steps of 1km.

12.2 Orbital Lifetime Prediction

The main part of the orbital decay computation is a Matlab code which reads one of the density .txt files and takes the satellite's area to mass ratio $\frac{A}{m}$, the drag coefficient C_D and the initial orbital altitude as inputs. Using orbit theory explained later in this section, it computes the time it takes for the satellite to reach an altitude of $100km$ in days and years. A satellite reaching an altitude of $100km$ is considered

"de-orbited" as it is the altitude at which space officially begins/ends. From here on, the satellite will soon begin to burn up.

The program computes the orbital decay rate in $\frac{m}{s}$ and multiplies it with a time step. This time step is chosen relatively to the orbital period because a small time step would cause the program to run for a long time and a large time step would cause large errors at lower altitudes. The resulting distance is subtracted from the current orbital altitude and the computation is repeated until an altitude of $100km$ is reached. The times and altitudes are saved in an array and plotted as can be seen in Figure 12.1. The decay rate depends on the ballistic coefficient B, orbital velocity V, orbit radius R_o, local density ρ and the co-rotation and wind correction factor F defined by King-Hele [41] [42]. The ballistic coefficient is a geometric parameter of the satellite, depending on its area to mass ratio and its drag coefficient. 'F' depends on the inclination of the satellite's orbit. It is 1 for polar orbits (so $i = 90°$) and decreases with decreasing inclination. The value is read of a graph obtained from King-Hele.

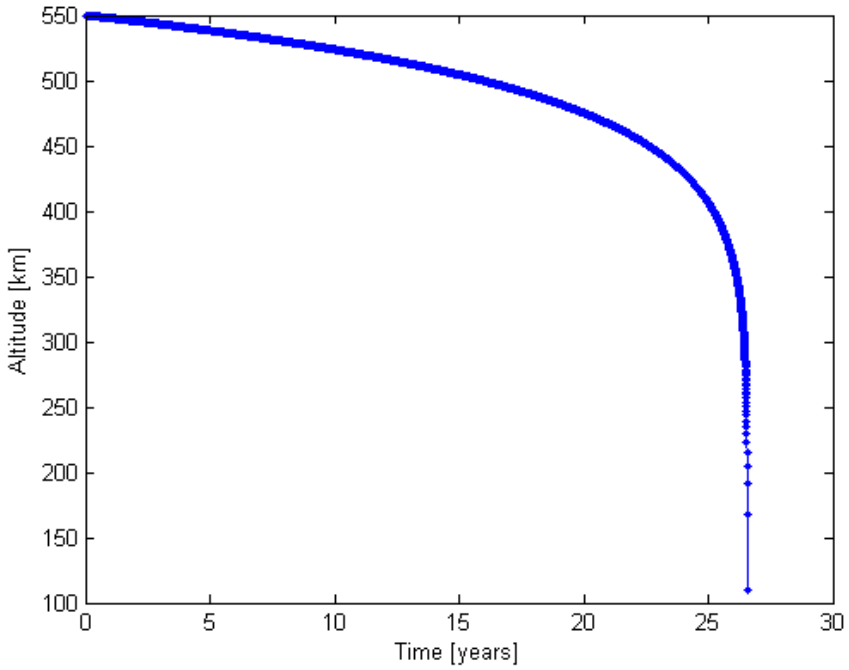

Figure 12.1: Sample graph of an orbital decay with $\frac{A}{m} = 0.01$, $C_D = 2.2$, $h_0 = 550km$, minimal solar and magnetic flux.

In order to obtain the altitude dependent orbital decay rate with respect to time, the first step is the basic drag formula as shown in Equation 12.1.

$$D = \frac{1}{2}\rho V^2 C_D S \tag{12.1}$$

where S in this case is later referred to as the satellite area in flight direction A_u, V is the orbital velocity, ρ is the local density and C_D is the drag coefficient. Knowing that $F = ma$, m being mass and a being acceleration, the formula can be solved for a_{drag}, which will be negative because the drag force causes a deceleration. $\frac{C_D S}{m}$ will from now on be replaced with B. Notice that the radius R_o is used in all equations using the assumption of dealing with circular orbits. Therefore the deceleration due to drag is indicated in Equation 12.2.

$$a_{drag} = \frac{1}{2} B \rho V^2 \tag{12.2}$$

and orbital relations, it follows that the change in radius due to drag over an orbital period is given by

Table 12.1: Observed and computed Orbital Decay based on Norad TLE data.

Date	**Observed Decay [m]**	**Computed Decay** [m]
14.04.2010	5.88	5.2522
20.09.2010	5.69	5.2380
05.04.2011	30.89	31.6630
03.08.2012	26.48	27.4778
22.12.2013	75.0496	76.1391

Equation 12.3.

$$\Delta R_{o_{drag}} = -2\pi B \rho R_o^2 \tag{12.3}$$

The formula for orbital velocity, is then indicated in Equation 12.4.

$$V = \sqrt{\frac{\mu}{R_o}} \tag{12.4}$$

Furthermore, the formula for the orbital period is shown in Equation 12.5.

$$P = 2\pi \sqrt{\frac{R_o^3}{\mu}} \tag{12.5}$$

The final equation, which represents the change in orbital radius with time, is shown in Equation 12.6.

$$\frac{dR_o}{dt} = -\frac{R_o^2 B \rho F V^3}{\mu} \tag{12.6}$$

Equation 12.6 is what the code finally uses in the loop. All parameters and constants use meters, kilograms, seconds and Newtons as units to ensure consitency.

12.3 Verification and Validation

In order to validate the code, data from existing space missions was obtained and compared to results produced by the simulation. Norad Two-Line-Element (TLE) data gathered and provided by Dr.ir. E.J.O. Schrama contained the necessary inputs for the code and actual decay data. The mean motion was used to derive the orbital altitude. Inclination, right ascension of ascending node and mean anomaly were used to determine the satellite's current latitude and longitude. Using 2 different data points, which provide the precise time at which they were taken, the time step and decay were obtained. Multiple sets of data points were randomly chosen out of the list. Here the GRACE 1 data set was used because information on its ballistic coefficient was found online [43]. Using the magnetic and solar flux values for the respective dates from NOAA [40], the computed decay differed slightly from the actual decay. A list with several data points and their computed/observed decay in meters can be found in Table 12.1

Deviations can be explained by the fact that the solar flux data is already averaged over an entire month, which does not exactly conform with the "atmosnrlmsise00" inputs. Additionally, the GRACE orbit was assumed to be completely circular ($e = 0$) and polar ($i = 90°$). In reality, the orbit has an inclination of 89° and an eccentricity varying between 0.0005 and 0.002, however these small deviations were assumed to be negligible.

Another error source is the large time step. Due to the TLE data points being taken less than daily, the time step multiplied by the decay rate is quite large and the decay rate is assumed constant over that time. To correct for this, the average decay rate is used between 1st and 2nd TLE point, which shows little to no difference for old data points (i.e. in 2010) but corrects the results quite substantially for the years 2013 and 2014. This shows that a sufficiently small time step needs to be used at low altitudes.

A last possible error source is the ballistic coefficient. This spacecraft parameter usually takes several measurements so it can be approximated because the C_D of a satellite is not determinable using methods

like wind tunnel tests for example. However, the decay data of the satellites can be gathered and used to determine the actual ballistic coefficient of the satellite. From this, the C_D can be derived and accurately determined as reference for similar future satellites.

Computing the decay rate for the SKY-FI mission yielded a decay time of 13.96 years using averaged magnetic and solar flux values and a ballistic coefficient of $B = 0.017 \frac{m^2}{kg}$ with an assumed $C_D = 2.2$. After 7.95 years, the satellite reaches an altitude of $500km$, which is the minimum operational altitude. Hence, the satellite needs to accommodate for an extra delta V budget to maintain a sufficient altitude until its end of life. This is explained in more detail in Chapter 13.

These results imply that there is no need for an additional sustainability plan when it comes to orbital lifetime. The satellites will "take care of themselves" within a sufficient amount of time. Regarding collision avoidance, the satellite will accommodate extra fuel to perform collision avoidance manoeuvres, which is also further elaborated upon in Chapter 13.

Chapter 13

Propulsion

In order to ensure that the satellites will fulfill their purpose of maintaining 90% coverage, a propulsion subsystem should be designed. This propulsion subsystem should provide enough delta-V for debris avoidance, constellation maintenance and orbit maintenance. Since the decay of the satellites is shorter than 25 years (even with the minimum solar spectrum), end of life delta-V is not needed.

13.1 Delta-V Budgeting

The three different manoeuvres needed are debris avoidance, constellations maintenance and orbit maintenance. Debris avoidance is needed due to the fact that there is a possibility that the satellite will have a collision and that has to be prevented. The constellation maintenance is needed to meet the requirements of coverage. The orbit maintenance is needed since it takes 8 years to reach the altitude of 500 km. At 500 km the coverage requirement is barely met. Thus the satellite cannot meet the requirements below 500 km. So the orbital maintenance delta V has to be designed so that the altitude after 10 years is 500 km.

13.1.1 Collision Avoidance

To determine the amount of delta-V needed for collision avoidance, first the probability of a collision per satellite has to be determined. This is done using the flux (Impacts/m^2/year) calculation [44]. The flux is calculated using Equation 13.1. The full derivation of this equation can be found Anderson [44].

$$F = H\,\phi\,\psi\,(F_1\ g_1 + F_2\ g_2) \tag{13.1}$$

Where all the right side variables except ψ are a function which are explained in Equations 13.2. ψ is a relation between the inclination and the flux, which has a value of 1.70 for 82 degrees inclination [44].

$$H = \sqrt{10^{e^{-(log_{10}(d)-0/78)^2/0.637^2}}} \tag{13.2a}$$

$$\phi = \frac{\phi_1}{\phi_1 + 1} \tag{13.2b}$$

$$\phi_1 = 10^{\frac{h}{200} - \frac{S}{140} - 1.5} \tag{13.2c}$$

$$F_1 = 1.22\ 10^{-5}\ d^{-2.5} \tag{13.2d}$$

$$F_2 = 8.1\ 10^{10}\ (d + 700)^{-6} \tag{13.2e}$$

$$g_1 = (1+q)^{23}\ (1+q')^{t-2011} \tag{13.2f}$$

$$g_2 = 1 + p\ (t - 1988) \tag{13.2g}$$

Where d is the orbital debris diameter in cm, t is the date in years, h is the altitude and S is 13-month smoothed solar radio flux in 10^4 Jy.

The orbital debris has a critical size of 1 cm [9]. This is due to the fact that at this size the subsystems are at danger. Smaller sizes can only damage the solar cells can make these produces less power. From this size and assumed that the average year the constellation is active is 2020, the flux can be calculated. Which is Flux = 2.2417 10^{-4}Impacts/m^2/$year$.

From the position accuracy of the satellite that is needed for SAR, a maximum positioning error of 14 meters is found. Thus the critical area for the flux is $28 \times 28m^2$, and the life time is 10 year. In Figure 13.1, the impacts can be seen depending on the size of the orbital debris. Since a critical debris size of 0.5 cm is chosen. There will be 1.76 possible impacts over the life time of a satellite.

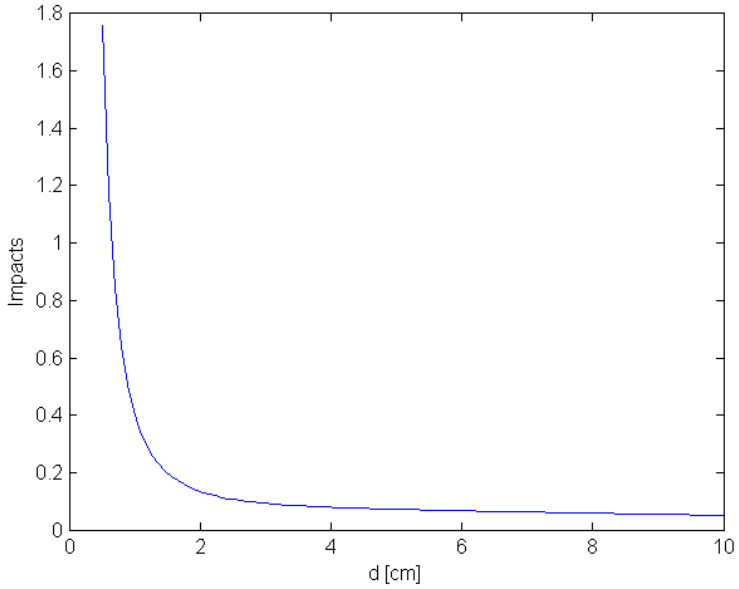

Figure 13.1: Number of impacts as a function of orbital debris size.

Yet due to the fact that the orbital debris also have an uncertainty, it is assumed that 3 debris avoidance maneuvers have to be done over the lifetime of a satellite.

From the fact that for the maneuver an average 250 meters altitude change has to be done, the delta V can be calculated using Equation 13.3. Where r_1 is the departure circular radius, r_2 arrival circular radius and μ is the standard gravitation parameter. From this it can be found that the delta V for debris avoidance will be 1.65 m/s.

$$\Delta V_{hohmann} = \sqrt{\frac{\mu}{r_1}}\left(\sqrt{\frac{2 \times r_2}{r_1 + r_2}} - 1\right) + \sqrt{\frac{\mu}{r_2}}\left(1 - \sqrt{\frac{2 \times r_1}{r_1 + r_2}}\right) \tag{13.3}$$

13.1.2 Constellation Maintenance

In order to maintain the constellation, and thus the 90 % coverage requirement, the satellites' position with respect to one another has to remain almost the same. For GEO satellites, this means that the Sun's gravity affects the inclination shift [7]. For LEO satellites this effect is negligible, as the effect is caused by the synchronicity with the sun [7]. The relative position can change due to unexpected events, and these events cannot be simulated. The events are expected to affect the decay time, and thus to take them into account, it is assumed that the C_d of a satellite is 20% higher than a other satellite. This will cause the orbital life time to decrease. The result of this different C_d value can be seen in Figure 13.2.

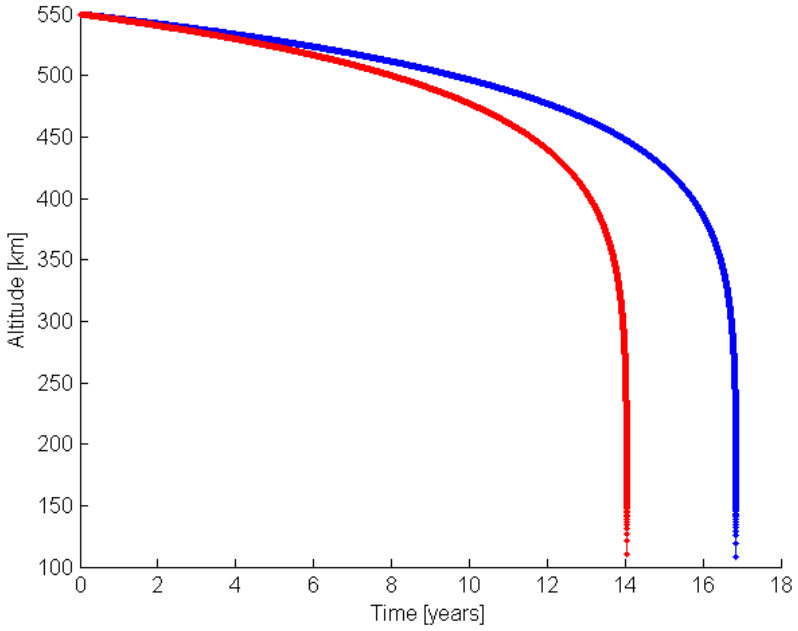

Figure 13.2: Decay of satellites with normal C_d in blue and with an increase of 20%C_d in red.

To counter this faster decay, a Hohmann transfer has to be done with an altitude change of 500 m. From Figure 13.2 it can be seen that this maneuver has to be done for 15 times. The calculation for the delta V can be seen in Equation 13.3. This results in a necessary delta V for the constellation maintenance of $4.1\frac{m}{s}$.

13.1.3 Orbital Maintenance

Since the orbital life time of the satellites has to be 10 years, as can be seen in the requirement table 1.1. As previously said, minimal altitude the system still meets its requirements is 500 km, which is after 8 years. A delta V has to be done to make sure the satellites reach 500 km after 10 years in stead of 8 years. This is done by small delta V from 549 km t 550 km. This has to be done for the first 2 years, 10 times every 0.20 years, at the beginning of life. From Equation 13.3 it can be found that the delta V for orbital maintenance is $4.39\frac{m}{s}$.

From this a simulation can be made as seen in Appendix A.7

13.1.4 Verification

The separate parts of the flux calculation can be done by hand. From this it is found that there is no error in this part of the simulation. The delta V calculation is based on a Hohmann transfer, which was also calculated by hand and the simulation was proven to be correct. This results in that the code has been verified.

13.2 System Selection

From the previous section it is found that the total delta V that is needed is $11.67\frac{m}{s}$ (with a 15% margin). Taking this delta V into account, it is possible to design and trade-off between different propulsion systems.

13.2.1 Propulsion System Trade Off

First the trade off can for the propulsion system can be made. The different propulsion systems can be seen in Figure 13.3. As can be seen here is that there is one main difference between the different design

options.

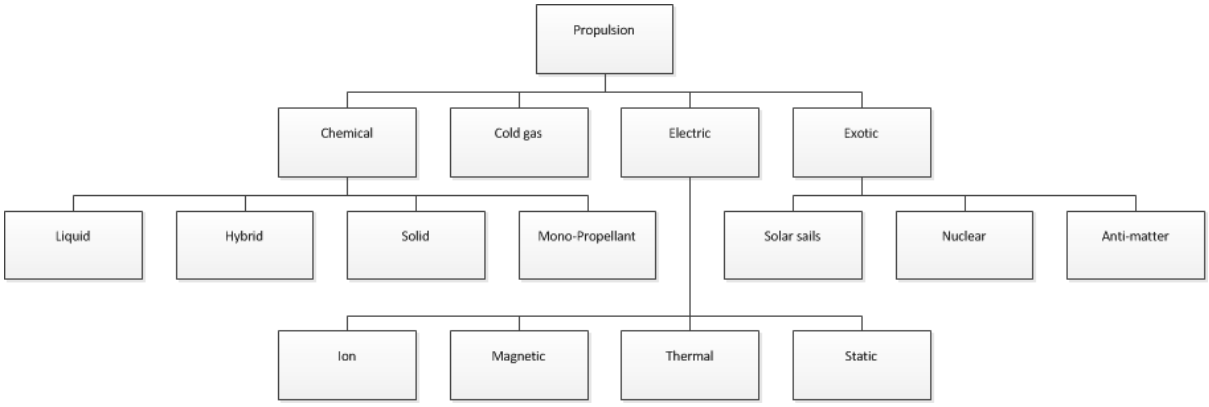

Figure 13.3: Design Option Tree for the propulsion subsystem.

The propulsion system can be cold gas, chemical (liquid, hybrid, solid, and mono-propellants), electric (ion, magnetic, thermal, or static), or exotic (solar sails, nuclear, antimatter).

Considering the monetary and time budget of the mission, exotic propulsion systems were quickly discarded, due to their low technology readiness level (a measure of what stage of development a system is) and high costs. It is not feasible to incorporate them in a large number of LEO satellites in the near future.

In order to compare the different systems, a figure of merit has to be stated. The specific impulse, I_{sp}, is a measure of the energy content of the propellants and how efficiently they are converted to thrust [3]. Therefore with a higher I_{sp} a smaller propellant mass is required to achieve the same thrust. This does not imply that the propulsion system with the highest I_{sp} is the lightest, as the specific impulse does not take into account the dry mass of the propulsion system. Using the I_{sp}, the propellant mass can be found through Tsiolkovsky's rocket equation 13.4

$$M_{prop} = M_{dry} \times \left(1 - 1/e^{\frac{\Delta V_{total}}{I_{sp} g_0}}\right) \tag{13.4}$$

This equation consists of several variables, including the specific impulse, the mass of the propellant, M_{prop}, the satellite dry mass (everything except for propellant), M_{dry}, the total velocity increment required for orbital maneuvers, ΔV_{total}, and the gravitational acceleration at sea-level, g_0. The only variable that has influence on the propellant mass for different propulsion systems is the specific impulse.

In order to select the best available propulsion subsystem, different criteria had to be selected, the combination of which will specify which system has the best characteristics. How these values are evaluated will be explained in Section 13.2.2. Three of the trade-off criteria are based on the physical limitations of the spacecraft, which are mass, volume and power. The lower these values, the better the system. Furthermore, the quicker the satellite can enter a new orbit, the better it is, because the communications subsystem is turned off while thrusting.

The choice rests on either cold gas, chemical, or electric propulsion system. From the chemical thruster family, the monopropellant, bipropellant, and hybrid thrusters were considered, as the solid rocket propulsion does not provide re-ignition or throttling. Unfortunately, satellite hybrid thruster data was too difficult to find, and therefore it is not considered anymore. The electric solid propellants are not flight tested yet [45]. On the other hand, for electric propulsion, either a resistojet or Hall Effect Thruster (HET) are the choices that are simple enough to be considered for this space mission.

13.2.2 Trade-off calculations

This section will explain how all the values in Table 13.1 are determined or found. To start off, the specific impulse, power and thrust are all given in the thruster's respective datasheets [46–49]. The only two trade-off criteria that aren't given are the total volume and mass, which will be estimated through preliminary equations. The only conclusion that could be made thus far is that the power consumed by

Table 13.1: Trade-off for various propulsion systems.

Type of propulsion	Estimated total mass $[kg]$	System volume $[cm^3]$	Specific Impulse [s]	Power use $[W]$	Thrust $[N]$
N_2 Cold Gas	2.3	35000	66	8	0.05
Mono-propellant [46]	2.5	4000	220	18	1
Bi-propellant [47]	3.6	6000	275	40	4
Hall-Effect [48]	1.2	3500	1300	300	0.015
Resistojet [49]	2	22000	99	30	0.1

the HET as found in [48] is about 1.6 times as much as the total system power, and therefore fails the trade-off.

From the propellant mass and type of system, the total propulsion subsystem mass can be estimated. The total mass is a sum of the feedsystem, tank, propellant, and thruster mass. The propellant mass is calculated through Tsiolkowsky's equation 13.4. The thruster mass was found through the supplier. For the tank mass, there are no accurate calculations but there are estimations. After knowing the propellant mass, the propellant volume can be calculated for a density, then the tank thickness for a cylindrical tank can be estimated through Equation 13.5 (assumes thin walls) [3]. Here the yield stress of a material, σ_y, is related to the tank pressure, P_t, the radius of the tank, r_t, and the tank's wall thickness, t, through the use of a safety factor, γ.

$$\sigma_y \ \gamma = \frac{P_t r_t}{t} \tag{13.5}$$

A safety factor of 2 was taken to ensure no structural failures. Simply put, the tanks are cylinders with spherical bulkheads, and have uniform thickness to avoid stress concentrations. The tank sizes and masses were determined for each case individually. For cold gas and the resistojet it was simply N_2 gas at 50 bar. For the mono-propellant there is diazene (hydrazine mono-propellant) at 10 bar and a pressurant (N_2) at 50 bar that has enough volume to fill both the N_2 and mono-propellant tank at 10 bar. This volume was estimated through the ideal gas equation 13.6, and a 10% margin was added to account for a minimum pressure difference across the pressure regulator.

$$P_1 V_1 = P_2 V_2 \tag{13.6}$$

Where P is pressure, and V is volume. Case 1 is only the nitrogen pressure at start (50 bar) and the volume of the pressurization tank, while case 2 is the volume of the two tanks + the feed system in between, with a pressure at 10 bar. This led to a pressurization tank that is 0.275 times the size of the large tank. The same pressurization calculations are used for the liquid bi-propellant system. The liquid propellants (MMH and N_2O_4) are at 10 bar each, and a pressurant (N_2) at 50 bars. Lastly, this particular Hall-effect thruster uses Xenon gas, where the pressurization sustem can work with the same principle as the cold gas thruster (blow-down).

The last mass component to be determined is the feedsystem, which differs per thruster type. The liquid bipropellant system requires 2 pressure regulators, 2 check valves (to prevent backflow) and 3 normally closed valves in addition to the components present on the off-the-shelf thruster. This is much heavier than the simple blowdown cold gas/resistojet/Hall-effect thruster systems which do not require any feed system components aside from a normally closed valve (which is usually included in the thruster mass given in the datasheet). Lastly for the mono-propellant a only a single normally closed valve and pressure regulator are required (since the thruster already includes normally closed valves).

A lightweight pressure regulator that fulfills the requirements was found to weigh 0.47 kg [50]. To avoid additional weights of NPT, BSP, and metric thread adapters, it was chosen to use the same threads everywhere. Since Swagelok uses metric ends, the check valves and normally closed valves will be also metric. A normally closed valve of 0.33 kg that uses 18 W [51], was found, but it was decided to use the same supplier (Swagelok) for the feedsystem to ensure no leakages, misfits or other failures will be present. This led to a total mass of 0.82 kg for the mono-propellant feed system.

The last trade-off criteria is the volume, which was determined through the feedsystem and thruster datasheets, and tank volume calculations. To determine the tank volume, the propellant volume calculations were made by dividing the propellant mass (found through Equation 13.4) with the density of the gas/liquid at the 10-50 bar of pressure (as previously stated). The tank volume was then calculated using the thickness and dimensions obtained from Equation 13.5.

13.2.3 Final Propulsion Design and Operation

After finding the trade-off data, Table 13.1 can be filled in. The cold gas and resistojet thruster system are too bulky, while the Hall-effect thruster uses too much power. No retailer data of existing small satellite hybrid thrusters (under $5N$) was found. Therefore only the liquid bi- and mono-propellant were found to conform to these requirements. Now, from the table it can be seen that the hydrazine mono-propellant is the design choice for this propulsion subsystem, as it uses less mass, volume and power than the bi-propellant.

In order to fulfill the requirements, a mono-propellant propulsion system was chosen with off-the-shelf feed system components and thruster. The total propellant mass as calculated from the total ΔV and Tsiolkovsky equation (Equation 13.4) is 0.565 kg. At 10 bar, the density of hydrazine is 1.02 g/cm^3 which leads to a propellant volume of 554 cm^3. The hydrazine tank size found through Equation 13.5 to be 14 cm in length, 4.2 cm outer radius, and 1.5 mm wall thickness, leading to a tank volume of 567 cm^3 on the inside, while only 554 cm^3 are required for the hydrazine. This extra margin was added to account for residual fuel, and allow for proper fuel flow throughout its lifetime. The pressurization tank is a spherical tank with 4.2 cm radius which provides 278 cm^3 tank volume

The tanks will be made out of annealed titanium (Grade 4), which has good formability and high yield strength (590 MPa) [52]. The same tank material is used for the nitrogen pressurization tank. In addition to the hole required for the feed system, the pressurization tank will have an additional hole to which a pressure transducer is attached. This is required in order to determine the propellant left in the propellant tank.

The location of the thruster is on the center of gravity of the satellite to avoid moments due to thrust. Furthermore, only one thruster system will be used to save mass. When accelerating and decelerating the satellite for quick maneuvers, first the system will thrust in flight direction (accelerate into transfer orbit), then the ADCS will yaw the satellite 180° (rotation), and lastly, at the correct part of the orbit, the system will fire the thruster again (decelerate into new orbit). The rotation takes 700 secs as computed with the ADCS programme as described in Appendix A.5, while the thruster acceleration and deceleration take up need to make a delta V maneuver of maximum 0.55 $\frac{m}{s}$. This corresponds to 755 seconds in total, since the acceleration due to the thruster system is 0.01 $\frac{m}{s^2}$. This is less than half an orbital period, meaning that the orbit transfer maneuvers can be properly performed.

Chapter 14

Final Design

For the final design, a more detailed view of each component in the subsystems can now be presented. The table below gives the mass, power required and cost for them:

14.1 Budget Breakdown

Table 14.1: The mass, power and cost budget breakdown of the entire SKY-FI satellite.

Subsystem	Components	Quantity	Total Mass (kg)	Total Power (W)	Total cost ($)
ADCS	Magnetorquers (MT6-2)	4	1.2	2	32,000
	3-axis Magnetometer	1	0.2	0.7	11,000
	3-axis Gyroscope	1	Negligible	0.015	10,000
	Sun Sensors	5	0.15	0.18	4,890
	Coarse Sun sensors	2	Negligible	Negligible	2,000
	ADCS Computer	1	0.35	0.12	8000
Subsystem Estimated Total			1.9	3.015	59890
Propulsion	Monopropellant (Hydrazine)	-	0.59	0	310
	Thruster MR103G	1	0.33	0.2	25000
	Tank (MP)	1	0.27	0	10500
	Tank (pressure)	1	0.2	0	12500
	N2 gas	-	0.009	0	100
	Check Valve	1	0.2	0	1000
	Pressure Regulator	1	0.47	0	2000
	Normally closed Valve	1	0.3	0.1	1000
	Pressure Transducer	2	0.2	0.1	1000
Subsystem Estimated Total			2.569	0.4	52410
Power	Batteries	112	10	-	42000

	Battery Management System	1	1	-	37660
	Solar Panels	108	12.75	-	216000
	Power Management Unit	1	4	0	15200
	Micro Stepper Motor	2	0.1	-	1000
	Hinge	2	0.3	-	1750
Subsystem Estimated Total			28.15	0	313610
Communication Subsystem					
User Link Transponder S-band	Input Ancillary	1	0.3	-	-
	RCVR LNA	1	0.4	1.8	-
	RCVR DC+ LO	1	0.5	11.0	-
	Input Ancillary	1	0.2		-
	DEMUX, single channel	7	1.2		-
	TWT RAD	2	2.5	6.4	-
	EPC Single	2	2.4	0.7	-
	MUX, single channel	7	3.3	-	-
	Output Ancillary	1	1.0	-	-
	Interconnects	1	4.7	-	-
Main Link Transponder Ku-band	Input Ancillary	1	0.3	-	-
	RCVR LNA	1	0.4	1.8	-
	RCVR DC+ LO	1	0.5	11.0	-
	Input Ancillary	1	0.2	-	-
	TWT RAD	2	2.5	9.7	-
	EPC Single	2	2.4	1.0	-
	Output Ancillary	1	1.0	-	-
	Interconnects	1	4.7	-	-
Inter Satellite Link Transponder Ka-band	Input Ancillary	2	0.6	-	-
	RCVR LNA	2	0.7	3.6	-
	RCVR DC+ LO	2	1.1	22.0	-
	Input Ancillary	2	0.3	-	-
	TWT RAD	2	3.0	18.3	-
	EPC Single	2	2.4	1.9	-

	Interconnects	2	4.0	-	-
Subsystem Estimated Total			40.6	89.2	1200000
Antennas	Patch Antennas	1	0.1	0	5000
	Parabolic Antennas	7	2.1	0	59500
	Inter-satellite Antennas	4	0.8	0	28000
Subsystem Estimated Total			3	0	92500
Command & Data Handling	C&DH Computer	1	2.02	0	270300
Thermal	Heat Patches	2	2	0.4	100000
	Multi Layer Insulation	2	3	0	65000
Subsystem Estimated Total			5	0.4	33000
Structures	Walls	6		0	-
	Columns	4		0	-
	Launch Attachment Rings	3		0	-
	Support Structures	-		0	-
Subsystem Estimated Total			22	0	350000
System Total			103.34	102.32	2101410

From the table, it can be seen that each satellite would weigh 103.34 kg, require a total power of 102.32 W throughout its operation, and would cost $714,204 for its development. Note that the power management unit contribution in terms of energy consumption adds 10% to the total satellite power usage. This would qualify the final design as a small satellite, and the corresponding value of its required power and cost are ones to be expected for other small satellites with similar purposes.

However, the required power and mass in the final design shows a very different and much higher value than the one estimated in the midterm report. The main reason for this is that the amount of electronics the communication architecture needed to fulfill the requirements was severely underestimated. As such, the mass and power required by all these parts become much bigger than even the total estimated mass and power of the whole satellite designed in the midterm report. This effects the other subsystems as well and causes their mass and power consumption to increase as well. For example, the higher power demand of the communication means that the number of batteries and the size of the solar panels needs to be increased significantly, which leads to a significant increase of their mass as well.

Another crucial part of the budget breakdown table is the cost budget. As elaborated in the market analysis section, with a total development cost of $714,204, this value should be enough to still be less than the provided budget of €500M. However, compared to the more definite value of the mass and required power of each satellite, some costs of the components are just estimated and yet to be validated. While the power subsystem and the ADCS subsystems cost values are known for sure, other subsystems, in particular the communication part, are mostly estimated compared to other satellites with similar purposes. Off-the-shelf components are available online for both the ADCS and the power subsystem, which is why their cost can be predicted more precisely. On the other hand, for some other much more specific parts, the cost cannot be accurately determined without actually ordering the parts themselves.

Another important remark regarding the cost budget is that the costs listed above are solely for material costs; it does not include the costs for man-hours and assembly. As the components and the assembly are very complex, the cost to employ the experts and the necessary tools needed for this will be quite expensive, even more than the material cost of $2.1M. It is assumed that this will cost around

$2.5M, which brings the total cost for each satellite to $4.6M. However, this cost per satellite is still within the given budget of €500M, especially since the cost of production can be reduced as more parts are assembled, so they will not be as expensive as the first satellite cost mentioned here.

With the final design known, a CATIA drawing is made in order to provide a better illustration of what the satellite will look like. This is done in Figures 14.1 and 14.2, where the latter is rendered with the outer panel taken out in order to show how the various subsystems will fit together inside the satellite:

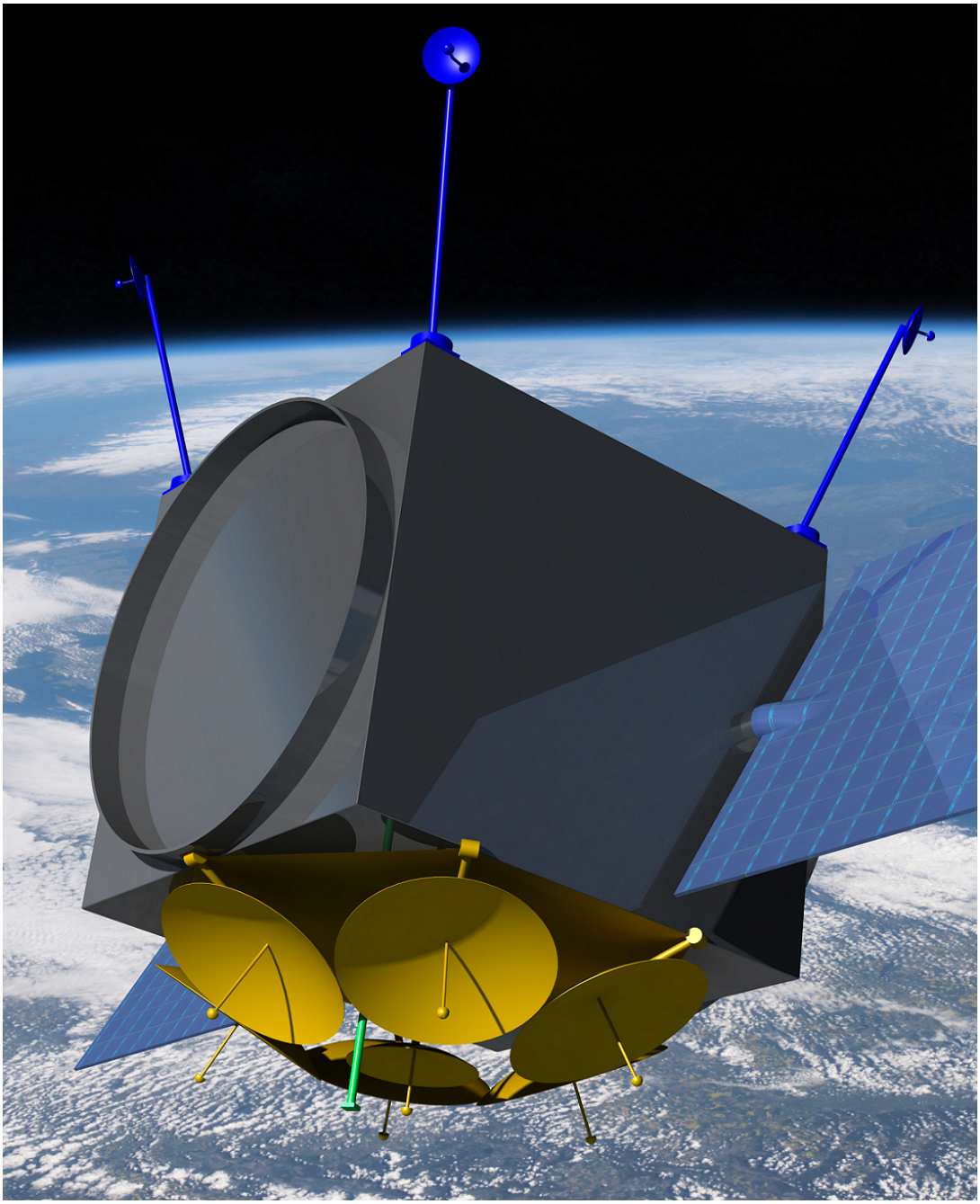

Figure 14.1: Full satellite with yellow antennas for ground coverage, blue for crosslink and green for ground station.

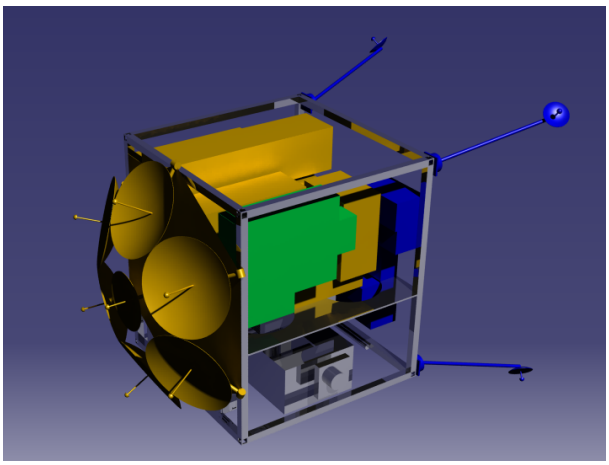

Figure 14.2: Inside of the Satellite with yellow antennas for ground coverage, blue for crosslink and green for ground station.

Chapter 15

Requirement Compliance Matrix

The requirements are shown in Chapter 1, from this the requirement compliance matrix can be made, this can be seen in table 15.1. As can be seen in the requirement compliance matrix, not all the requirements are met. It has been mentioned in Section 4.2 that apllication for ITU freqencies has not been part of the scope of this project. Furthermore, the cost associated with obtaining these frequencies was not included in the Section 14.1. Since it is a killer requirement, negotiations with ITU need to start as soon as possible during the post-DSE phase.

Table 15.1: Requirements compliance matrix.

Requirement ID.	Description	Req. Level (Rating)	Check	Value
Req-Top-1	The system shall be able to connect the user to the Internet.	Top-Level(Key)	✓	-
Req-Top-2	The system shall provide full coverage of the earth at any time with success rate of 90%	Top-Level	✓	94%
Req-Top-3	The system shall be able to transmit text messages at a data rate of 1 kilobit per minute	Top-Level(Key)	✓	1 kilobit per minute
Req-Top-5	The system shall be able to connect a phone call or send a picture at a data rate of 10 kilobit per second	Top-Level(Key)	✓	10 kilobit per second
Req-Top-6	The whole system's operation time shall be 10 years	Top-Level(Key)	✓	10 years
Req-Top-7	A portable device with an omnidirectional antenna shall be able to establish communication to the space segment when there is a non-obstructed field of view	Top-Level	✓	20 degrees ϵ
Req-Top-8	The system shall be realized within an initial (virtual) budget of 500 M€.	Top-Level (Killer)	✓	468.6 million
Req-Top-9	At the end of its life, the spacecraft shall have a minimal impact on the space debris density	Top-Level(Driving)	✓	-
Req-Top-10	The spacecraft shall comply with the ITAR regulations	Top-Level	✓	-

Req-Top-11	The spacecraft shall comply with the ITU regulations.	Top-level (Killer)		-
Req-Top-12	The system shall be able to locate the user within a 2 km radius within 1 hour.	Top-Level (Driving)	✓	$8.3m$ in 8.2 min
Req-Top-14	The user shall be able to successfully connect to the system within a period of 15 minutes.	Top-Level	✓	13 min max no connectivity
Req-Sys-1	The satellite shall de-orbit 25 years after End-of-Life.	System Level (Driving)	✓	5.9 years
Req-Top-6	The whole system's operation time shall be 10 years.	Top-Level	✓	10 years
Req-Sub-Payl-1	The payload shall provide a maximum data rate of 0.49 Mbits/s.	Subsystem-Level (Key)	✓	0.49 Mbits/s
Req-Sub-ADCS-1	The ADCS shall have a pointing accuracy of 5° with 3 sigma in 3 axes for the communication system.	Subsystem-Level	✓	5°, 3σ

Part II

Operations Management

Chapter 16

Launch Vehicle and Site

In this chapter, the launch vehicle will be selected first, and afterward the adapter and possible launch sites for this launcher will be chosen. Lastly, the launch window will be determined.

16.1 Launch Vehicle

In this section, the launch vehicle will be chosen from selected possible options. Afterward, the satellites will be placed in this launch vehicles by use of adapters, and the excess mass and volume will be determined for piggyback satellites to reduce the launch cost.

16.1.1 Launch Vehicle Selection

For the launch vehicle several possibilities were checked. These possibilities are traded off by looking at launch cost and the payload mass. A list of possible launch vehicles and their cost and payload mass (for the same altitude) can be seen in Table 16.1 [53–55].

Table 16.1: Launch vehicles cost and payload mass to LEO

Launcher	Cost [Million $]	Payload mass to LEO [kg]	Reliability [successful/total launches]
Rockot	20	1950	24/26
Epsilon	38	1200	1/1
Minotaur-C	20	1320	6/9

The cost of the Rockot launch vehicle was found to be 14 Million USD in 1999 through [56]. Taking into account inflation to 2015, the cost becomes 19.8 Million USD today. For the Epsilon and Minotaur-C, contemporary values were found, and thus did not have to be adjusted for inflation. From this table it can be seen that the Rockot launcher has to highest payload mass to LEO while still having the lowest cost. This can be (partly) attributed to the fact that the launch vehicles are old Russian missiles that are modified to be used as launch vehicles.

16.1.2 Rockot Launch Vehicle

For launch vehicles, the payload mass is dependent on the altitude the payload has to be launched. This can be seen in Figure 16.1. Since the inclination is 82 degrees, the payload mass of this launcher will be approximately 1550 kg. The payload fairing has an useful internal diameter of 2.1 m x 2.38 m and a height of 3.7 m.

Since a launch vehicle can only launch in a single plane, 12 satellites have to be launched per satellite. This means there would be 11 satellites in operation with one satellite as a spare satellite. This spare satellite will also get an additional delta V of 1 m/s to be able to get to the needed position in that

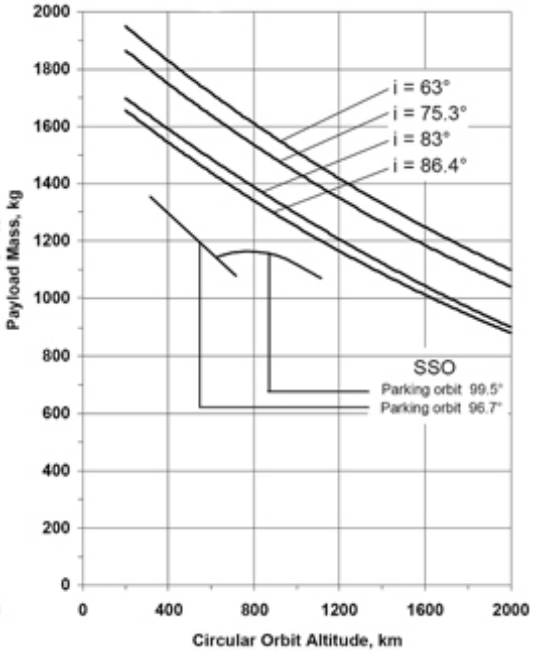

Figure 16.1: The possible payload mass with respect to altitude for the Rockot launch vehicle. Each line represents different orbit inclination.

plane. The spare satellite will also be at an slightly higher beginning altitude of 570 km to be able to easily go to a designated location within the orbit without using too much delta V. This will result in a total satellite mass of 1233 kg.

The satellites have a dimension of 0.59 x 0.59 x 0.67 meter. From the launcher dimensions seen in Figure 16.2, the satellites can be placed in a volume and mass efficient manner in the launcher.

From the launch guide an example of an adapter can be found for three satellites, which is found in figure 16.3. For this mission, it is possible to fit four satellites in one adapter. Since 12 satellites have to be launched per launcher, either three small adapters will have to be placed on top of each other, or one big adapter will be made for this. This can be seen in Figure 16.5 and Figure 16.4. The total adapter mass will then be approximately 150 kg [3].

This will result in a total payload mass of 1383 kg, which means 167 kg of mass is left for piggyback satellites. As can be seen in Figure 16.5, there is still some volume left under, above and next to the satellites . Although the adapter does have to be adapted to the piggyback satellites if they are placed next to the satellites, there will be enough volume to fit the piggyback satellites. This will decrease the cost of the launch, as the additional satellites will pay a part of the launch cost.

The Breeze upper stage of the ROCKOT launch vehicle will ensure the right inclination, altitude, plane spacing and satellite spacing. The satellite spacing is ensured by the adapter. The satellites will be locked in the adapter by a spring lock, which will be unlocked with a certain time slot.

As stated, a single launch costs 19.8 million USD in 2015 (14 million in 1999). Using a mass ratio of the SKY-FI payload over the total launched payload, and multiplying that with the 19.8 million yields a value of 17.7 million USD per launch, as seen in Equation 16.1.

$$Cost_{reduced} = \frac{M_{SKY-FI}}{M_{PayLauncher}} \times Cost_{2015} = \frac{1383}{1550} \times 19.8 = 17.7 \tag{16.1}$$

The launch cost is therefore 17.7 million USD.

16.2 Launch Site

In picking the launch site, it's critical that the launch can reach the required inclination of 82 degrees. Furthermore, the possible launch sites are also limited to the ones that are capable of launching the chosen Rockot launch vehicle. Under these conditions, from figure 16.6 it can be seen that only Plesetsk

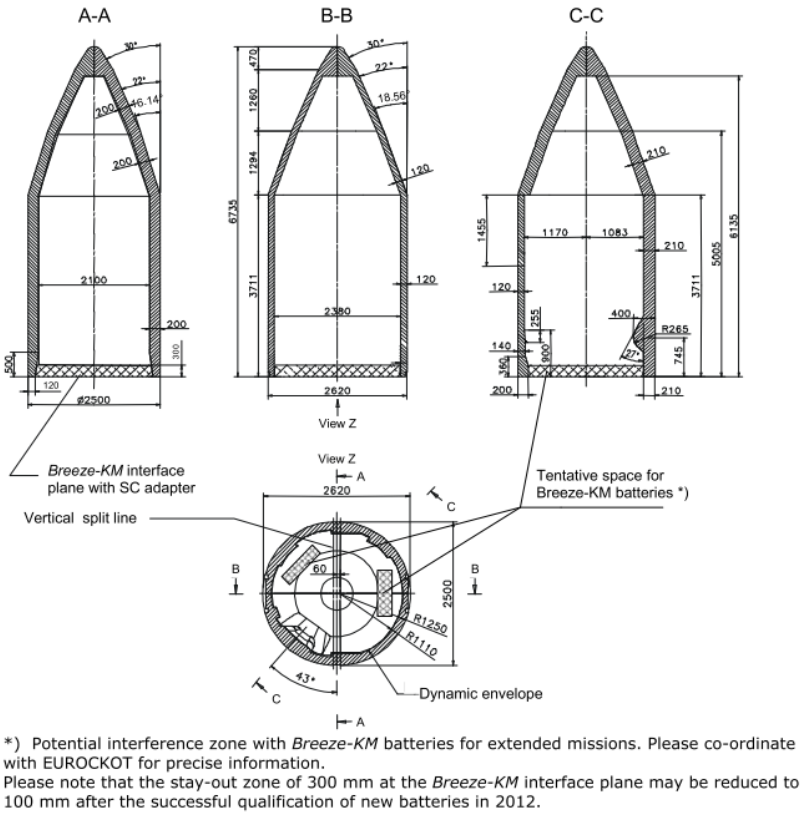

Figure 16.2: Maximum usable payload envelope of the Rockot Launcher, all dimension given in mm [35].

and Baikonur spaceport are able to launch at that inclination. However, since launch site Baikonur is not able to launch the Rockot launch vehicle, this leaves the launch site of Plesetsk cosmodrome to be selected [35].

16.3 Launch window

Since a launch constellation has to be made, the launch windows are very important to ensure that the constellation have proper plane spacing. From the orbital characteristics of the satellites, it is found that after one day the drift is 360 degrees which means that after single day, the plane is at the same location as the day before. This drift is used in order to retrieve the right time it takes between launches to reach the right plane spacing. The lane spacing is then found to be 11.8 degrees since the drift after one orbit equals 23.9 degrees. The next launch has to be after $\frac{11.8}{23.9} \times Period$, which is after 47.18 minutes.

It is obviously not possible to launch 19 satellites on the same day with a 47 minute spacing between each launch. Since the satellites will be at the same location after one day, the launches can be done consecutive after a x number of days and 47 min. Thus for each orbit the launch window is known, but the day of the orbit is not known yet since there are no reference about how long it will take to make the launch site ready for a second launch.

Since the constellation needs to be very close to each other, the launch windows needs to be small, and thus decided to be 20 minutes. Using this launch window, the upper stage can reach this designated plane location. Having this means the launch schedule can now be made, as shown in Table 16.2. The launch schedule can be changed if the storage of the satellites is not possible to launch such an high amount of satellites in such a short time span. Another reason why it could be changed is the availability of the launch vehicle, launch sites or the satellite parts. To counter this problem, either the spacing between launches can increase by a day or after a couple of launches (depending on the storage room), a break of x amount of time can be made to manufacture the new satellites or launch vehicles.

If the launch has to be postponed (for instance, due to bad whether), the launch day can just be

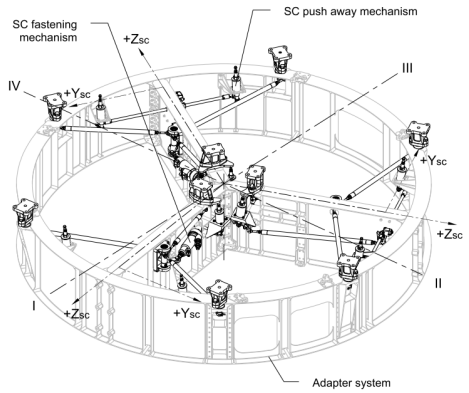

Figure 16.3: Example of a ROCKOT adapter for three satellites.

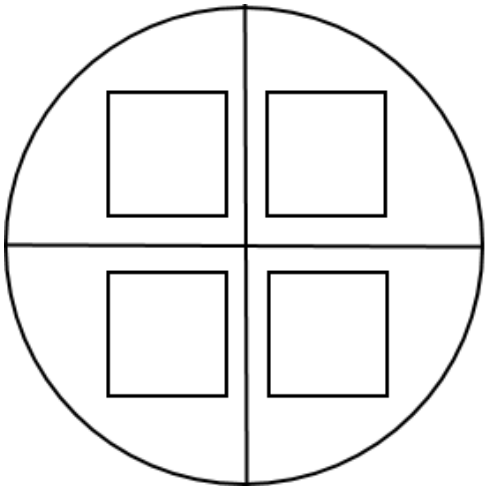

Figure 16.4: Schematic drawing of the adapter with 4 satellites.

postponed by one day since the drift will then be 360 degrees.

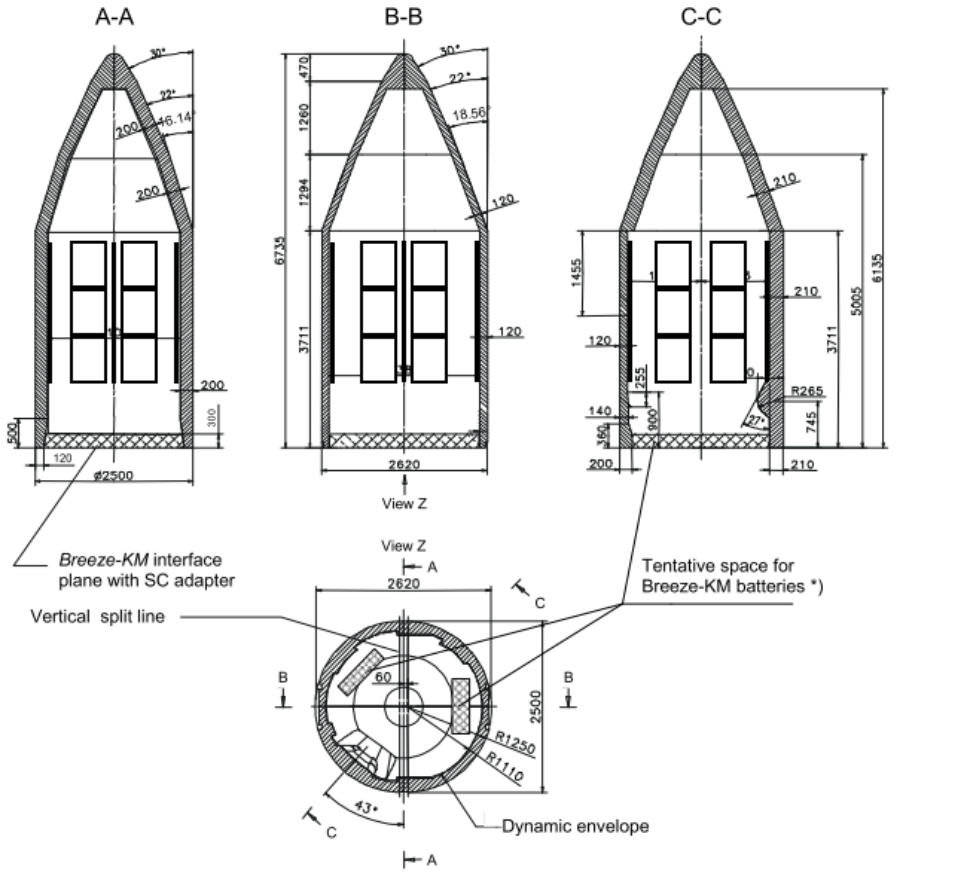

Figure 16.5: Satellites added in the Rockot payload envelope.

Figure 16.6: Possible launch sites in Russia along with their latitude and longitude position.

Table 16.2: Possible launch schedule and launch windows for ROCKOT launcher.

Launch day and orbit	Launch window
Orbit 1	23:50-00:10
Orbit 2	00:37 - 00:57
Orbit 3	01:24 - 01:44
Orbit 4	02:12 - 02:32
Orbit 5	02:58 - 03:18
Orbit 6	03:45 - 04:05
Orbit 7	04:33 - 04:53
Orbit 8	05:20 - 05:40
Orbit 9	06:07 - 06:27
Orbit 10	06:54 - 07:14
Orbit 11	07:41 - 08:01
Orbit 12	08:28 - 08:48
Orbit 13	09:16 - 09:36
Orbit 14	10:03 - 10:23
Orbit 15	10:50 - 11:10
Orbit 16	11:37 - 11:57
Orbit 17	12:24 - 12:44
Orbit 18	13:11 - 13:31
Orbit 19	13:58 - 14:18

Chapter 17

Market Analysis

In the Midterm Report [6] a market analysis was performed. The different concepts were judged on, among others, market perspective. The VLEO satellite constellation turned out to be the best choice overall and also for budget specifically. Budget being a critical constraint in the project, this chapter will show a new market analysis on the detailed VLEO final concept. Analysis will start with a cost analysis in Section 17.2. Several aspect of the design, manufacturing and operating process will be included. Section 17.3 will determine what the return on investment will be for the SKY-FI satellite communication system.

17.1 Market Size

This section gives a short summary of the market analysis that was performed in the baseline and mid-term reports. The size of the Mobile Satellite Services (MSS) market is estimated by summing the revenues of the biggest MSS providers Iridium, Inmarsat, Globalstar and Orbcomm which leads to a total market size in revenue of $1.9 billion. The number of subscriptions for Iridium is 739000 [57], for Inmarsat 369100 [58], for Orbcomm 976000 [59] and for Globalstar 639000 [60]. The data is from 2014 and comes from Annual Financial Reports to the United States Securities and Exchange Commission (SEC), to be found on the companies websites.
Additionally, there is a market for low-cost services that are not yet offered by the above mentioned companies. A study of McKinsey&Company [61] estimates that there are 1.1-2.8 billion individuals in mainly developing countries who cannot get online because they live outside of mobile cellular network coverage. However, these people will not be able to pay the high prices of the conventional MSS providers, but are potential customers of a low-cost, low-data rate service like SKY-FI.
The SKY-FI product is a low-data-rate service, comparable to the one Orbcomm is offering. Therefore, the targeted number of subscriptions is one million. The SKY-FI satellite constellation is designed to accommodate a user base of one million of which 5%, so 50000, are assumed to be connected at the same time. This number is feasible, considering the current market size and the growth potential of addressing unconnected individuals.
The pricing and therefore revenue of the SKY-FI service is based on the annual system operating cost and the desired return on investment. It is discussed in Section 17.2 and Section 17.3.

17.2 Cost Analysis

A cost analysis will be performed in this section. A number of costs will be estimated. The first cost that will be estimated is the non-recurring cost in Subsection 17.2.1. After that the recurring costs will be estimated in Subsection 17.2.2. The launch cost is a large part of the cost and will be treated separately in Subsection 17.2.4. Software cost will be estimated in Subsection 17.2.3. Finally, a the total cost will be discussed in Subsection 17.2.6. The analysis will be performed using the Small Satellite Cost Model (SSCM) as it is publicly available and concerns satellites, which weighs less than 1000 kg [3].

17.2.1 Non-Recurring Cost

Non-recurring costs specify the cost of all resources needed to design, develop, fabricate and test a system. This also includes qualification of the system. The final design will be estimated with SSCM. This model estimates the cost of research and development and the TFU. However, SSCM does not distinguish between recurring and non-recurring costs. The non-recurring cost is calculated as a fraction of the outcome of SSCM. For each subsystem different fractions have been determined. The fraction are displayed in Table 17.1.

Table 17.1: Recurring and Non-Recurring Cost of the TFU.

Subsystem	Weight [kg]	Cost TFU [k$]	Cost R&D [k$]	Non-Recurring [%]
Structures	21.16	543.6	1268.4	70
Thermal	5.00	111.5	261.5	50
Electrical	27.75	450	489.5	62
Propulsion	2.37	53.5	53.5	50
ADCS	2.40	100	61.3	38
CD&H	2.02	270.6	662.5	71
Communication	44.10	3081.25	7543.75	71
Total	**104.8**	**4610.45**	**10340.45**	

17.2.2 Recurring Cost

In the project also recurring costs are encountered. Recurring costs are defined as the cost of the following resources: labour and material used to fabricate, manufacture, integrate and assemble the satellite. Also the launch cost of the system rises with each satellite that needs to be launched.

However, higher production volume also leads to lower production cost per satellite. If the relation between the production volume and the satellite is known, the total satellite cost can be calculated. The total satellite cost is calculated using the TFU, number of satellites N_{sat} and a constant S, which can be found in literature [3]. A typical value in the Aerospace industry for production volumes of more than 100 satellites is S=0.80. The equation for this learning curve is given in Equation 17.1.

$$C_{TL} = C_{TFU} \times (N_{sat})^{(1+\frac{logS}{log2})} \tag{17.1}$$

The total recurring cost will amount to $182.6 million. It is clear now that serial production will result in a significant decrease per manufactured satellite.

17.2.3 Software Cost

Software is also an important component of the cost. The software cost can be estimated by determining the Source Lines of Code (SLOC). A distinction between flight software and ground software is made. The flight software consists of a number of parts: Executive, Communications, Command and Data Handling, Power Control, Attitude and Control, Uplink and Downlink, and Thermal Control. The ground software is assumed to be a fraction of the flight software SLOC [9]. Equation 17.2a gives us an overview of the software cost. The estimated amount is $27.8 million.

$$SLOC_{sat} = 7175 + 4320 + 10150 + 2160 + 8480 + 3610 + 4650 \tag{17.2a}$$
$$SLOC_{gr} = 0.25 \times SLOC_{sat} \tag{17.2b}$$
$$C_{SW} = SLOC_{sat} \times c_{SLOC_{sat}} + SLOC_{gr} \times c_{SLOC_{gr}} \tag{17.2c}$$

17.2.4 Launch cost

Every satellite mission includes a launch to insert the spacecraft in an orbit around the Earth. A satellite launch requires a launcher and launch site choice. This choice was made in Chapter 16. 19 launches will executed with the Russian Rockot launch system. Given the orbital height of 550 km and an inclination of 82° the Rockot launch system is able to insert 1550 kg into orbit. 12 satellites will be present in one launcher. The satellites weighs 103 kg each, will leads to a total payload mass for the launcher of 1257.6 kg. Also 150 kg of mass for the launch adapter will be added. So a total of 1407.6 kg will be used. This means still 142.4 kg is available which can be brokered. A single launch would cost $17.79 million. So a total of 19 launches would lead to a launch cost of $341.6 million.

17.2.5 Operating Cost

The operating cost consists of the cost of maintaining flight C_{satSW} and ground system software C_{grSW}, cost of mission operations C_{MO}, cost of maintaining acquired ground hardware C_{grHW}, cost of facilities C_{fac} and program management and systems engineering costs C_{PMSE}.

$$C_{satSW} = \frac{SLOC_{sat}}{16000} \times FTE_{eng} \tag{17.3a}$$

$$C_{MO} = N_{eng} \times FTE_{eng} + N_{tec} \times FTE_{tec} \tag{17.3b}$$

$$C_{grSW} = \frac{SLOC_{gr}}{28200} \times FTE_{eng} \tag{17.3c}$$

$$C_{grHW} = 0.135 \times C_{HWac} \tag{17.3d}$$

$$C_{fac} = (N_{GS} \times S_{fac} \times c_{fac} + S_{HQ} \times c_{HQ}) \times LAF \tag{17.3e}$$

$$C_{PMSE} = (C_{satSW} + C_{MO} + C_{grSW} + C_{grHW} + C_{fac}) \times 0.15 \tag{17.3f}$$

$$C_{op} = C_{satSW} + C_{MO} + C_{grSW} + C_{grHW} + C_{fac} + C_{PMSE} \tag{17.3g}$$

The set of equations has a number of input. The SLOCs to be maintained, the number of engineers and managers N_{eng} and technicians N_{tec}, the cost of the yearly hardware acquisitions C_{HWac} and the number of ground stations N_{GS} are constant. The other parameters (cost of a full-time equivalent of engineers FTE_{eng} and technicians FTE_{tec}, typical operation facility and headquarter sizes and cost S_{fac}, S_{HQ}, c_{fac}, c_{HQ} and Location Adjustment Factor (LAF)) are assumed to be constant. All values are based on historical data [9]. The technical operating cost of the system is then estimated to be $47.9 million.

General administrative cost and selling cost needs to be estimated as well. These costs were assumed to be $47.7 million. A comparison to the costs of Iridium [57], Orbcomm [59], Inmarsat [58] and Globalstar [60]. The total operating cost will amount to $95.6 million.

17.2.6 Cost Summary

The cost analysis will lead to a total cost. The total cost includes the non-recurring cost, recurring cost, software cost and launch cost. This will lead to the following costs.

17.3 Return on Investment

A project can only be financially feasible if the investors can earn back the initial investment including profit. The project requirements state that the project has a budget 500 million euros. As all costs are estimated in dollars are budget is 600 million dollars, given an exchange rate of $1,20 for every euro [62] (the average exchange rate in the period June 2014 - June 2015). The inflation since 2010 gives a factor of 1.1. So the total amount of the initial cost will amount €468.6 million. The yearly operating cost will €79.7 million. The overview can be seen in Table 17.2.

Table 17.2: Overview cost analysis of SKY-FI system.

Type of Cost	Amount [M$]	Amount [M€]
Non-Recurring	10.3	8.6
Recurring	182.6	152.2
Software	27.8	23.2
Launch	341.6	284.7
Total initial	**562.3**	**468.6**
Operating	95.6	79.7
Annual depriciation	56.0	46.7

The Return on Investment is determined by financial turnover T from subscription to the systems and the C_{year} cost per year. The Return on Investment is given in Equation 17.4. C_{year} is then again comprised of operating cost and the annual depreciation of the system.

$$RoI = \frac{T - C_{year}}{C_{year}} \tag{17.4}$$

(17.5)

The system will be designed for 1 million users. That is one-third of the current market for satellite communication. The subscription cost will be adjusted for inflation yearly. The number of paying costumers will fluctuate over during the operation life time of ten years. SKY-FI will be assumed to have 700 thousand subscriptions on average. Investors will need at least return on investment of 15%. Commercial activities in space are risky. Assuming investors need 15% return on investment, a yearly return of €70.3 million needs to be earned each year after deduction of costs. Assuming the average of 700 000 users, a monthly subscription to the system will cost €23.40 per user.

Chapter 18

Risk Assessment

This chapter gives an overview over the technical risks to which this mission is subjected. This was already done for the Baseline Report [2] and the Mid-Term Review [6], however now that one concept was chosen and designed in detail, some risks were added or changed. This chapter reviews previously identified risks and presents them with additional new risks in a new risk map and offers a contingency plan.

18.1 Risk Identification

First of all, the previously determined risks can be recalled from Table 18.1.

While developing the final concept, unidentified risks were found and have to be accounted for. These 'additional risks' are listen in Table 18.2.
The following lines will elaborate upon some of the risks that might be unclear:

Risk 2, a collision, has two major consequences: The system loses a satellite and creates a huge amount of space debris. The first would decrease the systems coverage and availability, while the latter violates the sustainability requirement.
Risk 4 refers to any subsystem of one respective satellite going out of service which renders the satellite useless.
An example for risk 5 would be a non-sufficient power supply by the solar cells, which impairs the payload's performance.
Risk 6 is based on the chance of human error or a software error at the ground station sending a command (i.e. to manoeuvre) which should not be sent.
Risk 10 could be caused by the launcher simply not responding to the launching signal, implying no damage to the satellite.
Risk 11 could be attributed to the satellite not being quite in range yet or the signal being corrupted.
The environmental hazards for risk 12 are things like humidity, dust or extreme temperatures which can damage or destroy the device.
Risk 13 could have a low battery power or user isolation as a cause.
In risk 14, extreme loading causes stresses, which lead to the user device breaking and therefore failing its purpose.
Lastly, risk 15 could be due to false programming (i.e. the device might emit an emergency signal without reason) or if the user accidentally calls the alarm.
There is only a limited amount of frequencies available for use in practice and therefore an (un)intentional conflict may arise.

User information made public due to someone listening in to calls would harm the systems reputation and might effect selling numbers.
Coverage would be incomplete due to the system not being deployed correctly which implies a failure to fulfill requirements.
The ITU sometimes changes which (band of) frequencies may be used for which services. If the frequency that the satellite system is using may not be used for the missions purposes anymore, the entire system

Table 18.1: Legend for former technical risk map.

ID	Risk	Category
1	A Communication Satellite (CS) does not respond or fails to receive a signal	satellite
2	A CS collides with another object	satellite
3	A CS is damaged by space weather	environmental
4	A CS subsystem fails to perform its specified task	satellite
5	A CS subsystem is under-performing	satellite
6	A CS receives a signal, which should not have been sent	ground station
7	A CS will be overloaded	satellite
8	The communication link fails to provide a sufficient data rate	transmission
9	The launcher explodes	launch
10	The launcher does not launch the payload	launch
11	The User Device (UD) fails to transmit a signal	transmission
12	The UD fails to work due to environmental hazards	environmental
13	The UD fails to connect to the satellite	transmission
14	The UD fails to work due to extreme loading	UD hardware
15	The UD transmits a false alarm	UD software
16	Interference due to a satellite using the same frequency band	transmission
17	Insufficient data encryption allows unauthorized listening in	transmission
18	A satellite orbits at a wrong inclination due to an erroneous launch	coverage
19	The ITU changes the frequency allocations	transmission
20	A crucial launch site is (temporarily) unavailable	launch
21	The antenna release mechanism fails to deploy the antenna (properly)	subsystem
22	The delta V budget accounted for is insufficient	sustainability
23	A software bug prevents the payload to perform its mission	software

Table 18.2: Legend for additions to the technical risk map.

ID	Risk	Category
24	The turn rate of the solar panels is insufficient	Power subsystem
25	The turn rate of the spacecraft is insufficient	ADCS subsystem
26	An unexpectedly intense solar flare causes the satellite to decay too fast	Environmental

goes out of service.
If the satellite cannot be launched into an orbit with the correct inclination, coverage will be incomplete. If the antenna does not deploy correctly, communication might be impossible for a satellite. If the entire mechanism is faulty then no satellite will be able to communicate with the ground.

If the satellite needs to accommodate fuel in order to reach a different altitude at its end of life but does not accommodate enough, sustainability regulations will not be met and might incapacitate certain orbits for future missions.
If the software is programmed erroneously, the payload might not be able to perform its mission, which would apply to every satellite since they will all use the same software.
The solar panels are required to constantly point towards the sun, which means an actuator has to be able to turn them fast enough so a constant power supply is assured.
The antenna is required to constantly point along the nadir vector, which means the ADCS needs to be able to constantly rotate the satellite while orbiting earth.
Solar flares affect the atmospheric density in space and the impact of the emitted particles cause unwanted disturbances to most spacecraft.

The risks from Table 18.2 are now presented in a risk map 18.3. Based on their probability and their severity, they are classified by how dangerous they are to the mission and how resources need to be distributed in order to account for them. Here, risks in the red areas are the most mission endangering while the green ones do not necessarily need to be accounted for at all. Unfortunately, the severity of a risk cannot be explicitly quantified. Catastrophic risk implies mission failure or significant non-achievement of performance [63]. Critical means that mission success is questionable or some possible reduction in technical performance. Marginal means that there is a degradation of secondary mission or small reduction in technical performance, while Negligible is inconvenience or non-operational impact. For each risk, the worst possible consequence is considered if there are multiple ones present. Note that this table does not state anything about how easily a risk will be treated, as a catastrophic and likely risk might still have a easy solution.

Table 18.3: Technical risk map.

Severity / Probability	Negligible	Marginal	Critical	Catastrophic
Likely			3	12
Probable	13,15			
Possible	5	11,17	4,10,26	2,20,22
Remote	18		1,7,19,21	14,24
Improbable	23		8,16,25	6,9

18.2 Risk Management

The newly discovered risks need to be accounted for in order to, again, guarantee a successful mission. This will be done as follows:

1. The satellite will be equipped with a transmitter, sending a constant signal to other satellites. If a satellite does not respond correctly then it won't get a signal anymore, which will cause it to reboot the system. Faulty signal reception due to pointing errors will be prevented by designing an ADCS with a sufficiently high accuracy.

2. Each satellite will regularly be checked for whether or not it is on a collision course with another space object. If a possible collision is detected, evasive manoeuvres will be initiated.

3. While space weather is not easy to influence, it can be predicted and irregular power output spikes can be used to overcome signal disturbances. All satellite components will be designed to withstand typical radiation levels due to solar eruptions.

4. All subsystems will be tested by sending a prototype into space and observe its performance and account for shortcomings.

5. All subsystems will be designed to deliver a better performance than they absolutely need, meaning safety margins are applied.
6. Ground station staff will be trained and made familiar with the system in order to avoid human error. Systems are inspected on a regular basis.
7. Each satellite will be prevented from overloading by relaying the processing of the data to a ground station.
8. The link will be optimized for the signal-to-noise ratio using a predetermined bandwidth range (using ITU standards).
9. A trade off will be made between launcher reliability and cost. Appropriate safety measures will be taken.
10. The launcher will be thoroughly examined and prepared.
11. The device will be equipped with a strong and long lasting power supply and users will be advised to use it where there is a free field of view to ensure a successful transmission.
12. The device will be designed waterproof and meshes are installed at all openings to prevent particle intrusion.
13. A 10% chance of not being able to connect to the satellite complies with the requirements. The coverage will be designed to ensure at least a 90% connection chance.
14. The device will be designed to withstand a load range which still is to be determined. It shall survive an airplane crash, assuming no large explosions occur which can melt the device.
15. The software will be tested for any possible malfunctions. User incompetence cannot be accounted for completely.
16. The ITU intends to prevent unintentional signal interferences by managing who may use which frequencies. QPSK modulation with 9/10 coding rate prevents unauthorized use of the signal.
17. A common encryption method will be used which is up to modern standards.
18. Multiple simulations will be performed, preferably by different people, in order to validate predicted orbit insertions.
19. The satellite will be able to use multiple frequencies. If a frequency is made unavailable for the satellite, it will be able to switch to another and continue its mission.
20. Before the first launch, all launch sites will be confirmed available. If not all orbits necessary are accessible, the mission is postponed.
21. The release mechanisms will be tested multiple times and possible failure scenarios will be simulated in order to guarantee their deployment.
22. Delta V budgets will be verified and compared to previous missions.
23. The software and all its subcomponents will be tested and validated before it is installed on the satellites board computer.
24. The solar panel deploy and pointing mechanism will be tested for its possible turn rates before the satellite is launched.
25. The actuators of the ADCS will be designed to overpower any other torques which might affect the satellite.
26. A delta V budget accounts for unplanned losses of altitude.

Chapter 19

Sensitivity Analysis

The final design has been assessed for risk in chapter 18. However, it is also important to know how susceptible the design is to changes in external factors. This chapter will discuss different factors. Section 19.1 will elaborate on the market size, Section 19.2 will discuss a change in the foreseen average data consumption by the connected user. Other factors are a change in required duration of service (19.3). Finally, SAR requirements might be revised, which is examined in Section 19.4, and a change in orbital altitude is looked into in Section 19.5. Finally, the sensitivity of the system to catastrophic failure of single satellites will be investigated in Section 19.6.

19.1 Market Size

The parameter that gives the most impact to the final design is the possible number of customers. This spacecraft is designed with a projection of 1 million active customers in mind, with around 5% of them considered to be using the service at all time. However, if the number of paying customer is reduced, this will directly affect the cost analysis and change the break even point. The possibility for this is not that unlikely, as the satellite telephone business is a rapidly growing one with more and more competitors getting in the business.

As a result of such a change, the cost budget will be reduced, and this will limit all parts of the subsystems. As a much lower budget means a much higher importance and weight in the cost criteria of the trade-off, it's possible that this would also lead to a major design overhaul. However, since this design already have a better cost trade-off compared to other possible design, it's very likely that such a major change in design is unnecessary. An alternative to this is to lower the number of redundant components for the subsystem, which would greatly increase the risk of failure. Another possible alternative is to buy cheaper, lesser quality components for the subsystem, which will negatively affects the performance of the spacecraft.

While having a reduced number of customer negatively impacts all parts of the subsystem, the communication subsystem do get some advantageous benefits from this change. This is because having a lower number of customer also means a lower number of required channels and capacity for the communication architecture, and this increase in data rate will in turn reduce the power requirement. This means a lower amount of necessary components which leads to lower mass and lower cost. However, there are still basic necessary components that will still remain for the communication architecture to function regardless of how the channels is lowered due to less customer demands, and the decrease in mass and cost budget is still really low compared to the reduced budget caused by having lower number of customers, as well as the negative impact it would have to the other subsystems.

19.2 User Data Consumption

The communication system design will have a capability to connect fifty thousand users, which can be found in Chapter 4. In this chapter also the assumption was formulated that the average data rate was a weighted average of two groups of users: high data rate users (phone call and internet) and low data rate users. Of course it is assumed users only use one of these services at once.

The assumed ratio between the two user groups can however be subject to change. For instance, the number of users trying to make a phone call might turn out to be higher than expected. This has some implications for the system. More phone call users means the data rate will increase. And a higher data rate would lead to a higher transmitting power, if the Signal to Noise Ratio (SNR) of 3 dB would be guaranteed. But since the spacecraft is optimised the power can not be changed.

Still, it is possible to connect more phone call users to the spacecraft. Without increasing the transmitting power the SNR will be lower. This will give consequences for the communication quality and a connection will not be guaranteed all the time. But as is stated in the Top Level Requirements the user is required to make a successful conversation 70 percent of the time. So small changes can be accommodated. Very large changes will pose a problem since the communication system will approach a operating limit. In that case extra phone call users will be blocked when there is no capacity.

19.3 Duration of Service

Currently, the required duration of service for the spacecrafts are ten years, and the spacecraft are designed accordingly to have a lifetime of ten years as well in order to minimize costs from the number of launches. However, should the required duration is to be increased, this will have major impact on the spacecraft's subsystems, in particular the power, ADCS and propulsion.

While the primary power source in the solar panel would be unaffected by this, it will directly affect the batteries as a secondary power source. The batteries have a limited lifetime before they're reduced too low in capacity, and there's already extra batteries stored to ensure enough power even with the current ten years duration. An increase in the satellite duration will lead to a higher need for batteries stored, which will increase the mass of the spacecraft.

Unlike with the power subsytem, the ADCS will suffer from a heavier impact due to the duration of service change. The ADCS components typically have a lower lifetime compared to components of other subsystems, and if the service duration is increased too high it will lead to the spacecraft not having a working ADCS system by the end of its lifetime, which would prove to be fatal.

In order to deal with this, an alternative would be to pick another ADCS component with a longer lifetime, though this compromise will come with the downside of a higher mass and power requirement. Another alternative is to have more launches which will allow subystem components with lower lifetime to be used, although the increased number of launches will increase the cost by a huge amount. As such, a large enough increase for the duration service will result in a very huge impact on the sensitivity of the spacecraft.

For the propulsion system, a higher amount of propellant mass will be needed to stay above the 500 km altitude that is needed to comply with the requirements. This will increase the propellant tank size and the total mass

19.4 Search and Rescue

Currently, the SAR design uses the Doppler shift tracking method to meet the required SAR accuracy and response time. If this required SAR accuracy are to be increased and the needed response time to be shorter, this will have some impact on the design of the spacecraft. The major parameter for the SAR requirements are how much data it can acquire, and so the passing time of the satellite over the SAR signal emitter as how often the satellite passes it will be the ones directly impacted by this change. The SAR capability only take a relatively very small part of the communication, and such a requirement change for the SAR will not affect the communication subsystem at all.

As the accuracy is increased and the response time needed to be shorter, this means that the satellite frequency and the time it spent getting data from the user must be higher. This means that the number of satellites will need to be increased in order to meet this higher demand. This will not affect the power or ADCS subsystem at all, and only minor changes (increase the number of planes or the number of satellites per pane) for the astrodynamics needs to be taken. Therefore, a change in the SAR requirements will not affect the sensitivity of the satellite that much.

19.5 Orbital Altitude

The orbital altitude is one the most important characteristics of the satellite system. Orbital altitude is the driving parameter for the design. It determines the footprint of the satellite, and as a result it determines the number of satellites required to provide worldwide coverage. Furthermore, the number of satellites leads to the number of users per satellites, which then determines the power and weight of the spacecraft. It is apparent what the orbital altitude means for the spacecraft. A specific altitude might not be available for such a large constellation.

A relatively small change of the orbital height in the region of the final design (550 km), will mostly affect the orbital decay of the spacecraft. In Chapter 9 this was extensively discussed. A decision to lower the spacecraft will lead to a faster orbital decay, which should be countered by an orbital maintenance manoeuvre. This is solved by increasing the amount of propellant on board. This will not be a problem.

Lowering the spacecraft will also as mentioned earlier decrease the footprint. In this case it should be checked whether the coverage requirements are still satisfied. If the altitude has to be lowered by a large distance, more satellites will have to be added which will increase the cost, even though the power, mass and size per satellite will decrease due to the fact that less users will be needed per satellite.

19.6 Satellite Failure

Ability to satisfy the coverage requirement depends on the satellites actually performing their operations. However, satellites can always fail, which means they are no longer able to perform their mission. Several reasons, such as debris collision or satellite component failure, can cause catastrophic satellite failure. This section is concerned with the question how failed satellites affect the overall performance of the system.

In the table it shown how the system coverage is influenced by failing satellites. The simulation results are given in the table. It shows that the system will continue to operate properly in case of a satellite failure. Not included in the analysis is the fact total number of users for the systems stays the same, so the number of users per satellite increase. If the number of users increases, only some of the users can actually set up a connection with the satellite. The satellite is only able to account for 239 connections. The last column in Table 19.1 shows to what percentage of active users a satellite connection is available.

Table 19.1: Influence of number of failing satellite on the provided coverage.

Missing Satellites	Coverage [%]	Availability [%]
0	94.79	100
5	94.50	97.5
10	94.25	95.2
20	93.35	90.5
40	92.59	81.0
80	88.78	61.8

Chapter 20

Operations and Logistics

The operations and logistics are divided into 5 separate parts, launching logistics, manufacturing, transportation, ground station operation and space operation, after which the block flow diagram is shown of the full operations. A part of this chapter is from the Midterm report [6], which is refined and completed here.

Launching logistics

As explained in Chapter 16, the 12 satellites will be launched into orbit through the EUROCKOT launch vehicle. 12 satellites will be launched in a single plane, one of which is a spare satellite that is needed in case of an unforeseen failure of a satellite, as explained in Chapter 18. The full launch logistics are explained in Chapter 16 where the launch schedule can also be found.

Manufacturing

There are 209 operational satellites distributed over 19 planes, and a spare satellite in each plane, leading to a total of 228 satellites that will have to be manufactured. Since a large amount of satellites have to be produced, a production facility is needed. It is beneficial to perform manufacturing as close to the launch site as possible, in order to minimize transportation logistics of the completed satellite. In addition to a production facility, a storage place for this large number of satellites has to be found. Since the launch site is near a train station, the manufacturing and storage can be done near a train station on the same line.

The antennas, the structure, and the propellant tanks have to be specially made for this mission, which will increase the cost. While the propulsion system, thermal control, solar panels and battery's can be bought and shipped directly.

Transportation

If manufacturing can be done near a train station leading to the launch site, all the separate parts have to be flown in to the Archangel Talagi airport. Then the manufacturing can be done and the launch vehicle and satellite can be transported towards the launch site using the train rails.

In the event that manufacturing near the train rails of the launch site is not possible, the satellites will be manufactured in a different country. The satellites will then be transported to the launch site using the train rails and the designated airplanes from the ROCKOT user guide [35]. This shall increase the cost due to the safety measurements that have to be taken into account.

Ground station operation

The ground stations will have to be operated in such a manner that communication, tracking, and all the manoeuvres will be made possible. This means that there are several subtypes of operation which have to be performed at the same time. Additionally, staff needs to be present at all times, since even in the middle of the night a SAR signal could be transmitted. As a result, workers also need to be organised in shifts. If possible, however, the SAR signal can be automatically sent to the emergency number from

the ground station, reducing the required number of ground station operatives. The amount of ground stations are determined in Chapter 4.

Space operation

Finally, all spacecraft have to be tracked which will be more work for a constellation of a couple of hundred spacecraft. For this a delta V is designed in Chapter 13. This delta V is able to orbit maintenance, constellation maintenance and collision avoidance. When one of these manoeuvres are needed to be done, the ground station will send the signal.

When these 5 separates parts are combined a block flow diagram can be made, this can be seen in Figure 20.1

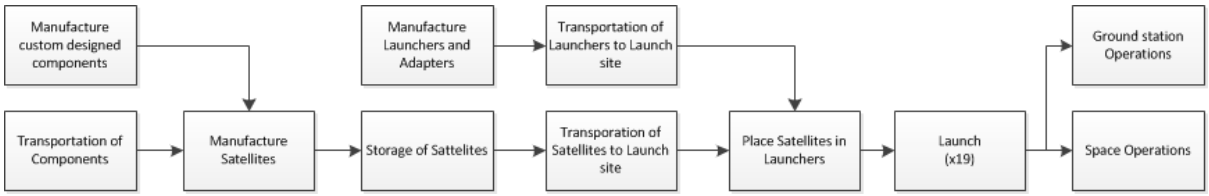

Figure 20.1: Block flow diagram of the Operations and Logistics.

Chapter 21

Production Plan

In Figure 21.3 the flow diagram of the production plan can be seen. The Batteries, Battery Management System (BMS), Power Management Unit (PMU), sun sensors, magnetometers, magnetorquers, ADCS computer, solar arrays, stepper motor and thruster are all developed and produced by different companies while other elements such as the antennas, propulsion tanks and the satellite body structure have to be custom made.

The structure of the satellite can be seen in Figure 21.1. The middle plate is used to separate the communication hardware on top and the other subsystems below. Making this structure is the first step of the production. Then the communication hardware can be added on top of the middle plate. The multiplexers will be in the middle while the amplifiers and the converters are on the outside. Once this has be done the ADCS system will be added. During this assembly the battery packs are made and then assembled on the bottom plate of the satellite. Meanwhile the propulsion system can be produced and assembled onto the satellite. Then the thermal control, MLI, and the outside polished aluminium plates can be placed. Now that the inside structure is finished. The antennas and solar panels can be assembled and then added to the satellite. The ground link antenna assembly is illustrated in figure 21.2. Following this, a satellite is completely assembled.

Since a high amount of satellites have to be produced, several subsystems such as the propulsion system, battery packs, solar panels or the antennas can all be made in bulk and stored to speed up the production. However, this requires a large storage space. When a satellite is finished, it has to be stored until the rest of the satellites are finished as well.

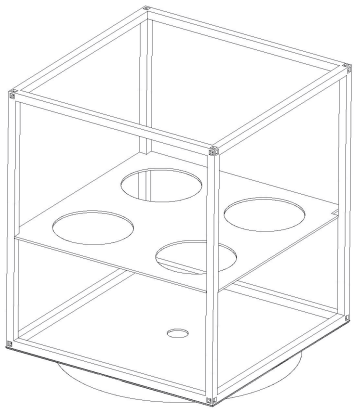

Figure 21.1: Primary structure of the Satellite.

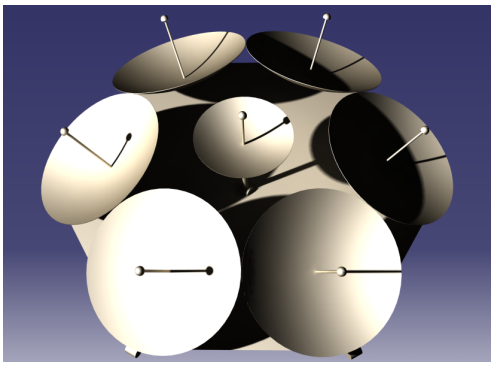

Figure 21.2: Assembly of Ground link antenna.

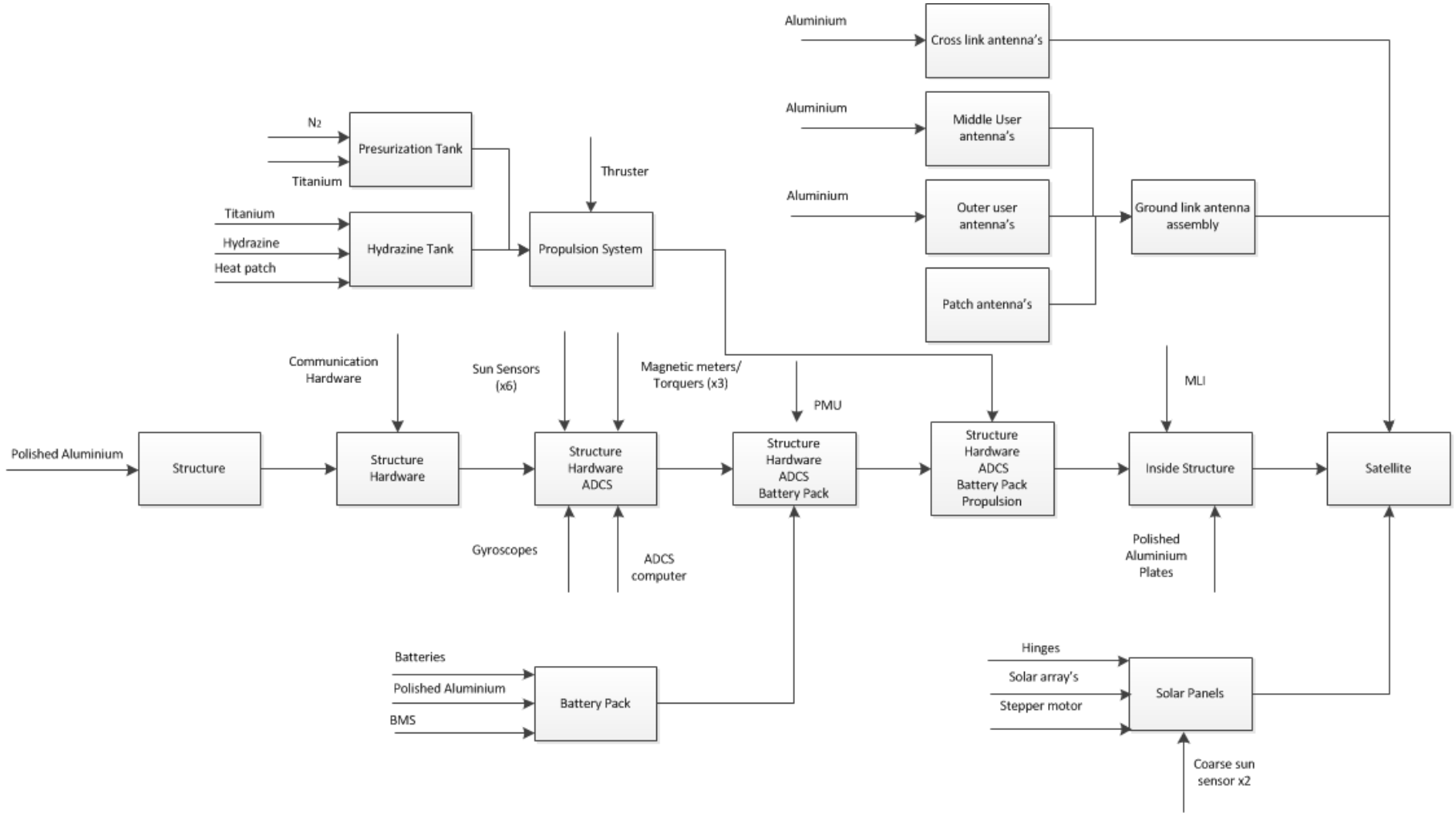

Figure 21.3: Production plan where activities are chronologically ordered.

Chapter 22

Project Design and Development

Since at the end of the DSE the project is not finished. A plan has to be made to what still needs to be done after the DSE. First the project development will be discussed in Section 22.1, which will explain the regulation and technical design that will be done after the DSE. In section 22.2 the Post DSE activities will be explained, which will explain the manufacturing, testing and launching of the system. After which the Post DSE gannt chart is shown in section 22.3 to summarize these two sections.

22.1 Project Development

Two roles have been identified in the development of the project after the DSE. One is obtaining the correct certification (managerial side) while the other is the techincal side (design development & testing) of the satellite. Both of these run in parallel and should be done in such a way to prevent holding back each other. Therefore careful planning and timely arrangement of paperwork has to be maintained till the nominal mission.

Regulation Compliance

Before starting detailed design of the satellite, an application for frequency to the ITU has to be made, otherwise the detailed design of the antennas cannot be performed.The ITU negotiations last around two years, based on the fact that there are little ITU meetings across the year. After a range of ITU frequencies is obtained (which is a milestone), together with permission of ITAR, an authorization to proceed with the design is obtained.

After a flight model has been built, then the negotiations with EUROCKOT for purchasing launchers for the 209 (+19 spare) satellites has to begin. Legal permission needs to be obtained for transporting Hydrazine and $LiFePO_4$ outside Russia. EUROCOKOT can provide the permissions for them within Russia. Furthermore, negotiations with other potential buyers of the free space in the launcher, need to be performed in parallel with the aforementioned permissions.

Technical Design

Right-after the completion of the DSE, the next steps in the traditional way of designing a system is the Detailed Design phase. During this phase every detail is designed and analyzed. The final production of the satellite will be conducted based on these design details. Design of tooling and detailed scheduling of the production will also need to take place during this phase. Major changes to the design have finished and calculations for the satellite are done by finite elements and related CFD programs. Detailed design phase finishes with the first flight test model built.

The two main functions , Regulation compliance and Design & Development testing, merge at satellite launch.

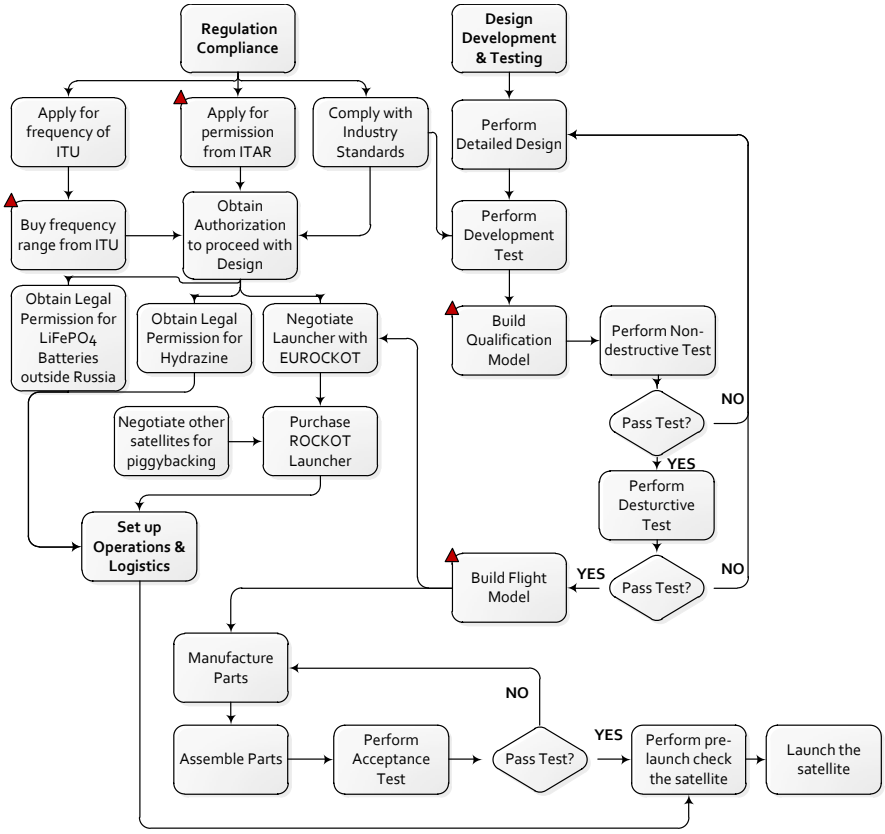

Figure 22.1: Project Design and Development Logic.

22.2 Post DSE Activities

Manufacturing and Assembly

Manufacturing has to be done once the negotiations with EUROCKOT has been completed, sinnce the manufacturing will be done near the launch site and the adapters depend on the type of launcher. First the custom parts have to be manufactured. Then the several subsystems can be assembled and finally the full satellite can be assembled. The production phase can be divided into manufacturing division and assembly division. Concept of batches and production line stations will be used during the production. The complete concept of the production plan can be found in Chapter 21. Several parts and assemblies will have to be stored in a storage or buffer stations near the manufacturing factory. Since the satellite itself is not big, the transportation of the finished satellite is not going to be a big problem.

Testing

Now that all the subsystems have been designed into detail, an acceptance test need to be performed to see if all the subsystems will meet the requirements under the simulated space conditions.

Once all the subsystems have been tested. The whole system will be tested. This is first done by simulating the space conditions, including all harsh conditions from launching to flying in the space. Temperature, pressure, vibrations, and load experience will be tested. Once this has been approved, two prototype satellites will be launched into space to test the system. Two satellites are needed due to the fact that the cross-link communication and formation flying has to be tested.

Launching

Once all the satellites have been manufactured, they will be sent to the chosen launching site to be mounted on the launchers. The specific site and launchers choices are discussed in the Chapter 16.

Inside the chapter, the launching windows and schedule are determined as well.

22.3 Post DSE Gantt Chart

In order to visually represent the timeline of what happens after the DSE, a Gantt chart is devised and presented in Figure 22.2. Important milestones such as, for instance, building all the pre-flight models are also indicated (with red triangles). Of course the time frame is an estimation and will be subjected to changes as the design matures.

ID	Task Name	Start	Finish	Duration
1	Freeze Design	13/07/2015	13/07/2015	0d
2	Apply for ITU Frequency	03/07/2015	11/07/2017	740d
3	Obtain Frequency range from ITU	11/07/2017	11/07/2017	1d
4	Detailed Design	13/07/2015	13/03/2017	610d
5	Negotiate with ITAR	03/07/2015	11/07/2016	375d
6	ITAR approval	11/07/2016	11/07/2016	0d
7	Development Test	11/07/2016	18/09/2016	70d
8	Build a Qualification Model	18/09/2016	17/10/2016	30d
9	Qualification Model Built	17/10/2016	17/10/2016	0d
10	Non-destructive Testing	17/10/2016	15/11/2016	30d
11	Destructive Test	15/11/2016	14/12/2016	30d
12	Build Flight Model	14/12/2016	13/03/2017	90d
13	Flight Model Built	13/03/2017	13/03/2017	0d
14	Manufacture Parts	13/03/2017	08/09/2017	180d
15	Parts Assembly	08/09/2017	06/12/2017	90d
16	Acceptance Test	06/12/2017	04/01/2018	30d
17	Pre-launch Inspection	04/01/2018	10/01/2018	7d
18	Launch	10/01/2018	28/01/2018	19d
19	Nominal Mission	28/01/2018	25/01/2028	3650d
20	End-of-Life (De-orbit)	25/01/2028	22/01/2034	2190d

Figure 22.2: Post-DSE Gantt Chart.

Chapter 23

RAMS Characteristics

This chapter presents the Reliability, Availability, Maintainability and Safety (RAMS) characteristics of the SKY-FI mission. These are not specific mission or design goals but rather elements which should be accounted for in every project. Due to the fact that the satellites cannot undergo maintenance in space, this chapter does not include maintainability characteristics. However, this is accounted for in the reliability and redundancy of the system as a fail safe design philosophy was employed.

Reliability

The reliability of a system can be determined by finding the reliability of each system component and their mechanisms. The launcher reliability is the easiest to determine because it is defined as the ratio of successful to total launches. In the case of Rockot, 24 out of 26 launches were successful. This yields a reliability of 0.923. Since 19 launches will be performed, the total reliability is $0.923^{19} = 0.219$. This is already too low to assure a successful mission. Therefore, in order to achieve a successful mission, a proper fail-safe design should be made. The Rockot launch vehicle ordered through EURockot (the Rockot supplier) already includes an insurance of up to €100M [35], in case the launch fails due to launcher problems. Due to the low cost of the SKY-FI satellites, the insurance fully covers the launch and satellite cost.

Since making a complete fail-safe system would imply nearly doubling the mass of each subsystem, it was instead decided to design for fault avoidance. For the satellites themselves, the subsystems include design margins (such as additional propellant, additional batteries) in the case of an unexpected event. The tanks themselves are also designed with a safety margin and, wherever possible, the maximum load of a system was taken as the design point. With respect to communication success, a QPSK modulation with a 9/10 code rate. This improves the robustness of the communication as it improves error detection in signals.

Most satellite components are of the shelf products which have already been used in different system and are therefore provided with a reliability margin. This will be used for the SKY-FI satellite. During production each system is acceptance tested and screened such that no errors in production and assembly remain undetected and unfixed.

Using this philosophy, the reliability of the system and thus also fault avoidance have improved. Now the total reliability has to be calculated by multiplying all the subsystem reliabilities. The failure chance of a component was determined for each subsystem. Upon doing this, the design philosophy and redundancy types have to be taken into account. Equations 23.1, 23.2 and23.3, are cases for single system reliability, reliability with system redundancy, and reliability with partitioned (per part) redundancy [3].

$$R = e^{-N\lambda t_{mis}} \tag{23.1}$$

$$R = 1 - \left[1 - e^{-N\lambda t_{mis}}\right]^2 \tag{23.2}$$

$$R = \left(1 - \left[1 - e^{-N\lambda t_{mis}}\right]^2\right)^N \tag{23.3}$$

Where R is the reliability, N is the number of parts, λ is the failure rate of a part, and t_{mis} is the mission lifetime. A reliability of 0.78 for ADCS is found, accounting for redundancy. The batteries and power subsystem have a reliability of 0.97 due to redundancies and over-designing. The communication and antenna subsystem has a reliability of 0.88 with partial redundancies, since they use a lot of electronics. The thermal subsystem has a reliability of 0.98 with 2x redundancy for the active part. The propulsion subsystem has a reliability of 0.97 with feed system redundancies and after passing acceptance testing. Lastly, the structure, upon passing acceptance testing, has a reliability of 0.99. This results in a total reliability of 0.63 per satellite for a duration of 10 years.

This low reliability comes from the fact that once a single part starts under-performing or fails while another part can take over, the satellite is deemed to fail. If other subsystems can take over, the reliability of the ADCS improves to 0.96. The antenna system reliability then would improve to 0.95, since a satellite can survive and perform its tasks without all cross-link antennas deployed. This means that there will be a total reliability of 0.84. The chance of no satellites failing is therefore 16%.

In order to account for the failure of a satellite, past the limits of the fail-safe design, an extra satellite per plane is added. Furthermore, the calculations presented are estimates, and as the level of pre-launch testing increases the reliability of the satellite system can only increase. As far as

Availability

Availability of the system is defined in one of the top level requirements. For 10 years after launch, a user will be able to connect to the satellite with a 90% chance for success and make use of its functions. This was accounted for in the design of multiple subsystems. The power subsystem, ADCS, propulsion and orbit design were all designed with regard to this requirement. The power subsystem makes sure that the communication subsystem is constantly supplied with sufficient power, the ADCS ensures that the antenna is always nadir pointing, the propulsion subsystem keeps the satellite at a sufficient altitude before the mission ends and the orbit constellation was designed so the whole earth could be covered by this system.

Safety

There are several types of safety that have to be taken into account: safety during manufacturing, operations and launch.

During operations, safety hardly needs to be accounted for since there are not many people in space. Re-entry might pose a threat to humans where the satellite crashes down, however most parts of the satellite are expected to burn up in the atmosphere. According to Nick Johnson, NASAs chief scientist for orbital debris, re-entry does not pose a significant threat to humans: "The risks are extremely small. To date, no incidents of human injury or significant property damage from reentering debris have been reported throughout the entire Space Age."[64].

The critical functions for safety during manufacturing and launch are listed below.

- Battery catching fire during transportation
- Battery catching fire during manufacturing
- Hydrazine catching fire during transportation
- Hydrazine catching fire during manufacturing
- Launch vehicle crashes

Safety during manufacturing is important due to the fact that the satellites require thrusters and batteries. Both of them can cause (in the worst case) lethal accidents during transportation and manufacturing. During transportation the batteries are required to fulfil all safety requirements and correct documentation has to be written, both according to the IATA regulation [65]. The regulations for the thrusters are mainly focused on the hydrazine tanks. The safety procedures are defined by ASD Eurospace[66]. These regulations are also implicated during manufacturing.

Safety during launch is mainly focused on the launch vehicle and the launch site. Due to the fact that the reliability of the Rockot launch vehicle is not perfect, there is a probability that a launch vehicle will crash. Since the Plesetsk launch site is in such a remote area, a crash of the launch vehicle will not impose any danger for humans. Also EURockot (in charge of the launch) has the responsibility over this phase of the mission and thus insure that the regulations are followed.

Conclusion

The purpose of this report was to present the result of this project developed in 10 weeks by 10 students as part of the Design Synthesis Exercise at the TU Delft Faculty of Aerospace Engineering. The result is a constellation of 228 satellites, including 19 spares, spread over 19 orbits with each orbit accommodating one redundancy satellite. In this report, different subsystems of the satellite are designed in a detailed level all in order to meet the top level requirements of the mission. The system provides a global communication network capable of transmitting phone calls, text messages and emergency signals as well as providing search and rescue capabilities and access to the Internet at an average data rate of 2kpbs and a peak data rate of 10kbps per user. Single users can be assigned higher data rates up to 50kbps if no other users are connected to a satellite or by reducing the data rates of other users. Users anywhere on earth will be able to use the system successfully at least 90% of the time and can be located via Doppler-tracking for SAR purposes if they are connected to a satellite.
Inter satellite communication, additional ground stations, gateway antennas and smart digital on-board signal routing allow for fast connections, low latency and reduced need for expensive ground operations. The communication payload consists of four transponders which are made of flight-proven and reliable components, accommodating 245 users per satellite.
Each satellite weighs 103kg and is 60cm $\times$ 60cm $\times$ 65cm large. The total spacecraft power is 102W, which is provided by two deployable solar cells with a total array size of $0.86m^2$ that are capable of pitching towards the sun with a negligible error, furthermore the satellite will yaw to provide optimal orientation towards the sun while the ISL antennas, mounted on motors will yaw in the opposite direction. A battery with 60Wh capacity provides power during eclipse.
The satellites will remain operative for 10 years at an altitude from 500-550 km and will de-orbit 5.9 years after its end of life, thus leaving no extra space debris behind.
The satellites will have an Attitude Determination and Control System (ADCS) that provides three-axis control to point the ground communication antennas towards earth and the solar panels towards the sun. This is accomplished with an assembly of 4 magnetorquers.
The thermal control system makes sure that the electronics and the propulsion system can operate within their designed temperature ranges. To achieve that, heaters are implemented to prevent the propulsion tank from freezing during the eclipse.
After the technical design is completed, a thorough analysis of the mission operations is made. It includes launcher selection, market analysis, operations, production plan, sensitivity and risk assessment. This will ensure the success and the completeness of the mission. The following are several recommendations on how to increase the systems potential and usability. First of all, although the constellation was optimized by using more accurate orbital models for the earth and the earth's surface, a better value for the spacing of the planes and overlapping area can be determined. By doing so, the number of satellites can be reduced and with it the cost of the entire mission. During the design of the subsystems, many experimental or relatively new technologies were not used due to reliability issues. However these subsystems can be redesigned using these technologies in order to further improve the systems performance. Especially with the updated design of the communication subsystem, the capacity can be improved to support more people with a higher data rate to cope with increasing Internet demand. Regarding the antenna, better modelling of the gain pattern might give insight into a slightly different communications array, for example one large parabolic reflector with multiple feeds. Furthermore, collaboration with scientist to use the system for research is recommended as the system can be a potent tool. In the end, it can be concluded that the design can be realised under the current virtual budget of €500m and meets all the design requirements, thus it can be considered a success.

List of References

[1] Airbus Defense and Space, "Partner in Oneweb Satellite Constellation," http://airbusdefenceandspace.com/newsroom/, Accessed on: 19-06-2015.

[2] Angelovski, S., Antonio, Y. A., de Jong, G., Carrera, A., Chen, Y., Freiherr von der Goltz, J. H., ten Hove, G. R. W., Bussink, T., Rado, K., and El Sioufy, J. K., "DSE - Internet via the satellite for everyone, everywhere, anytime." Tech. rep., Technical University Delft, 2015, Baseline Report.

[3] Wertz, J. R. and Larson, W. J., *Space Mission Analysis and Design*, Microcosm Press, 3rd ed., 2010.

[4] Klees, R. and Dwight, R., "AE2220-I Applied Numerical Analysis," TU Delft Blackboard, 2014, Lecture Notes Reader.

[5] Noomen, R., "AE2230I Lecture 15+16," TU Delft Blackboard, Accessed on: 7-5-2015.

[6] Angelovski, S., Antonio, Y. A., de Jong, G., Carrera, A., Chen, Y., Freiherr von der Goltz, J. H., ten Hove, G. R. W., Bussink, T., Rado, K., and El Sioufy, J. K., "DSE - Internet via the satellite for everyone, everywhere, anytime." Tech. rep., Technical University Delft, 2015, Mid-Term Report.

[7] Fortescue, P., Swinerd, G., and Stark, J., *Spacecraft Systems Engineering*, John Wiley & Sons, 4th ed., 2011.

[8] Union, I. T., "Environmental protection of the geostationary-satellite orbit," https://www.itu.int/dms_pubrec/itu-r/rec/s/R-REC-S.1003-0-199304-S!!PDF-E.pdf, 1993, Accessed on: 6–5–2015.

[9] Wertz, J. R., Everett, D. F., and Puschell, J. J., *Space Mission Engineering - The New SMAD*, Microcosm Press, 2011.

[10] NASA, "Propagation Effects Hand- book for Satellite Systems Design," Book, 1983.

[11] Iridium, "Homepage," https://www.iridium.com/, Accessed on: 1–5–2015.

[12] Roddy, D., *Satellite Communications*, fourth edition ed., 2006.

[13] Balanis, C. A., *Antenna Theory: Analysis and Design*, Wiley, 3rd ed., 2005.

[14] "Antenna Theory," http://www.antenna-theory.com/antennas/reflectors/dish3.php, Accessed on: 13-06-2015.

[15] Limited, S. S., "Determining the focal length of a parabolic dish," Internet: http://www.satsig.net/focal-length-parabolic-dish.htm, Accessed on: 16–6–2015.

[16] "FocalLength," http://www.satsig.net/focal-length-parabolic-dish.htm, Accessed on: 03-06-2015.

[17] Limited, S. S., "The Antenna Feed," Internet: http://happy.emu.id.au/lab/rep/rep/9510/txtspace/9510_017.htm, Accessed on: 16–6–2015.

[18] "FocalLength," http://www.analyzemath.com/parabola/parabola_focus.html, Accessed on: 03-06-2015.

[19] "substrate," http://www.rogerscorp.com/acs/products/32/RT-duroid-5880-Laminates.aspx, Accessed on: 13-06-2015.

[20] Thales, "Microwave Telecom," https://www.thalesgroup.com/en/canada/space/microwave-telecom, Accessed on: 26–6–2015.

[21] L-3, "Space TWTs, LTWTAs & EPCs," http://www2.l-3com.com/eti/product_lines_space_twt.htm, Accessed on: 26–6–2015.

[22] Cubesatshop, "NanoPower Solar P110-A/B," http://cubesatshop.com/index.php?page=shop.product_details&flypage=flypage.tpl&product_id=70&category_id=17&option=com_virtuemart&Itemid=79, 2015, Accessed on: 12–6–2015.

[23] Faulhaber, D. F., "AM2224-ww-ee," http://www.micromo.com/media/pdfs/AM2224_FPS.PDF, 2014, Accessed on: 12–6–2015.

[24] KG, D. F. F. G. . C., "Spur Gearheads series 2.22," http://www.clyde-space.com/products/electrical_power_systems/smallsat_power, 2014, Accessed on: 23–6–2015.

[25] Space, C., "Smallsat Power," http://www.micromo.com/media/pdfs/22-2_FMM.PDF, 2015, Accessed on: 15–6–2015.

[26] Stoyan Nihtianov, A. L., *Smart Sensors and MEMS: Intelligent Devices and Microsystems for Industrial Applications*, chap. 15, Woodhead Publishing Limited, 2014, p. 463.

[27] Corporation, A., "Digital Sun Sensors (DSS)," http://www.adcole.com/aerospace/digital-sun-sensors/, Accessed on: 24-06-2015.

[28] Analog Devices, I., "MEMS Gyroscope list," http://www.analog.com/en/products/mems/mems-gyroscopes.html, Accessed on: 22-06-2015.

[29] Integrated, M., "MAX21000 Gyroscope specs," http://www.maximintegrated.com/en/products/analog/sensors-and-sensor-interface/MAX21000.html, Accessed on: 19-06-2015.

[30] Oelze, H. W., "CubeSat Magnetorquers produced by ZARM," http://www.zarm-technik.de/downloadfiles/ZARMTechnikAG_CubeSatTorquers_web2010.pdf, Accessed on: 10–6–2015.

[31] Hibbeler, R. C., *Mechanics of Materials*, Prentice Hall, 9th ed., January 2013.

[32] Pisacane, V. L., *Fundamentals of Space Systems*, Oxford University Press, 2nd ed., 2005.

[33] Widder, D. V., *The heat equation*, Vol. 67, Academic Press, 1976.

[34] David, G. G., "Spacecraft thermal control handbook," *Fundamental Technologies*, Vol. 1, 2002.

[35] EUROCKOT Launch Service Provider, *Rockot User's Guide*, issue 5, revision 0 ed., August 2011.

[36] Pisacane, V. L., *Fundamentals of Space Systems*, Oxford University Press, USA, 198 Madison Avenue, New York, 2005.

[37] United Nations Office for Outer Space Affairs, http://www.unoosa.org/pdf/spacelaw/sd/2004-B5-10.pdf, 2004, Accessed on: 20–5–2015.

[38] Mathworks, "Matblab atmosnrlmsise00 function documentation," http://nl.mathworks.com/help/aerotbx/ug/atmosnrlmsise00.html?refresh=true, Accessed on: 23-06-2015.

[39] MathWorks, http://nl.mathworks.com/help/aerotbx/ug/atmosnrlmsise00.html, Accessed on: 20–5–2015.

[40] NOAA, "Homepage," ftp://ftp.swpc.noaa.gov, Accessed on: 18–5–2015.

[41] King-Hele, D., *Satellite orbits in an atmosphere, theory and applications*, chap. 2.5, Blackie, 1987, pp. 30–31.

[42] Doornbos, E., *Thermospheric density and wind determination from satellite dynamics*, Ph.D. thesis, TU Delft, 2011.

[43] Hongzheng, C., "Near Real-Time Global Density Estimation Using Satellite Precision Orbit Ephemerides," http://swfound.org/media/94993/Cui-Near_Realtime_Atmospheric_Density-Nov2012.pdf, Accessed on: 11–6–2015.

[44] Anderson, B. J., "Natural Orbital Environment Guidelines for Use in Aerospace Vehicle Development," *NASA*, 1994.

[45] Sawka, W. and McPherson, M., "Electrical Solid Propellants: A Safe, Micro to Macro Propulsion Technology," AIAA, AIAA, July 2013, 49th AIAA/ASME/SAE/ASEE Joint Propulsion Conference. doi:10.2514/6.2013-4168.

[46] Rocketdyne, A., "Monopropellant Rocket Engines," Datasheet found on https://www.rocket.com/propulsion-systems/monopropellant-rockets, Accessed on 15–06–2015.

[47] MOOG, "Bipropellant Thrusters," Datasheet found on http://www.moog.com/products/thrusters/bipropellant-thrusters/, 2013, Accessed on 16–06–2015.

[48] ALTA, "Mini Hall Thruster HT-100," Datasheet via ALTA-space website, http://www.alta-space.com/uploads/file/brochures/Brochure_2013_HT100_D.pdf.

[49] Surrey, "Low Power Resistojet," Datasheet, January 2014, http://www.sstl.co.uk/getattachment/9deb85e0-a017-4915-8feb-ce30d4819752/Low-Power-Resistojet.

[50] Swagelok, "Pressure Regulators K Series," http://www.swagelok.com/downloads/webcatalogs/EN/MS-02-230.pdf, Accessed on 16–06–2015.

[51] HYDAC, "2/2 Solenoid Directional Valve Poppet Type, Direct Acting Normally Closed Metric Cartridge 250 bar," http://www.hydac.com/fileadmin/pdb/pdf/PRD00000000000000000000005949030011.pdf, Accessed on 16–06–2015.

[52] Boyer, R., Welsch, G., and Collings, E. W., *Materials Properties Handbook: Titanium Alloys*, ASM International, 1994.

[53] EUROCKOT, "EUROCKOT launch services," http://http://www.eurockot.com/rockot/launch-vehicle/, Accessed on: 16-06-2015.

[54] Morita, Y., "A New Type of Launch Vehicle: A Rocket with Artificial Intelligence," http://global.jaxa.jp/article/interview/vol58/index_e.html/, Accessed on: 21–5–2015.

[55] Clark, S., "Minotaur rocket poised to send research to new heights," http://spaceflightnow.com/minotaur/stps26/101118preview/, November 2010, Accessed on: 21–5–2015.

[56] Harvey, B., *The Rebirth of the Russian Space Program 50 Years After Sputnik, New Frontiers*, Praxis Publishing, 2007.

[57] Iridium, "Iridium Announces Fourth Quarter and Full Year 2014 Results," http://files.shareholder.com/downloads/ABEA-3ERWFI/106554385x0x812109/5e07ffc9-b1fc-4a5f-911a-9539ef7aabad/IRDM_News_2015_2_26_Financial_Releases.pdf, February 2015, Accessed on: 1–5–2015.

[58] Inmarsat, "Inmarsat plc reports Preliminary Full Year Results 2014," http://www.inmarsat.com/wp-content/uploads/2015/03/Inmarsat_plc_Preliminary_Results_2014.pdf, February 2015, Accessed on: 1–5–2015.

[59] ORBCOMM, "ORBCOMM announces fourth quarter and full year 2014 results," http://www.orbcomm.com/uploads/files/ORBCQ414FY2014EarningsRelease.pdf, March 2015, Accessed on: 1–5–2015.

[60] Globalstar, "Globalstar Annual Report 2014," http://www.globalstar.com/en/index.php?cid=6062&fileLink=http://irxml.corporate-ir.net/filings/toc.data?id=10117559&sXbrl=1&compId=203507, March 2015, Accessed on: 30–6–2015.

[61] Sprague, K., Manyika, J., Chappuis, B., Bughin, J., Grijpink, F., Moodley, L., and Pattabiraman, K., "McKinsey&Company - Offline and falling behind - Barriers to internet adoption," http://www.mckinsey.com/insights/high_tech_telecoms_internet/offline_and_falling_behind_barriers_to_internet_adoption, September 2014, Accessed on: 1–5–2015.

[62] USFOREX, "Historical Exchange Rates June 2014 - June 2015," http://www.usforex.com/forex-tools/historical-rate-tools/historical-exchange-rates, Accessed on: 19-06-2015.

[63] Curran, R., Hamann, R. J., and van Tooren, M. J. L., "Workshop PM-SE," TU Delft DSE Lecture Slides, 2009, Workshop 2.

[64] Newcomb, T., "Near Real-Time Global Density Estimation Using Satellite Precision Orbit Ephemerides," http://newsfeed.time.com/2011/09/22/satellite-falling-to-earth-nasa-scientist-puts-it-into-perspective/, Accessed on: 15–6–2015.

[65] IATA, *Lithium Battery Guidance Document*, IATA, 2015.

[66] Eurospace, A., *Exemption of propellant-related use of hydrazine from REACH authorisation requirement*, ASD Eurospace, 2012.

Appendix A

ICD

A.1 Astrodynamics Interface Control Document

An ICD describes the interface of the software tools which have been created. The astrodynamics software ICD calculates the propagation of the orbits, satellite location and provide images of coverage and orbits. The program is written in MatLab. The program can be run by invoking the script via the command line. The program used is named Coverage.m

The input of Coverage.m is:
Number of Planes
Number of Satellites per Plane
Inclination
Number of orbits

The output of Coverage.m is:
Orbit characteristics
% Coverage over time
Average % Coverage
Video of constellation for amount of orbits selected

A.2 Link Budget

The linkbudget calculation sheet is presented below for the ground users and the ground station. The intersatellite link budget is shown separately in Table A.2.

	User (worst case)	User (best case)	User (best case side ant)	User (worst case side ant)	Station (worst case)	Units
Space Segment						
Total number of users	50000	50000	50000	50000	1	people
Number of satellites	209	209	209	209	1	units
Users per beam	35	35	35	35	1	
Frequency	2,20	2,20	2,20	2,20	12,00	GHz

Beam Width	60,00	60,00	38,50	38,50	120,00	deg
Coverage Area	1145,92	1145,92	471,81	471,81	4583,66	deg2
Antenna Efficiency	70,0%	70,0%	70,0%	70,0%	70,0%	%
Antenna Gain	9,60	9,60	23,34	23,34	7,99	dBi
Antenna Diameter	0,16	0,16	0,25	0,25	0,01	m
Satellite Tx Power	20,50	14,80	3,480	1,020	6,3	W
Backoff and Line Loss	-3,0	-3,0	-3,0	-3,0	-3,0	dB
EIRP per Anteanna beam	19,72	18,30	25,76	20,43	12,98	dBW
Propagation Range	644,4	550,0	1.294,0	700,0	1.816,0	km
Space Loss	-155,48	-154,11	-161,54	-156,20	-179,22	dB
Atmospheric Losses	-3,0	-3,0	-3,0	-3,0	-7,0	dB
Net Path Loss	-158,48	-157,11	-164,54	-159,20	-186,22	dB
Ground Segment						
Diameter	0,12	0,12	0,12	0,12	2,62	m
Beamwidth	79,55	79,55	79,55	79,55	0,667939	deg
Antenna Efficiency	55,0%	55,0%	55,0%	55,0%	70,0%	%
Gain, G	0,50	0,50	0,50	0,50	48,81	dBi
Line Loss	-0,5	-0,5	-0,5	-0,5	-3,0	dB
Receive Carrier Power C	-138,26	-138,30	-138,28	-138,27	-124,42	dBW
System Noise Temperature	27,0	27,0	27,0	27,0	27,0	dB-K
G/T	-26,50	-26,50	-26,50	-26,50	21,81	dB/K
Receiver C/No	63,34	63,30	63,32	63,33	77,18	dBW
Data Rate	55,90	55,90	55,90	55,90	67,27	dB-Hz
Available Eb/No, Downlink	7,44	7,40	7,42	7,43	9,91	dB-Hz

End-to-End Eb/No	6,94	6,90	6,92	6,93	6,91	dB
Required Eb/No	3,89	3,89	3,89	3,89	3,89	dB
Link Margin	**3,0**	**3,0**	**3,0**	**3,0**	**3,0**	dB
Number of Channels	7	7	7	7	1	
Number of Users/Channel	5	5	5	5	1	
Single User Data Rate	0,07	0,07	0,07	0,07	4,8	Mbps
Code Rate,	0,9	0,9	0,9	0,9	0,9	

A.3 User Beam Coverage

This program will briefly describe how to use the spotbeam.m. The final result of the beam coverage software is a plot that shows the surface covered by the antennas with the signal strength. The program is written in MatLab. The program can be run by invoking the script via the command line.

There are three main steps in the program. The first step gives an overview of how the antennas should be positioned, and the beam-width they should be designed for.

The input of the first part of spotbeam.m is

- Altitude
- Central antenna half power beam-width
- Required coverage area

The output of the first part is:

- Required outer antenna half-power beam-width
- Antenna layout
- Antenna angular offset
- Beam pattern that should be designed for

Upon having the required antenna beam-widths, the gain plots can be created. This is the second part, which is purely antenna theory. It serves to show that the half power beam-width that is required is achieved.

The input of the second part of spotbeam.m is

- Frequency of the signal
- Focal length
- Antenna diameters
- Aperture efficiency

The output of the second part is:

Table A.2: Intersatellite Link

	Ground User	Units
Space Segment		
Frequency	30	GHz
Beam Width	10	deg
Coverage Area	31,83	deg^2
Antenna Efficiency	70,0%	-
Antenna Gain	25,3	dBi
Antenna Diameter	0,07	m
Satellite Tx Power	6,4	W
Backoff and Line Loss	-2,0	dB
EIRP per Anteanna beam	31,36	dBW
Propagation Range	3.328,6	km
Space Loss	-192,44	dB
Atmospheric Losses	0,0	dB
Net Path Loss	-192,44	dB
Ground Segment		
Diameter	0,07	m
Beamwidth	10	deg
Antenna Efficiency	70,0%	-
Gain, G	25,30	dBi
Line Loss	3,0	dB
Receive Carrier Power C	-135,79	dBW
System Noise Temperature	27,0	dB-K
G/T	-1,70	dB/K
Receiver C/No	65,81	dBW
Data Rate	55,90	dB-Hz
Available Eb/No, Downlink	9,92	dB-Hz
End-to-End Eb/No	6,92	dB
Required Eb/No	3,89	dB
Link Margin	**3,0**	dB
Number of Channels	2	-
Required Data Rate	0,7	Mbps
Code Rate, ρ	0,9	-

- Antenna gain plots
- Antenna gain at different beam-widths

Now for the last part, the output of the first two parts is combined to achieve a complete representation of signal strength and coverage of the antenna pattern.

The input of the third part of spotbeam.m is

- Altitude
- Antenna gains at different beam-widths
- Antenna layout
- Antenna angular offset

The output of the third part is:

- Antenna footprint pattern with signal strength

A.4 Doppler Tracking Interface Control Document

This ICD describes the interface of the software tools which have been created. For the Doppler tracking. The script is programmed with Matlab and is calles doppler_locate.m and recalls functions that are also used for the astrodynamics.

The input of doppler_locate.m is

- Latitude and longitude of user device
- Transmission frequency
- Minimum required elevation of a satellite
- Inclination
- Number of orbits
- Orbit altitude
- Orbit inclination
- Orbit right ascension node

The first step is to calculate the Doppler shift that is observed on the satellite for the given orbital parameters and user device location.
The second step is to take the this observations and recreates the position with a linear iteration method as described in Section 5.2.

The output of doppler_locate.m is:

- Estimated observer latitude and longitude
- Estimated observer frequency
- Standard deviation of the latitude and longitude
- Standard deviation of the frequency

A.5 ADCS Interface Control Document

This ICD describes the interface of the ADCS software. Two codes were written during the development of this subsystem. The first one was used to find a pointing accuracy requirement and the second one was used to find an appropriate magnetorquer dipole for this mission. Both codes were written in Matlab.

A.5.1 pointingaccuracy.m

This code relates a percentage in coverage loss for one beam to a minimum pointing accuracy using simple geometry. Using the percentage of acceptable loss and the footprint radius as inputs, the program computes the overlap of 2 circles corresponding to the non-overlapping areas being equal to the input percentage of the whole circle's area. The output is the angle between the 2 beams creating those circles depending on the satellite's altitude.

A.5.2 DisturbanceTorques.m

This code uses satellite geometry, mass, solar panel specs, assumptions on the satellite's residual dipole and reflectivity factor and a magnetorquer dipole as inputs. The outputs are the following:

- Gravity gradient induced torque
- Solar radiation induced torque
- Magnetic field induced torque
- Aerodynamic drag induced torque
- Magnetorquer induced torque
- Maximum rotation manoeuvre time

A.6 Decay Interface Control Document

This ICD describes the interface of the decay simulation software. It computes the time it takes for a satellite to reach an altitude of 100km. The program is programmed in Matlab. As mentioned in the Sustainability and Decay chapter, the program consists of 3 parts out of which only the third is used repeatedly. The first two were used to create data files which feed the third code.

Additionally, an extra piece of code was written which was used to validate the above described program. It reads TLE data, obtains relevant information from it and compares it to what the code would compute.

A.6.1 average.m

This script reads data files obtained from the NOAA website, containing both magnetic and solar flux historical data. The program reads these files and produces the following outputs for both:

- average
- maximum
- minimum
- median

A.6.2 DensityComputation.m

The input of DensityComputation.m are the 4 values computed by average.m. It returns the following documents:

- Altitude_Density_allavg.txt
- Altitude_Density_allmed.txt
- Altitude_Density_allmax.txt
- Altitude_Density_allmin.txt
- Altitude_Density_dgdmax.txt

- Altitude_Density_asfmax.txt

These are lists containing a density assigned to a certain altitude in steps of 1km. They use different settings of solar and magnetic flux to find the average, maximum and minimum possible density.

A.6.3 DecayComputation.m

The inputs of DecayComputation.m are one of the .txt files mentioned above to be chosen by the user, the initial orbital altitude and the co-rotation and wind correction factor based on the orbit inclination which is read of by a graph. It only has one output, which is the time it takes for the satellite to reach 100km. The result is presented in days and years. If required, a few command lines can be un-commented and the program will plot the orbital radius with respect to time.

A.6.4 ODValidation.m

This code uses 2 preferably consecutive TLE data points of, in this case, the Grace 1 mission and reads the mean motion, time, right ascension of the ascending node, inclination and mean anomaly from it. In addition to this, it takes the average and daily solar flux as well as the past and present magnetic flux as inputs. Using the exact same functions as the 'to be validated' code, it computes the numerically obtained decay and the actual decay of the mission.

A.7 Delta V Interface Control Document

This ICD describes the interface of the delta V software. The code has be written in Matlab and consist of the calculation of the three different types of delta V and the total propellant mass needed for that. The name of the program is deltaV.m

The inputs of the program are

- altitude
- inclination
- Operation year
- Solar Flux
- Operation lifetime
- Size area
- Specific impulse
- mass spacecraft

The outputs of the program are

- Probability of collision
- delta V for debris avoidance
- delta V for orbital maintenance
- delta V for constellation maintenance
- propellant mass

A.8 Thermal Interface Control Document

This chapter describes the interface of the thermal analysis simulations. The thermal analysis consists of two parts, one function calculates the amount of heat captured and emitted by the spacecraft and the second part computes the heat distribution of a flat plate by means of a finite difference method.

A.8.1 sc_body_heat.m

Inputs:

1. α_s Solar absorbance.
2. ε infrared emissivity.

Outputs

1. Temperature vector of cold case.
2. Orbit angle vector, corresponding to the temperature vector above.
3. Added heat vectors for
   (a) Heat due to solar radiation.
   (b) Heat due to albedo effect.
   (c) Heat due to IR radiation.
4. Table for cold case containing the net heat flow for each side of the spacecraft.
5. Table for hot case containing the net heat flow for each side of the spacecraft.
6. Temperature of hot case.

Fixed values in the program which can be altered

1. Spacecraft internal heat dissipation.
2. Solar flux for hot and cold case.
3. Boltzman constant.
4. View factor of solar and albedo radiation.
5. Area of each of the spacecraft sides.
6. Earth seasonal fluctuation factors.

A.8.2 heat.m

This program Inputs

1. α Heat dissipation.
2. Total time to evaluate.
3. Length of x-direction.
4. Length of y-direction.
5. Number of points in x-direction.
6. Number of points in y-direction.

Outputs

1. (a) Vector containing temperature values.
   (b) Plot of the temperature vector.
2. (a) Vector of x-axis.
   (b) Vector of y-axis.
3. Stability value, see Formula (10.9).

4. Vector containing error for each time-step.

Fixed values which can be altered

1. Initial condition, set to 259 [K].
2. Boundary conditions,
   (a) For $x = 0$, or $y = 0$: 326 [K].
   (b) For $x = L_x$, or $y = L_y$: 259 [K].

A.9 Structural Analysis Interface Control Document

This section shows the logic of the structural analysis program. Generally, the following inputs and outputs are obtained from the program:

[b] Inputs:

- Material properties: density, Young's modulus and yield stress.
- Thickness of component.

[b] Constant values:

- Accelerations from launcher manual.
- Mass of spacecraft
- Dimensions of spacecraft

[b] The outputs are generated in tables, all present in Chapter 11. Summarising:

- Von Mises stress.
- Natural frequency.
- Critical buckling stress.

The text in Chapter 11 clearly explains which formula is used and whether the component is evaluated for buckling or natural frequency failure.

The thickness has to be iterated manually. By adjusting the thickness, one can rerun the program and obtain the Von Mises stress, buckling stress and natural frequency.

A.10 Sun Pointing Angle Interface Control Document

This ICD describes how the Matlab code determines the angular velocity of the yaw motion of the satellite and pitch motion of the solar panels when given a input of specific time. With the Matlab code, the maximum value from these graphs can be obtained. These are the values that are needed to determine whether the ADCS system and motor in the solar panel is able to cope with required rate.

The name of the Matlab program is called rotations.m. Functions of the standard transformation matrix around U, V, W axis with respect to time are used for the rotation calculations. They are in separate files and will be recalled to be used in the main program.

The input of is

- Mean anomaly 'θ'
- Inclination angle (It is constant for the designed constellation, but it can be changed for verification and validation of the code)
- Right ascension of the ascending node 'Ω' and 'β'

After the transformations, the relation between the vehicle based reference system and the ECI can be established. The angle of projection between two frames can be found with the arc cosine and the rate can be found with the gradient of two consecutive points, which will be the rate of angle changing.

The output of rotations.m is:

- the projection of the angles between the vehicle reference frame and ECI frame
- The plot of rate of change of these angles (angular velocity of yaw and pitch motion)
- The maximum values of these plots